8-2010

DEVELOPMENT OF TISSUE ENGINEERED TEST SYSTEMS TO STUDY MAMMARY CELL INTERACTIONS IN VITRO

Cheryl Cass
Clemson University, parzel@clemson.edu

DEVELOPMENT OF TISSUE ENGINEERED TEST SYSTEMS TO STUDY MAMMARY CELL INTERACTIONS *IN VITRO*

A Dissertation
Presented to
the Graduate School of
Clemson University

In Partial Fulfillment
of the Requirements for the Degree
Doctor of Philosophy
Bioengineering

---

by
Cheryl Anne Parzel Cass
August 2010

Accepted by:
Karen J.L. Burg, Ph.D., Committee Chair
Lisa Benson, Ph.D.
Timothy Burg, Ph.D.
Didier Dréau, Ph.D.
Richard Groff, Ph.D.

ABSTRACT

The work described in this dissertation was conducted in the interdisciplinary research environment of the Clemson University Institute for Biological Interfaces of Engineering. A note at the beginning of each chapter acknowledges, as relevant, collaborating doctoral students and reminds the reader where work from each chapter has been presented or published. The overall goal of this work was to develop tissue engineered test system methodologies to allow the study of mammary cell interactions *in vitro*. The background, as described in Chapter 1, was published in part in Philosophical Transactions of the Royal Society A in 2010. The studies were designed to encompass both microfabrication technology as well as traditional 3D gel-based macrofabrication techniques, both of which will ultimately be necessary to design and fabricate biologically relevant 3D composite breast tissue cultures. The first step was to assess the effectiveness of microfabrication technology (a custom inkjet bioprinter) to eject cellular and acellular bio-inks into specified two-dimensional patterns on a variety of surfaces. Hence Chapter 2 addresses the overall project feasibility; studies are described wherein printing parameters are modified to identify optimal model conditions. These particular studies were designed to 1) evaluate the effect of stage height on cell viability, 2) identify the relationship between the rate of nozzle firing and the viscosity of a bio-ink, and 3) determine the accuracy of cell placement in a printed co-culture pattern. This work was presented at the 2008 Hilton Head Conference on Regenerative Medicine (stage height) and the 2009 Annual Conference of the Society For Biomaterials (nozzle firing). Chapter

3 addresses one of the major limitations of bioprinting, that of cartridge nozzle clogging, and evaluates the effectiveness of ethylenediaminetetraacetic acid as an anti-scalant and anti-aggregant in 2D high-throughput bioprinting. This work was published in 2009 in the Journal of Tissue Engineering and Regenerative Medicine. Furthermore, Chapters 4 and 5 describe the high resolution capability of the custom bioprinting system, which was demonstrated by 1) printing mono- and co-culture patterns and 2) applying thermal inkjet technology to stain histological samples and cell monolayers, which will be important in the future analysis of test systems. Work described in Chapter 4 was presented in part at the 2009 Annual Meeting and Exposition of the Society For Biomaterials and the 2009 IEEE Engineering in Medicine and Biology Society Conference, while work described in Chapter 5 was presented in part at the 2010 Annual Meeting and Exposition of the Society For Biomaterials. As a final bioprinting-based study, Chapter 6 describes the printing of high-resolution patterns of murine cells in 2D to evaluate paracrine signaling among adipocytes and cancer cells. To achieve this end, D1 and 4T1 cells were printed in co-culture patterns and the effect of 4T1 cells on the proliferation of D1 cells treated with an adipogenic cocktail was evaluated. This work was presented at the 2010 IEEE Engineering in Medicine and Biology Society Conference.

Before merging inkjet technology with traditional 3D gel-based culture techniques, 3D gels with incorporated 3D rigid substrates were developed to sustain anchorage dependent stromal cells in a breast tissue co-culture model. As described in Chapter 7, the differences in the activity of stromal cells (adipocytes) seeded on beads versus cells suspended in a gel were determined, as was the effect of adipocytes (seeded

on beads and directly in a gel) on mammary epithelial cells. This work will provide a foundation on which tissue test systems with biologically relevant features may be built.

Chapter 8 presents work dedicated to education and outreach in tissue engineering. Specifically, a series of classroom teaching modules are presented that can be used to demonstrate basic tissue engineering concepts, such as the effect of the shape of a medical implant on surrounding tissue or the effect of scaffold surface texture on cell attachment. The long-term goal of this work will be to enhance science, technology, engineering, and mathematics education teaching methods and to enhance graduate student communication skills with a non-scientific audience.

DEDICATION

This work is dedicated to my parents, JoAnne and Joe, my brother, Joey, my step-parents, Debbie and Ron, and my new Cass family, Fran and David. I never could have completed this degree without your love and support. To my husband, Brian: Thank you for always believing that I could actually achieve this and for helping me maintain balance throughout the process. I love you so much, and I can't wait to explore the world with you. It's time to fly!

ACKNOWLEDGEMENTS

I would like to thank my advisor, Dr. Karen Burg for her guidance and support and for the opportunity to pursue this degree. I would also like to thank my committee members, Dr. Lisa Benson, Dr. Timothy Burg, Dr. Didier Dréau, and Dr. Richard Groff for investing their time in my research endeavors.

Many people from the Department of Bioengineering and Institute for Biological Interfaces of Engineering and from the rest of the Clemson community have also given me their assistance throughout the course of my graduate education including Mrs. Cassie Gregory, Mrs. Maria Martin, Dr. Brian Booth, and Mrs. Linda Jenkins. I would also like to thank Mrs. Brenda Hungerford from T.L. Hanna High School and Ms. Lydia Beall from the Boston Museum of Science for assisting in the implementation of educational demonstrations. I could not have completed this dissertation without the support and friendship of the other graduate students and postdocs at Clemson, especially Cheryl Gomillion and Dr. Chih-Chao Yang.

Funding for this work was provided by the National Science Foundation Emerging Frontiers in Research and Innovation (EFRI) grant and the Department of Defense Era of Hope Scholars Award.

TABLE OF CONTENTS

Table of Contents (Continued) ..... Page

Table of Contents (Continued) ..... Page

LIST OF TABLES

LIST OF FIGURES

List of Figures (Continued)

List of Figures (Continued)

List of Figures (Continued)

CHAPTER 1

Select information in this chapter was published in Philosophical Transactions of the Royal Society A (TC Burg et al., 2010).

LITERATURE REVIEW

Anatomy of the Human Breast

The human breast (**Figure 1.1**), like other organs in the body, is comprised of a functional parenchyma (the mammary gland) and a stroma of supportive connective tissue (Forsyth, 1991; American Cancer Society, 2010). Among these highly innervated tissues is a local network of blood and lymphatic vessels. Parenchymal tissue contains milk-producing lobular structures and ducts, which function in milk transport (Akers, 2002; Gray, 1985). Each breast contains approximately 15-20 lobes that branch into smaller lobules and that have individual excretory ducts, also known as lactiferous tubules, which eventually converge at the nipple (Baker *et al.*, 2001). Lobes are connected by the fibrous tissue of the breast and are separated by intervals of adipose tissue. The volume of the breast is composed primarily of adipose tissue. The fundamental unit of adipose tissue is a fat lobule, which consists of approximately 10^2-10^3 mature adipocytes.

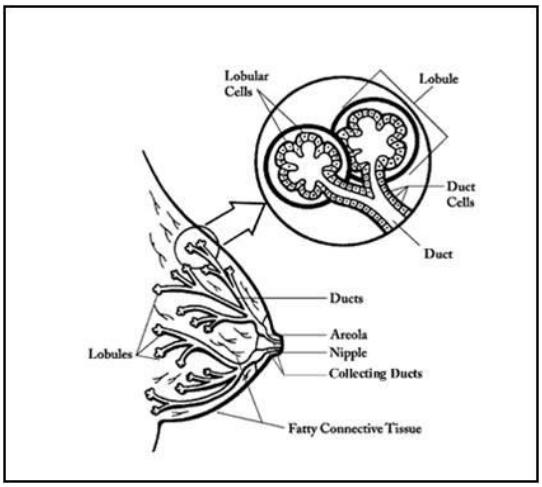

***Figure 1.1: Bulk anatomy of the female breast. The mammary epithelium (ducts and glands) is embedded within fatty connective tissue*. (American Cancer Society, 2010)**

The primary cellular and protein based components of functional secretory glands in the breast, termed acini or alveoli, include luminal epithelial cells, myoepithelial cells, and a basement membrane; in a normal human breast, the basement membrane is responsible for separating the epithelium from the connective tissue (Gudjonsson *et al*., 2003). As depicted in **Figure 1.2**, a single layer of luminal epithelial cells surrounds the inner lumen of each gland constituent (Nelson & Bissell, 2006). Normal luminal epithelial cells (labeled LEP in Figure 1.2) form tight junctions and are polarized; that is, they have distinct apical (facing the lumen) and basolateral (interacting with other) surfaces (Lodish *et al*., 2004). Directly adjacent to the single layer of luminal epithelial cells is a layer of myoepithelial cells (labeled MEP in Figure 1.2). These cells are primarily responsible for the deposition of basement membrane (labeled BM in Figure 1.2) proteins and for the maintenance of luminal epithelial cell polarity (Polyak & Hu, 2005). The prefix "myo," often associated with "muscle," is appropriate for this cell type

because they are also contractile in nature; they are responsible for contributing to the milk secretion process during lactation (Schmeichel & Bissell, 2003).

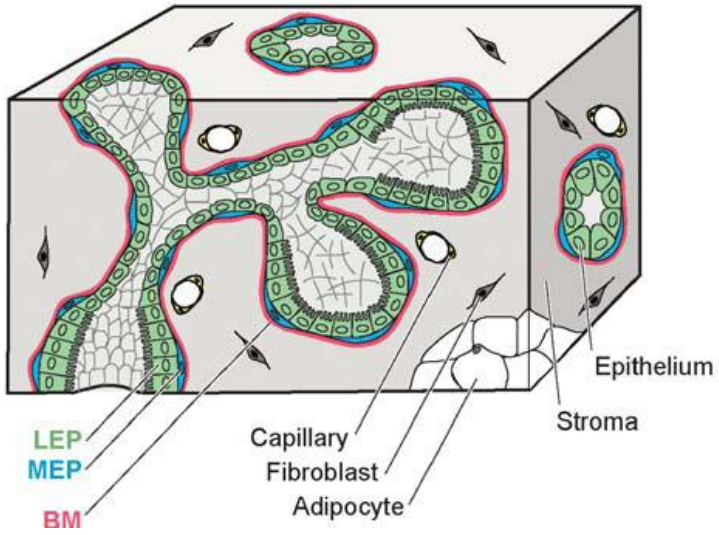

Figure 1.2: Composition and structure of mammary tissue. The parenchyma is separated from fatty connective tissue by a layer of basement membrane. (Nelson & Bissell, 2006)

Histologic analyses have shown that ductal myoepithelial cells form a more continuous barrier layer, when compared to the crescent-shaped myoepithelial cells in the mammary alveoli. This intermittent configuration can result in direct contact of luminal epithelial cells with basement membrane proteins in the alveoli structures, thus resulting in an altered microenvironment (Dairkee *et al*., 1985; Deugnier *et al*., 2002). Body cells and cap cells are also present within the structure of the alveoli. Body cells (usually occur in several layers within the terminal end bud of a murine mammary gland) (Sternlicht *et al.,* 2006) represent those that undergo programmed cell death (apoptosis)

to facilitate lumen formation during stages of breast development. Cell death via apoptosis can be distinguished from necrotic cell death by identification of distinct apoptotic morphological changes including cell shrinkage, chromatin condensation, nuclear fragmentation, and cytoplasmic budding or "blebbing" (Kim, 2005; Potten, 2004). Cap cells (typically there is a single layer of cells directly adjacent to myoepithelial cells) (Hinck and Silberstein, 2005) are proliferative in nature and are thought to be the progenitor cells responsible for the establishment of both luminal epithelial and myoepithelial cells during development (Harris *et al*., 2004). A basement membrane, also termed basal lamina, acts as a barrier separating parenchymal and stromal tissues. Its primary constituents include Type IV collagen, fibronectin, enactin, and laminin (Lanza, 2000; Liotta *et al*., 1984).

Collagen IV	A structural and adhesive protein that is exclusive to basement membranes and that is mostly non-helical, sheet-forming, and does not form fibrils (Ratner *et al*., 1996).
Fibronectin	An adhesive glycoprotein that can be incorporated into collagens and that has integrin binding capabilities (Lodish *et al*., 2004).
Enactin	Also referred to as nidogen, enactin is primarily responsible for crosslinking Type IV collagen and laminin (Lodish *et al*., 2004).
Laminin	An adhesive protein with multiple binding sites that forms 2D sheet-like networks with Type IV collagen (Lodish *et al*., 2004).

Adipose tissue is a highly specialized connective tissue that insulates and cushions the body (Fruhbeck, 2008), and it operates as an energy reserve and hormone regulator at the system level of body functions (Dugail & Hajduch, 2007; Hoggard *et al.*,

2004). The principal cellular component of adipose tissue is a collection of lipid-filled cells known as adipocytes that are adhered to a collagen fiber matrix (Iyengar *et al*., 2005). Other cellular components of adipose tissue include fibroblastic connective tissue cells, leukocytes, macrophages, and preadipocytes (committed precursor cells that, once filled with lipid, will differentiate into mature adipocytes) (Gomillion *et al.*, 2006). While white adipose tissue is not as highly vascularized as its brown counterpart (the main function of white adipose tissue is centered on energy storage), each fat cell in the white adipose tissue construct is in contact with at least one capillary, which provides a vascular network for continued growth of the tissue (Beylot, 2007; Patrick, 2000). White adipose cells store triglycerides as a nutrient source, though the transport of these molecules out of each cell is still not well understood (Civelek *et al*., 1996).

Breast Tissue Development

Unlike most exocrine glands in the human body, mammary gland development occurs in distinct stages throughout the lifetime of a female, with a majority of developmental and morphological processes taking place in adulthood (Daniel & Smith, 1999). Developmental progression of the mammary gland is known to persist because of the interactions between both genetic and environmental conditions; microenvironmental influences include primarily systemic hormonal cues and the mechanically and chemically-based communication that occurs among cells and matrix components in the stromal and epithelial tissues.

The extent of mammary gland branching at birth is minimal. The initiation of mammary tissue development in females is similar to that of males in the womb. Embedded within mesenchymal tissue at approximately 10-24 weeks into fetal development are 15-25 rudimentary ducts that form via elongation and luminalization of the embryonic mammary anlage (initial cluster of embryonic cells that eventually develops into an organ). Studies have shown that most of the epithelial cells are of the luminal lineage (Fridriksdottir *et al.*, 2005; Sternlicht, 2006). It has also been demonstrated that early stage morphogenesis in the fetus is not hormone dependent, and will occur even in the absence of receptors for estrogen, progesterone, growth hormone and prolactin (Sternlicht *et al.*, 2006).

Following embryonic and fetal development of the mammary tissue, a lag phase ensues, during which the morphogenetic capability of the gland becomes quiescent until puberty. At the onset of puberty, an influx of systemic hormones (mainly estrogen at this adolescent stage) results primarily in ductal extension and branching and production of new fatty tissue to increase the bulk of the breast tissue (Robinson *et al.*, 1999). In contrast to fetal development, pubertal breast development will not persist in the absence of hormones (LaMarca & Rosen, 2008).

Consistent with adolescent breast development, pregnancy results in further extension and branching of ductal structures and is associated with added fatty tissue mass. During pregnancy, progesterone is primarily responsible for these architectural changes and for the budding of alveoli, which will ultimately become milk-producing entities. The hallmark events of pregnancy include an early growth phase of the lobular

clusters, as well as a late differentiation stage during which epithelial cells arrange themselves into specialized secreting units (Russo *et al*., 2001a). Specifically, luminal epithelial cells will further differentiate into lobuloalveolar cells, which are capable of secreting milk (Tong & Hotamisligil, 2007). Therefore, the mammary gland will never reach a terminally differentiated and fully active state unless it is influenced by the events of a full-term pregnancy and parturition.

There are no major architectural changes to the mammary tissue during the lactation phase, as the breast in this case becomes terminally differentiated to its most active state of producing and secreting milk. Milk production will commence in the presence of circulating lactogenic hormone complex, which includes estrogen, progesterone, prolactin, and other metabolic hormones. When progesterone signals cease, secretion of the synthesized milk product can occur (Pang & Hartmann, 2007).

The commencement of involution occurs post-pregnancy, with absent or inconsistent nursing practices, when physical suckling cues no longer prompt the mammary gland to continue lactating (Nelson & Bissell, 2006). When the breast is no longer needed as a milk producing organ, the extensive production and secretion units (lobuloalveoli) rapidly collapse and resorb via methodical apoptotic processes. The epithelial tissue is replaced with fibrous and fatty connective tissue in a response that is deemed a "non-inflammatory tissue remodeling process" (Schedin *et al*., 2007).

Later in life with the onset of menopause, the major hormonal changes that can be observed in the human female breast include a decrease in the levels of estrogen and progesterone. Structurally, the basement membrane surrounding glandular tissue may

experience thickening and the stromal tissue is replaced predominately with fat. The proliferative capacity of the post-menopausal breast also significantly declines (Walker & Martin, 2007).

Breast Tumor Initiation

The schematics presented in **Figure 1.3** show alterations in tissue architecture during initial tumor growth and invasion. Though studies have been conducted to better understand the genetic and microenvironmental influences on tumor initiation, the origin of breast cancer remains largely unknown (Polyak, 2007). In the normal breast, parenchymal tissue remains compartmentalized via the maintenance of a basement membrane, shown in Figure 1.3 as a continuous black line. A single layer of polarized luminal epithelial cells (red luminal cells) and basal myoepithelial cells (black luminal cells) forms the lumen of a ductal structure; beyond the basement membrane is a normal distribution of stromal cells including fibroblasts (pink stromal cells), adipocytes (yellow stromal cells), inflammatory cells (blue stromal cells), and vascular cells (red stromal cells). The arrows indicate normal cell signaling.

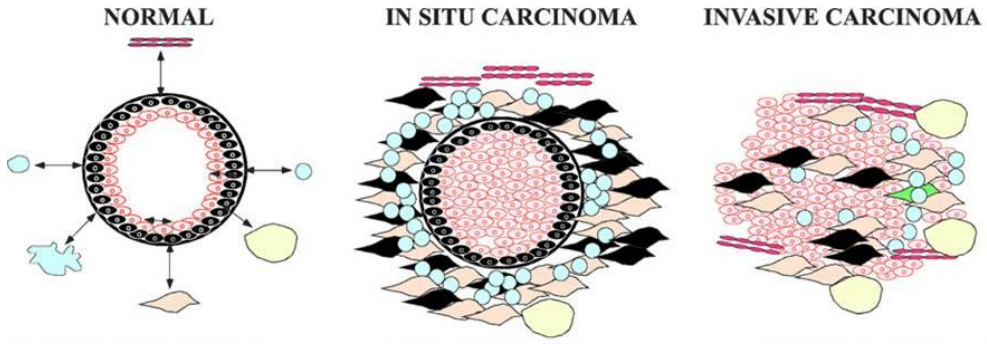

Figure 1.3: Alterations in tissue architecture during cancer growth and invasion. (Polyak & Hu, 2005)

When malignant transformation occurs, ductal carcinoma *in situ* (DCIS) will rapidly ensue. During this time of abnormal cell proliferation, stromal cells increase in number, and luminal epithelial cells can no longer maintain polarity. Luminal epithelial cells will proliferate until the lumen of the ductal structure becomes obstructed. Within this phase, the basement membrane remains continuous until the number of myoepithelial cells (responsible for the deposition of basement membrane) diminishes to a point where an intact layer can no longer be maintained. As DCIS progresses to invasive carcinoma, there is a complete loss of myoepithelial cells and of the basement membrane typically maintained by these cells. The architectural result of invasive carcinoma is a complete absence of parenchymal compartmentalization and the distribution of tumor cells within the tissue stroma. At this point, breast cancer poses such a threat because of the high concentration of local blood and lymphatic vessels in the stroma through which migratory cells can metastasize (Yu *et al.*, 2005).

Why Study Cells in Three Dimensions?

The spectrum of culture systems from 2D to 3D to animal models is vast and, while animal models provide a 3D architecture for cell growth, they are expensive and complex, and it often becomes difficult to isolate and study a single variable (Yamada & Cukierman, 2007). Additionally, animal models may not provide a suitable representation of the human organ or tissue in question. For example, unlike murine mammary tissue in which epithelial structures are surrounded by fat, human parenchymal components are in direct contact with collagen-based stromal tissue (Ronnov-Jessen *et al*., 1996). This detail is represented histologically in **Figure 1.4** (Lee *et al*., 2003; Russo *et al*., 2001a; Russo *et al*., 2001b).

One of the major environmental factors, which contributes to the maintenance of cell function integrity *in vitro,* is the substrate on which cells are grown. Traditional cell culture methods involve the seeding, growth, differentiation, and long-term culture of primary and immortalized cells on rigid plastic substrates. Though a multitude of cell types can actually remain viable on these artificial surfaces through many successive passages, their ultimate behavior in monolayer culture may not successfully recapitulate *in vivo* activity. For example, Emerman and colleagues (1977) demonstrated that primary murine mammary epithelial cells cultured on rigid plastic surfaces always failed to secrete casein (a milk protein), even when the cells were supplemented with lactogenic hormones.

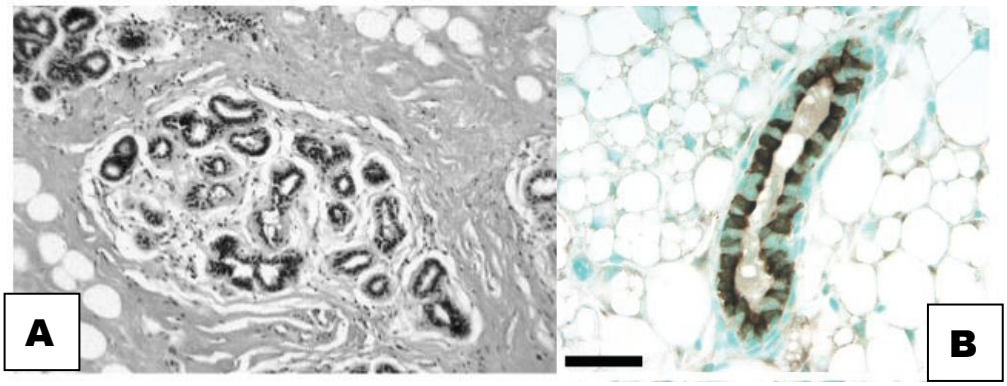

Figure 1.4: Comparison of human and murine mammary tissue. A) Human parenchymal tissue is surrounded by collagenous tissue with sporadic fat lobules while B) murine parenchymal tissue is surrounded almost entirely by fat. (Lee et al., 2003; Russo et al., 2001a; Russo et al., 2001b)

Conversely, when these cells were cultured on floating collagen membranes, they secreted casein and grew in a similar manner to differentiated secretory cells *in vivo*. Furthermore, cells that were maintained on floating collagen substrates and that were supplemented with lactogenic hormones secreted approximately 25-200 times the amount of casein into the culture media. This indicates that the effect of lactogenic hormones was significantly increased when cell attachment to an extracellular matrix-based substrate was achieved (Emerman *et al*., 1977). In addition, murine mammary epithelial cells cultured on attached Type I collagen membranes synthesized significant amounts of casein; this casein was, however, degraded over time or cells failed to secrete it into the culture medium. This result suggests that the physical state and resultant stiffness of the substrate (in this case floating versus attached Type I collagen), and not just the surface alone, can have an effect on cellular activity (Lee *et al*., 1985).

Other cell types, particularly primary cells that have been harvested directly from a mammalian source, cannot actively proliferate and die in two-dimensional culture. This is not surprising because all cells in the body grow within a 3D context. Often, primary cells that remain in 2D culture through several passages and undergo multiple cell division cycles will become undifferentiated and lose their specialized function (Wicha *et a*l., 1982). The proliferation capacity of primary murine mammary tumor epithelial cells was improved via three-dimensional organization within a Type I collagen gel. Cells were either cultured in a gel suspension or sandwiched between two gel layers, and they were maintained in culture for 26 days unlike their monolayer counterparts, which detached from their culture surface over time. Three-dimensionally-maintained cells were transplanted into parenchymal-free fat pads of mice, and histologic analyses showed epithelial-based outgrowths (Yang *et al*., 1979). Furthermore, 2D cultures often lack stromal components; this is a significant omission considering stromal tissue comprises approximately 80% of the bulk volume within a resting breast (Kim *et al*., 2004). It has been discussed by Gospodarowicz and associates that cell shape as it relates to its attachment substrate via integrin-ligand binding plays a major role in the determination of cellular growth and behavior. Ultimately, adaptation of a cell's cytoskeleton can affect binding of and response to mitogenic agents. It is believed that binding sites on the cell can become either cryptic or exposed, depending on how well the culture surface mimics the *in vivo* environment. In the body, local alterations in the extracellular matrix may be responsible for controlling this mechanism (Gospodarowicz *et al*., 1978).

From Reconstruction to Tissue Modeling

Puleo and colleagues (2007) noted two major tissue engineering applications, including scaffold-based cellular constructs for organ and tissue repair and high-throughput cultivation of cellular microenvironments for examination of disease progression and drug efficacy. Tissue engineering strategies may be employed in the development of *in vitro* breast tissue models that are more structurally similar to native tissue and therefore have enhanced potential for use in testing regimens of drug therapies and vaccines. Researchers can also use these engineered tissue models to study the physical and chemical interactions that occur among cells and extracellular matrix components and to better understand the progression of transformed epithelial cells into tumors and metastasis of tumor cells. Thus, methods of breast tissue engineering may be useful in the treatment and prevention of breast cancer. Using 3D breast tissue test systems, breast cancer cells and normal human mammary cells can be observed in a variety of relevant conditions in order to deduce why variations in subsequent cellular processes and matrix mechanics lead to cancer progression and thus what therapies will be useful.

Over 20 years ago, collagen gels were used to stabilize mammary cell boluses so that paracrine signaling could be evaluated and compared to that observed in 2D monolayer culture (Miller *et al.*, 1989). In a study by Zhang and colleagues, alginate-poly-L-lysine-alginate (APA) microcapsules were used to encapsulate MCF-7 cells. The authors demonstrated that the capsule microenvironment (i.e. liquid vs. gelled) had an effect on cell viability and activity. Additionally, when compared to an MCF-7

monolayer, encapsulated cells were more resistant to drug regimens; the authors recommend the use of these microencapsulated multicellular tumor spheroids in high-throughput drug screening processes (Zhang *et al*., 2006; Zhang *et al*., 2005). To date, the use of chitosan in three-dimensional breast tissue model applications has been minimal, though Dhiman and associates have demonstrated chitosan's utility as a three-dimensional matrix for MCF-7 cells. In their initial study, Dhiman and coworkers prepared chitosan microbead scaffolds with varying degrees of deacetylation for *in vitro* culture. The growth response of MCF-7 cells cultured on three-dimensional scaffolds was evaluated in static conditions and was shown to be superior to that of MCF-7 cells in monolayer culture (Dhiman *et al*., 2004). Three-dimensional chitosan scaffolds were then used as model systems for initial drug testing protocols. When MCF-7 cells were grown in 3D, they secreted more cathepsin-D in the presence of tamoxifen, but the subsequent uptake of cathepsin-D was inhibited. Chitosan scaffolds are porous, and therefore scaffolds densely populated with cells can provide tumor spheroid-like structures without loss of nutrient and waste transport capabilities. Thus, it was hypothesized that drug-resistance is not solely a result of poor diffusion of drugs to the interior of a spheroid; since, in this study, the three-dimensional nature of the culture was sufficient to allow MCF-7 cells to endure tamoxifen treatment more readily than MCF-7 cells in 2D monoculture. The results imply that the 3D architecture of the cellular construct led to increased drug resistance (Dhiman *et al*., 2005).

Matrigel is one of the most commonly used extracellular matrix (ECM) substrates for the preparation of normal and malignant cell culture models (Debnath & Brugge,

2005; Weaver *et al*., 1995). In breast tissue modeling applications, Matrigel has been used traditionally to induce hollow mammary acini formation via polarization of normal luminal epithelial cells. In 2003, Debnath and colleagues discussed morphogenesis and oncogenesis of MCF-10A human mammary epithelial cells grown in Matrigel, using an overlay method. They aimed to provide a model that could answer questions pertaining to oncogenes and the ultimate signaling pathways that promote epithelial organization; these explanations could likely not be deduced using standard two-dimensional culture. The authors provide protocols for implementation of viral vectors that allow stable gene expression, along with protocols for three-dimensional basement membrane culture (Debnath *et al*., 2003). Then, in 2008, Krause and associates co-cultured 3D mammary acini models using MCF-10A mammary epithelial cells as well as primary human fibroblasts obtained from reduction mammoplasty samples. This novel culture system was developed in an effort to better understand stromal-epithelial interactions in the mammary tissue and the overall effect on tissue development. Co-cultures (or a control mono-culture of MCF-10A cells) were maintained up to six weeks in either Type I collagen or a combination of collagen and Matrigel. When compared to mono-culture controls, the primary stromal fibroblasts: 1) in Type I collagen allowed a more rapid onset of cellular organization, likely resulting from fibroblast assistance in cell-cell communication and 2) in Type I collagen and matrigel allowed the formation of ductal structures (Krause *et al*., 2008).

Porous microparticles consisting of either poly(D,L-lactide-*co*-glycolide) or polylactide (PL) were constructed by Sahoo and colleagues to determine their efficacy as

cellular scaffolds. A portion of poly(vinyl alcohol) (PVA) or chitosan was also incorporated into the structure of the microparticles in select experimental samples on which MCF-7 cells were seeded. The authors concluded that (PL-PVA) beads better supported MCF-7 cell growth than Dhiman's chitosan scaffolds and were thus also suitable for the preliminary investigation of chemotherapeutics (Sahoo *et al.*, 2005).

Microfabrication Tools

Previous *in vitro* studies have demonstrated the importance of spatial alignment of cells in culture when attempting to more accurately mimic the *in vivo* microenvironment, which can include cell-cell and cell-ECM contacts in addition to physical forces and soluble factors (Falconnet *et al*., 2006; Hebner *et al*., 2008). The ability to define cell placement and therefore spatial location within a 3D tissue can lead to better predictions of cell function and an overall increase in the stability of cell phenotype (Sodunke *et al.*, 2007). Conventional cell seeding methods are inadequate in the development of an *in vitro* tissue test system because they involve the random placement of cells, and therefore lack the precision necessary for spatial control. This point is important because evidence indicates that interactions among malignant cells with the surrounding stromal tissue influence patterns of tumor growth and metastasis (Iyengar *et al*., 2003). Bissell and LaBarge note that the microenvironments of both normal and malignant cells are responsible for controlling phenotypic expression (Bissell & Labarge, 2005).

As a result, many studies have been conducted to assess the relevance of current microfabrication tools, and new technologies are being designed and developed, which

can be applied to these sought after culture models. Microfabrication tools allow the creation of select biomaterial surface variations as well as the precise placement of cellular components (Khetani & Bhatia, 2006). One advantage of microfabrication technology is that cultures will be small in size, thus requiring smaller amounts of expensive and scarce reagents (Park & Shuler, 2003). Inkjet-based microfabrication, known as bioprinting, can provide a foundation for developing such *in vitro* breast tissue models (Mironov *et al*., 2006b). The modified inkjet printer may be a useful tool for creating three-dimensional *in vitro* models because it offers an inexpensive and high-throughput solution to microfabrication, and because the printer can be easily manipulated to produce varying tissue attributes (Zhang *et al*., 2008).

Several limitations of the technology have also been mentioned, including the ejection of satellite drops (outliers that disrupt pattern resolution), transmission of heat and shear force to bio-inks, and inability to thoroughly clean cartridge reservoirs (Barbulovic-Nad *et al*., 2006). The reality is that, no matter the intended application, ink-jet printing has many logistical barriers that must be addressed in order to realize the high throughput precision fabrication of complex, 3D tissues. Khademhosseini and Langer (2007) previously discussed cell printing as a powerful "bottom-up" tissue engineering approach. They note that technical limitations associated with this method include nozzle clogging and sustainability of printed tissue constructs. Parzel and colleagues addressed the former limitation, and provided a solution for the restricted number of drops and cells that can be printed prior to clogging and printhead failure. In previous work using the HP26 printhead to print a serum-free cell culture medium, nozzles failed, i.e. the nozzles

did not eject a drop when fired after only a relatively short amount of printing time. This failure was generally attributed to clogging by adsorbed proteins (for which reason only serum-free medium is used) and cellular components, in addition to aggregated cells. The authors assessed the efficacy of ethylene diamine tetraacetic acid (EDTA) as an anti-scalant and anti-aggregant in 2D bioprinting applications and demonstrated enhancement of the printer's high-throughput potential following addition of EDTA to a bio-ink (Parzel *et al.*, 2009).

The earliest bioprinting technology literature discusses precise deposition of organic molecules, molecular aggregates, cells, and single-celled organisms such as bacterium (Goldmann & Gonzalez, 2000; Wilson & Boland, 2003). The earliest accepted applications of bioprinting included 3D organ printing and tissue printing for high-throughput drug screening (Mironov *et al.*, 2006a). Although traditional tissue engineering approaches were proven successful, the bioprinter addressed the problem of slow and non-uniform migration of cells within a rigid scaffold. Wilson and Boland describe the current state of bioprinting hardware and software, and the process involved in the conversion of off-the-shelf consumer products to laboratory tools. Specifically, the paper feed mechanism must be disabled, hardware sterilized, and printing platforms enclosed in sterile environments. Because some cells are too large to fit through inkjet cartridge nozzles, Wilson and Boland developed a piezo-driven printhead with nine available bio-ink reservoirs (2003). In a subsequent publication, Boland describes an improvement to the system which allows 3D printing of biological materials. Thermo-

reversible gels were used as "bio-paper" while cells were suspended in reservoirs and served as ink (Boland *et al.,* 2003).

Further advances in cell printing ensued with the addition of a z-axis stepper motor and the investigation of rheologic properties of proposed bio-inks. Also described was the development of CAD (computer aided design) models to facilitate the 3D layering of engineered tissues (Varghese *et al*., 2005). The advances in computer-aided tissue engineering, which is being applied to the development of biological tissues and organ substitutes, were presented (Sun *et al*., 2004). Boland again reviewed critical printing parameters such as ink temperature, and speculated that the bioprinting system is suitable for living systems because only a 4-10 degree increase in temperature is expected as the bio-ink is ejected in fractions of a second. Additionally, the simultaneous printing of biomaterials and cells was described. Specifically, cells were printed in a suspension of calcium-chloride, which acts as a crosslinker for alginate supports. The idea of incorporating controlled-release units into the bio-ink, which could be precisely placed within an area of the engineered tissue, was also discussed (Boland *et al*., 2006).

To demonstrate the value of inkjet based bioprinting in patterning biological materials, Roth and coworkers printed Type 1 collagen onto glass coverslips in various patterns including lines, circles, dot arrays, and gradients. A smooth muscle cell line and primary neurons were seeded manually onto these substrates and preferentially adhered to the printed collagen patterns (Roth *et al*., 2004). In 2004, a similar bioprinting system was used to validate printing of viable mammalian cells. Chinese hamster ovary (CHO) cells and embryonic rat motorneurons were suspended in phosphate buffered saline and

printed onto agar and collagen-based "bio-paper". Less than 8% of the CHO cells were estimated to be lysed during the printing process, and maintenance of motorneuron cell morphology was confirmed by observing extension of cell processes following 7 days in culture (Xu *et al.,* 2004). Similarly, cell viability of human fibroblasts was assessed using an alamarBlue® assay after cells were printed using piezoelectric controlled inkjet printing. Changing the amplitude and the rise time of the electrical pulse appeared to have no statistically significant effect on fibroblast viability (Saunders *et al*., 2008). Yet again, viability of human osteosarcoma cells was assessed with a LIVE/DEAD® viability/cytotoxicity assay, in this case with a BioLP™ (Biological Laser Printer). The expression of heat shock protein by these cells was also monitored, and cells were found to be minimally affected by the printing process (Barron *et al*., 2005).

In addition to validating normal cell morphology of printed mammalian cells using thermal inkjet printing technology, Xu investigated whether printed cells could maintain basic cellular processes and specific function. The electrophysiology of embryonic hippocampal and cortical neurons was assessed following the inkjet printing process, using a whole-cell patch clamp technique. None of the recordings showed a significant difference from the control, unprinted cells (Xu *et al*., 2006). Subsequently, he also demonstrated the effectiveness of the inkjet printer as a tool for enhanced gene transfection. Because of the shear stresses that cells experience during ejection from a nozzle, their membrane pores become enlarged, allowing the entrance of plasmid vectors into the intracellular compartment (Xu *et al*., 2009).

In 2D, muscle-derived stem cell microenvironments were engineered with bioprinting techniques to create a specific pattern of immobilized growth factor. The presence of patterned BMP-2 (bone morphogenetic protein) affected whether stem cells differentiated toward an osteogenic or myogenic lineage (Phillippi *et al*., 2008). The potential of hydrogels as bio-inks in bioprinting applications is considerable, largely due to the tunable nature of these materials. For example, adhesive peptides and growth factors can be incorporated into the matrix and gels can be modified following printing with the implementation of smart materials (e.g. those that are pH and temperature sensitive (Fedorovich *et al*., 2007). In 2006, a custom inkjet printer was used to deposit patterns of FGF-2 (fibroblast growth factor) onto fibrin substrates in order to evaluate the effect of growth factor saturation on cell proliferation (Miller *et al*., 2006). Then, in 2007, another group used printing technology to guide the differentiation of neural stem cells. To do so, several protein components and growth factors including FGF-2, CNTF (ciliary neurotrophic factor), and FBS (fetal bovine serum) were printed onto hydrogel scaffolds, and selective differentiation by neural stem cells seeded on each of the proteins ensued (Ilkhanizadeh *et al*., 2007).

Overall, the major hurdle involved in the development of an *in vitro* breast tissue model appears to be the implementation of appropriate microenvironmental signaling mechanisms. In order to build a successful model, the collective culture of stromal and parenchymal cells (e.g. fibroblasts, adipocytes, endothelial cells, inflammatory cells, luminal epithelial cells, myoepithelial cells) will be required. Unfortunately, each of

these cell types requires its own unique, extremely dynamic, and non-linear set of physical, biochemical, and electrical signals to appropriately stimulate cell activity.

References

Akers RM. 2002. Lactation and the Mammary Gland. Ames: Iowa State University Press. 278.

American Cancer Society. http://www.cancer.org. 2010.

Baker JA, Soo MS, Rosen EL. 2001. Artifacts and pitfalls in sonographic imaging of the breast. AJR Am J Roentgenol 176(5):1261-6.

Barbulovic-Nad I, Lucente M, Sun Y, Zhang M, Wheeler AR, Bussmann M. 2006. Bio-microarray fabrication techniques--a review. Crit Rev Biotechnol 26(4):237-59.

Barron JA, Krizman DB, Ringeisen BR. 2005. Laser printing of single cells: statistical analysis, cell viability, and stress. Ann Biomed Eng 33(2):121-30.

Beylot M. 2007. Adipose Tissue and Adipokines in Health and Disease. Totowa, NJ: Humana Press.

Bissell MJ, Labarge MA. 2005. Context, tissue plasticity, and cancer: are tumor stem cells also regulated by the microenvironment? Cancer Cell 7(1):17-23.

Boland T, Mironov V, Gutowska A, Roth EA, Markwald RR. 2003. Cell and organ printing 2: fusion of cell aggregates in three-dimensional gels. Anat Rec A Discov Mol Cell Evol Biol 272(2):497-502.

Boland T, Xu T, Damon B, Cui X. 2006. Application of inkjet printing to tissue engineering. Biotechnol J 1(9):910-7.

Burg TC, Parzel CA, Groff RE, Pepper M, Burg KJL. 2010. Building off-the-shelf tissue engineered composites. Philosophical Transactions of the Royal Society A 368:1839-1862.

Civelek VN, Hamilton JA, Tornheim K, Kelly KL, Corkey BE. 1996. Intracellular pH in adipocytes: effects of free fatty acid diffusion across the plasma membrane, lipolytic agonists, and insulin. Proc Natl Acad Sci USA 93(19):10139-44.

Dairkee SH, Blayney C, Smith HS, Hackett AJ. 1985. Monoclonal antibody that defines human myoepithelium. Proc Natl Acad Sci USA 82(21):7409-13.

Daniel CW, Smith GH. 1999. The mammary gland: a model for development. J Mammary Gland Biol Neoplasia 4(1):3-8.

Debnath J, Muthuswamy SK, Brugge JS. 2003. Morphogenesis and oncogenesis of MCF-10A mammary epithelial acini grown in three-dimensional basement membrane cultures. Methods 30(3):256-68.

Debnath J, Brugge JS. 2005. Modelling glandular epithelial cancers in three-dimensional cultures. Nat Rev Cancer 5(9):675-88.

Deugnier MA, Teuliere J, Faraldo MM, Thiery JP, Glukhova MA. 2002. The importance of being a myoepithelial cell. Breast Cancer Res 4(6):224-30.

Dhiman HK, Ray AR, Panda AK. 2004. Characterization and evaluation of chitosan matrix for *in vitro* growth of MCF-7 breast cancer cell lines. Biomaterials 25(21):5147-54.

Dhiman HK, Ray AR, Panda AK. 2005. Three-dimensional chitosan scaffold-based MCF-7 cell culture for the determination of the cytotoxicity of tamoxifen. Biomaterials 26(9):979-86.

Dugail I, Hajduch E. 2007. A new look at adipocyte lipid droplets: towards a role in the sensing of triacylglycerol stores? Cell Mol Life Sci 64(19-20):2452-8.

Emerman JT, Enami J, Pitelka DR, Nandi S. 1977. Hormonal effects on intracellular and secreted casein in cultures of mouse mammary epithelial cells on floating collagen membranes. Proc Natl Acad Sci USA 74(10):4466-70.

Falconnet D, Csucs G, Grandin HM, Textor M. 2006. Surface engineering approaches to micropattern surfaces for cell-based assays. Biomaterials 27(16):3044-63.

Fedorovich NE, Alblas J, de Wijn JR, Hennink WE, Verbout AJ, Dhert WJ. 2007. Hydrogels as extracellular matrices for skeletal tissue engineering: state-of-the-art and novel application in organ printing. Tissue Eng 13(8):1905-25.

Forsyth IA. 1991. The mammary gland. Baillieres Clin Endocrinol Metab 5(4):809-32.

Fridriksdottir AJ, Villadsen R, Gudjonsson T, Petersen OW. 2005. Maintenance of cell type diversification in the human breast. J Mammary Gland Biol Neoplasia 10(1):61-74.

Fruhbeck G. 2008. Overview of adipose tissue and its role in obesity and metabolic disorders. Methods Mol Biol 456:1-22.

Goldmann T, Gonzalez JS. 2000. DNA-printing: utilization of a standard inkjet printer for the transfer of nucleic acids to solid supports. J Biochem Biophys Methods 42(3):105-10.

Gomillion CT, Parzel CA, Burg, KJL. 2007. Tissue Engineering, Breast. Encyclopedia of Biomaterials and Biomedical Engineering. New York:Taylor & Francis.

Gospodarowicz D, Greenburg G, Birdwell CR. 1978. Determination of cellular shape by the extracellular matrix and its correlation with the control of cellular growth. Cancer Res 38(11 Pt 2):4155-71.

Gray H. 1985. Anatomy of the Human Body. Philadelphia: Lea & Febiger.

Gudjonsson T, Ronnov-Jessen L, Villadsen R, Bissell MJ, Petersen OW. 2003. To create the correct microenvironment: three-dimensional heterotypic collagen assays for human breast epithelial morphogenesis and neoplasia. Methods 30(3):247-55.

Harris JR, Lippman ME, Morrow M, Osborne CK. 2004. Diseases of the Breast. Baltimore: Lippincott, Williams, and Wilkins.

Hebner C, Weaver VM, Debnath J. 2008. Modeling morphogenesis and oncogenesis in three-dimensional breast epithelial cultures. Annu Rev Pathol 3:313-39.

Hinck L and Silberstein GB. 2005. Key stages in mammary gland development: The mammary end bud as a mobile organ. Breast Cancer Research 7:245-251.

Hoggard N, Hunter L, Duncan JS, Rayner DV. 2004. Regulation of adipose tissue leptin secretion by α-melanocyte-stimulating hormone and agouti-related protein: further evidence of an interaction between leptin and the melanocortin signaling system. Journal of Molecular Endocrinology 32:145-153.

Ilkhanizadeh S, Teixeira AI, Hermanson O. 2007. Inkjet printing of macromolecules on hydrogels to steer neural stem cell differentiation. Biomaterials 28(27):3936-43.

Iyengar P, Combs TP, Shah SJ, Gouon-Evans V, Pollard JW, Albanese C, Flanagan L, Tenniswood MP, Guha C, Lisanti MP, Pestell RG, Scherer PE. 2003. Adipocyte-secreted factors synergistically promote mammary tumorigenesis through induction of anti-apoptotic transcriptional programs and proto-oncogene stabilization. Oncogene 22(41):6408-23.

Iyengar P, Espina V, Williams TW, Lin Y, Berry D, Jelicks LA, Lee H, Temple K, Graves R, Pollard J, Chopra N, Russell RG, Sasisekharan R, Trock BJ, Lippman M, Calvert VS, Petricoin ER 3rd, Liotta L, Dadachova E, Pestell RG, Lisanti MP, Bonaldo P, Scherer PE. 2005. Adipocyte-derived collagen VI affects early mammary tumor progression *in vivo*, demonstrating a critical interaction in the tumor/stroma microenvironment. J Clin Invest 115(5):1163-76.

Khademhosseini A, Langer R. 2007. Microengineered hydrogels for tissue engineering. Biomaterials , 28:5087-5092.

Khetani SR, Bhatia SN. 2006. Engineering tissues for *in vitro* applications. Curr Opin Biotechnol 17(5):524-31.

Kim JB, Stein R, O'Hare MJ. 2004. Three-dimensional *in vitro* tissue culture models of breast cancer-- a review. Breast Cancer Res Treat 85(3):281-91.

Kim R. 2005. Recent advances in understanding the cell death pathways activated by anticancer therapy. Cancer 103(8):1551-60.

Krause S, Maffini MV, Soto AM, Sonnenschein C. 2008. A Novel 3D *In Vitro* Culture Model to Study Stromal-Epithelial Interactions in the Mammary Gland. Tissue Eng Part C Methods 14(3):261-71.

LaMarca HL, Rosen JM. 2008. Minireview: hormones and mammary cell fate--what will I become when I grow up? Endocrinology 149(9):4317-21.

Lanza R, Langer R, Vacanti, J. 2000. Principles of Tissue Engineering. San Diego, CA: Elsevier Science.

Lee EY, Lee WH, Kaetzel CS, Parry G, Bissell MJ. 1985. Interaction of mouse mammary epithelial cells with collagen substrata: regulation of casein gene expression and secretion. Proc Natl Acad Sci USA 82(5):1419-23.

Lee AV, Zhang P, Ivanova M, Bonnette S, Oesterreich S, Rosen JM, Grimm S, Hovey RC, Vonderhaar BK, Kahn CR, Torres D, George J, Mohsin S, Allred DC, Hadsell DL. 2003. Developmental and hormonal signals dramatically alter the localization and abundance of insulin receptor substrate proteins in the mammary gland. Endocrinology 144(6):2683-94.

Liotta LA, Rao NC, Barsky SH, Bryant G. 1984. The laminin receptor and basement membrane dissolution: role in tumour metastasis. Ciba Found Symp 108:146-62.

Lodish H, Berk A, Matsudaira P, Kaiser C, Krieger M, Scott M, Zipursky S, Darnell J. 2004. Molecular Cell Biology. New York: W.H. Freeman and Company.

Miller FR, McEachern D, Miller BE. 1989. Growth regulation of mouse mammary tumor cells in collagen gel cultures by diffusible factors produced by normal mammary gland epithelium and stromal fibroblasts. Cancer Res 49(21):6091-7.

Miller ED, Fisher GW, Weiss LE, Walker LM, Campbell PG. 2006. Dose-dependent cell growth in response to concentration modulated patterns of FGF-2 printed on fibrin. Biomaterials 27(10):2213-21.

Mironov V, Boland T, Trusk T, Forgacs G, Markwald RR. 2003. Organ printing: computer-aided jet-based 3D tissue engineering. Trends Biotechnol 21(4):157-61.

Mironov V, Drake C, Wen X. 2006a. Research project: Charleston Bioengineered Kidney Project. Biotechnol J 1(9):903-5.

Mironov V, Reis N, Derby B. 2006b. Review: bioprinting: a beginning. Tissue Eng 12(4):631-4.

Nakamura M, Kobayashi A, Takagi F, Watanabe A, Hiruma Y, Ohuchi K, Iwasaki Y, Horie M, Morita I, Takatani S. 2005. Biocompatible inkjet printing technique for designed seeding of individual living cells. Tissue Eng 11(11-12):1658-66.

Nelson CM, Bissell MJ. 2006. Of extracellular matrix, scaffolds, and signaling: tissue architecture regulates development, homeostasis, and cancer. Annu Rev Cell Dev Biol 22:287-309.

Pang WW, Hartmann PE. 2007. Initiation of human lactation: secretory differentiation and secretory activation. J Mammary Gland Biol Neoplasia 12(4):211-21.

Park TH, Shuler ML. 2003. Integration of cell culture and microfabrication technology. Biotechnol Prog 19(2):243-53.

Parzel CA, Pepper ME, Burg T, Groff R, Burg KJL. 2009. EDTA enhances high-throughput two-dimensional bioprinting by inhibiting salt scaling and cell aggregation at the nozzle surface. Journal of Tissue Engineering and Regenerative Medicine 3:260-268.

Patrick CW, Jr. 2000. Adipose tissue engineering: the future of breast and soft tissue reconstruction following tumor resection. Semin Surg Oncol 19(3):302-11.

Phillippi JA, Miller E, Weiss L, Huard J, Waggoner A, Campbell P. 2008. Microenvironments engineered by inkjet bioprinting spatially direct adult stem cells toward muscle- and bone-like subpopulations. Stem Cells 26(1):127-34.

Polyak K. 2007. Breast cancer: Origins and evolution. The Journal of Clinical Investigation 117(11):3155-3163.

Polyak K, Hu M. 2005. Do myoepithelial cells hold the key for breast tumor progression? J Mammary Gland Biol Neoplasia 10(3):231-47.

Potten CaW, J. 2004. Apoptosis - The Life and Death of Cells. New York, NY: Cambridge University Press.

Puleo CM, Yeh HC, Wang TH. 2007. Applications of MEMS technologies in tissue engineering. Tissue Eng 13(12):2839-54.

Ratner BD, Hoffman AS, Schoen FJ, Lemons JE. 1996. An Introduction to Materials in Medicine. San Diego, CA: Academic Press.

Robinson GW, Karpf AB, Kratochwil K. 1999. Regulation of mammary gland development by tissue interaction. J Mammary Gland Biol Neoplasia 4(1):9-19.

Ronnov-Jessen L, Petersen OW, Bissell MJ. 1996. Cellular changes involved in conversion of normal to malignant breast: importance of the stromal reaction. Physiol Rev 76(1):69-125.

Roth EA, Xu T, Das M, Gregory C, Hickman JJ, Boland T. 2004. Inkjet printing for high-throughput cell patterning. Biomaterials 25(17):3707-15.

Russo J, Hu YF, Silva ID, Russo IH. 2001a. Cancer risk related to mammary gland structure and development. Microsc Res Tech 52(2):204-23.

Russo J, Lynch H, Russo IH. 2001b. Mammary gland architecture as a determining factor in the susceptibility of the human breast to cancer. Breast J 7(5):278-91.

Sahoo SK, Panda AK, Labhasetwar V. 2005. Characterization of porous PLGA/PLA microparticles as a scaffold for three dimensional growth of breast cancer cells. Biomacromolecules 6(2):1132-9.

Sanjana NE, Fuller SB. 2004. A fast flexible ink-jet printing method for patterning dissociated neurons in culture. J Neurosci Methods 136(2):151-63.

Saunders RE, Gough JE, Derby B. 2008. Delivery of human fibroblast cells by piezoelectric drop-on-demand inkjet printing. Biomaterials 29(2):193-203.

Schedin P, O'Brien J, Rudolph M, Stein T, Borges V. 2007. Microenvironment of the involuting mammary gland mediates mammary cancer progression. J Mammary Gland Biol Neoplasia 12(1):71-82.

Schmeichel KL, Bissell MJ. 2003. Modeling tissue-specific signaling and organ function in three dimensions. J Cell Sci 116(Pt 12):2377-88.

Sodunke TR, Turner KK, Caldwell SA, McBride KW, Reginato MJ, Noh HM. 2007. Micropatterns of Matrigel for three-dimensional epithelial cultures. Biomaterials 28(27):4006-16.

Sternlicht MD, Kouros-Mehr H, Lu P, Werb Z. 2006. Hormonal and local control of mammary branching morphogenesis. Differentiation 74(7):365-81.

Sun W, Darling A, Starly B, Nam J. 2004. Computer-aided tissue engineering: overview, scope and challenges. Biotechnol Appl Biochem 39(Pt 1):29-47.

Tong Q, Hotamisligil GS. 2007. Developmental biology: cell fate in the mammary gland. Nature 445(7129):724-6.

Varghese D, Deshpande M, Xu T, Kesari P, Ohri S, Boland T. 2005. Advances in tissue engineering: cell printing. J Thorac Cardiovasc Surg 129(2):470-2.

Walker RA, Martin CV. 2007. The aged breast. J Pathol 211(2):232-40.

Weaver VM, Howlett AR, Langton-Webster B, Petersen OW, Bissell MJ. 1995. The development of a functionally relevant cell culture model of progressive human breast cancer. Semin Cancer Biol 6(3):175-84.

Wicha MS, Lowrie G, Kohn E, Bagavandoss P, Mahn T. 1982. Extracellular matrix promotes mammary epithelial growth and differentiation *in vitro*. Proc Natl Acad Sci U S A 79(10):3213-7.

Wilson WC, Jr., Boland T. 2003. Cell and organ printing 1: protein and cell printers. Anat Rec A Discov Mol Cell Evol Biol 272(2):491-6.

Xu T, Jin J, Gregory C, Hickman JJ, Boland T. Inkjet Printing of Viable Mammalian Cells. Biomaterials, 2005, 26(1):93-99.

Xu T, Gregory CA, Molnar P, Cui X, Jalota S, Bhaduri SB, Boland T. 2006. Viability and electrophysiology of neural cell structures generated by the inkjet printing method. Biomaterials 27(19):3580-8.

Xu T, Rohozinski J, Zhao W, Moorefield EC, Atala A, Yoo JJ. 2009. Inkjet-mediated gene transfection into living cells combined with targeted delivery. Tissue Eng Part A 15(1):95-101.

Yamada KM, Cukierman E. 2007. Modeling tissue morphogenesis and cancer in 3D. Cell 130(4):601-10.

Yang J, Richards J, Bowman P, Guzman R, Enami J, McCormick K, Hamamoto S, Pitelka D, Nandi S. 1979. Sustained growth and three-dimensional organization of primary mammary tumor epithelial cells embedded in collagen gels. Proc Natl Acad Sci U S A 76(7):3401-5.

Yu J, Li G, Li J, Wang Y. 2005. The pattern of lymphatic metastasis of breast cancer and its influence on the delineation of radiation fields. Int J Radiat Oncol Biol Phys 61(3):874-8.

Zhang X, Wang W, Xie Y, Zhang Y, Wang X, Guo X, Ma X. 2006. Proliferation, viability, and metabolism of human tumor and normal cells cultured in microcapsule. Appl Biochem Biotechnol 134(1):61-76.

Zhang X, Wang W, Yu W, Xie Y, Zhang X, Zhang Y, Ma X. 2005. Development of an *in vitro* multicellular tumor spheroid model using microencapsulation and its application in anticancer drug screening and testing. Biotechnol Prog 21(4):1289-96.

Zhang C, Wen X, Vyavahare NR, Boland T. 2008. Synthesis and characterization of biodegradable elastomeric polyurethane scaffolds fabricated by the inkjet technique. Biomaterials 29(28):3781-91.

CHAPTER 2

Select results in this chapter were generated by an Institute for Biological Interfaces of Engineering interdisciplinary team, including Clemson University doctoral student Matthew Pepper, and were presented at the 2008 Hilton Head Conference on Regenerative Medicine (Parzel et al., 2008) and the 2009 Annual Meeting and Exposition of the Society For Biomaterials (Parzel et al., 2009a).

ESTABLISHMENT OF PROJECT FEASIBILITY

Modification of Printing Parameters to Establish Optimal Model Conditions

The following studies were performed to establish the utility of inkjet technology to build *in vitro* test systems. Printing parameters such as stage height and rate of nozzle firing were manipulated to aid in the development of bioprinting protocols for a variety of bio-ink solutions. Furthermore, preliminary patterning experiments were conducted to determine if the bioprinter hardware and software could pattern cells consistently and reliably and, if not, what changes need to be made to prevent technical limitations.

Stage Height

Materials and Methods

To understand the effect of stage height on viability of normal mammalian cells, D1 murine mesenchymal stem cells (American Type Culture Collection (ATCC), Manassas, VA) were printed at various heights using a modified HP 540 (Hewlett Packard, Palo Alto, CA) series thermal inkjet printer shown in **Figure 2.1**. The hypothesis was that cell viability would decrease as distance increased, due to increased cell velocity with travel from the nozzle to the print surface.

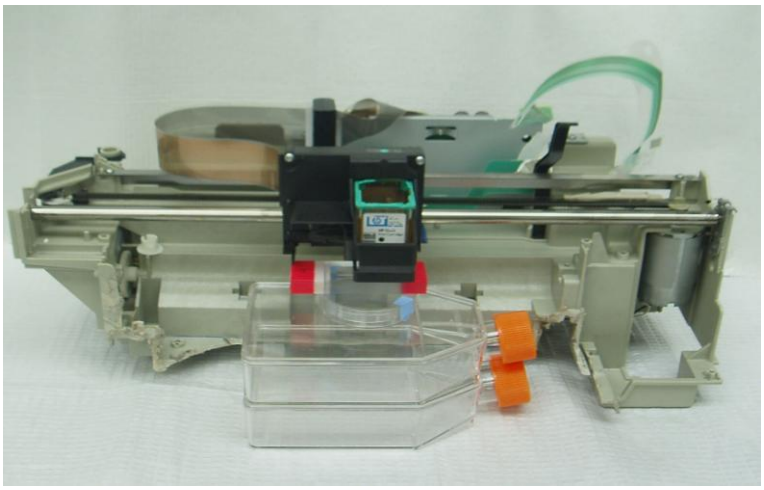

Figure 2.1: Modified HP 500 Series thermal inkjet printer and stage configuration

The printing height was easily altered using glass microscope slides (VWR, West Chester, PA) taped into stacks, as depicted in **Figure 2.2**, which also illustrates the corresponding distance to the printhead in millimeters. Polystyrene culture slides (Nalge Nunc International, Rochester , NY) were used as the ultimate printing surfaces, and they were pre-wetted with a solution of fetal bovine serum (FBS) (Mediatech, Inc., Manassas, VA) and Dulbecco's Modified Eagle's Medium (DMEM) (ATCC) (1:1) for 1 hour in a 75mm sterile plastic petri dish (VWR). D1 cells (ATCC) were selected for assessment of viability. Using aseptic cell culture techniques, D1 cells were suspended into serum-free culture medium at a concentration of $1x10^6$ cells/mL. A 250µL volume of the cell suspension was loaded into an ink cartridge well, which had been cleaned using 100% ethanol (Pharmco-Aaper, Shelbyville, KY), and subsequently rinsed with sterile distilled water, using volumes that filled the entire cartridge. Distilled water was also printed from the cartridge to ensure rinsing. A solid circular pattern with a diameter of 0.15

inches was created in an MS Word document (Microsoft® Office Word 2003, Microsoft Corporation, Redmond, WA), and 10 passes of the printer were used to create the pattern in triplicate. Cells were incubated for 30 minutes to facilitate attachment, after which 20mL of culture medium was added to each dish containing a slide. Controls were also prepared on the polystyrene slides by manually seeding (i.e. pipetting) $5x10^5$ cells onto the slide surface. The controls were implemented to ensure that the slides provide a favorable growing surface for the D1 cells; excessive necrosis of printed cells could then be likely attributed to the printing process.

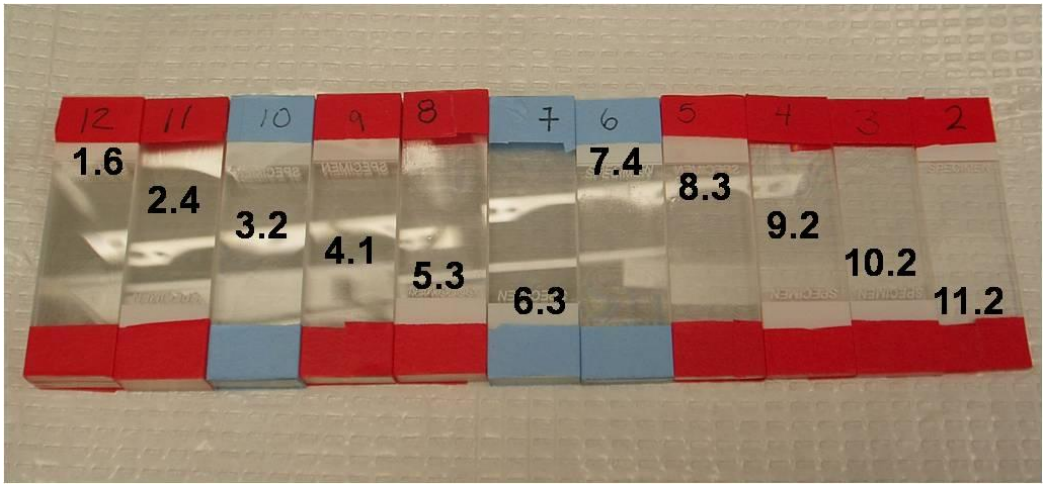

Figure 2.2: Glass slides stacked to achieve printing height differentials. Final distance from the surface of each set of stacked slides to the printhead is listed in millimeters.

D1 cells were assessed for viability using a LIVE-DEAD® viability kit (Invitrogen, Carlsbad, CA) at 24 hours and 7 days post printing (post seeding for control slides). A solution was prepared by adding 20µL of 2mM EthD-1 stock reagent

(fluoresces red in the presence of necrotic cells) and 5µL of 4mM calcein AM stock reagent (fluoresces green in the presence of live cells) to 10mL of phosphate buffered saline (PBS) (Sigma-Aldrich, St. Louis, MO) and vortexing. Cells were covered with the LIVE/DEAD® solution and incubated for 45 minutes, protected from light. Samples were viewed under an Axiovert 135 fluorescent microscope (Zeiss, Germany) using a fluorescein optical filter for calcein detection (485 +/- 10nm) and a rhodamine optical filter (530 +/- 12.5nm) for EthD-1 detection. Images were captured using a ProgRes™ C10^{Plus} digital camera (Chori Imaging Corporation, Yokohama, Japan). Qualitative assessments were made regarding the effect of printer height on the viability of cells.

Results and Discussion

A negligible number of necrotic cells was present in all of the printed cell cultures at 24 hours, as seen in **Figure 2.3,** following incubation with the LIVE/DEAD® solution. The control samples did show that the polystyrene slide provided a favorable growing surface for the D1 cells. Since the greater distance of 11.2mm is far beyond the distance at which a discernible pattern would likely print, the stage height does not appear to be of concern when considering cell viability in future experiments. To understand the effect of stage height on quantitative variations of cell viability, cells should be printed at the aforementioned distances onto a variety of surfaces (e.g. wet, dry, collagen coated) and evaluated using a dye exclusion test since the LIVE/DEAD® assay does not account for dead cells suspended in the reagent medium.

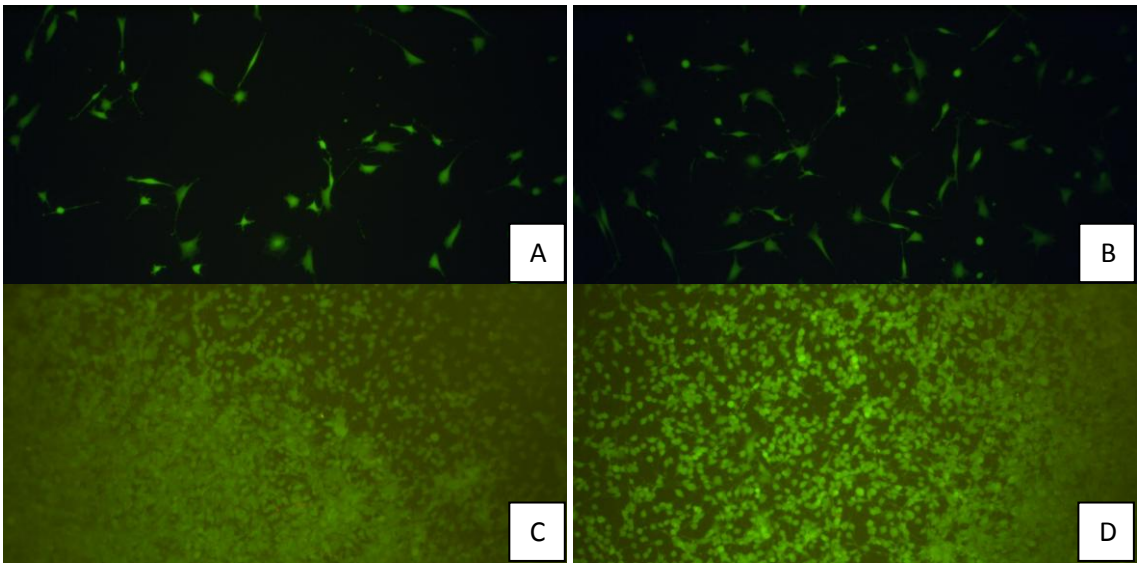

Figure 2.3: D1 cells printed from a modified HP 500 series thermal inkjet printer. A) D1 cells printed from a height of 1.6mm and incubated for 24 hours. B) D1 cells printed from a height of 11.2mm and incubated for 24 hours. C) D1 cells printed from a height of 1.6mm and incubated for 7 days. D) D1 cells printed from a height of 11.2mm and incubated for 7 days. All images were captured using a 10x objective.

Rate of Nozzle Firing

Materials and Methods

The waveform that "fires" an HP26 cartridge, i.e., produces a droplet, will quickly heat the resistor in a nozzle chamber and cause formation and the ejection of a drop of ink. The parameters of this waveform shown in **Figure** were examined in order to optimize the electronics that create the firing pulse. The amplitude is found from literature reviews (Harmon & Widder, 1988); however, the role of the period and pulse width in ejecting a droplet of biomaterial must be determined.

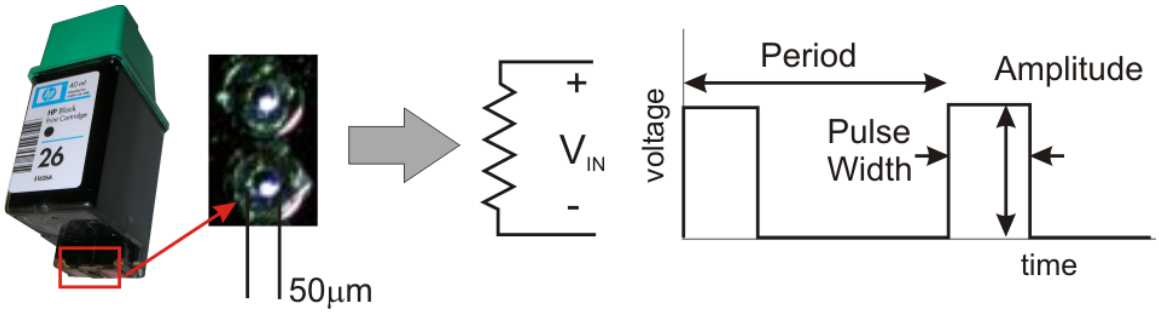

Figure 2.4: Cartridge with magnified nozzle orifice and electrical model with firing waveform.

In the first experiment, the cartridge was loaded with suspended D1 cells at a concentration of $7.7x10^6$ cells/mL in a 1:1 solution of Hanks Balanced Salt Solution (HBSS) (Sigma) and serum free-DMEM (ATCC); ethylenediaminetetraacetic acid (EDTA) (0.53mM) was added to reduce clogging (Parzel *et al.*, 2009b). An initial firing frequency of 1000Hz (period=1ms) with a 2µs pulse width was used until the cartridge stopped producing drops; the frequency was then reduced until printing commenced. A series of 30,000 drops was printed in the first 30 seconds and the results evaluated. Printing continued for 30 second intervals and the results were evaluated at the cumulative printing times of 1, 1.5, 2, and 2.5 minutes.

The following scale was created to evaluate the printed drops:

- 1 = good
- 0.5 = printed with satellites around main drop
- 0 = not all drops printed

Two evaluators (not blinded) rated drops macroscopically, whereby a "good" rating was standardized based on the macroscopic appearance of ink printed from an unclogged nozzle.

In the second experiment, glycerol (99.6%, Acros Organics, Fair Lawn, NJ) was printed in varying viscosities. Solutions were prepared by diluting glycerol in distilled water to concentrations ranging from 50%-75% volume ratio of glycerol in water. The frequency (1/period) was increased to determine the maximum firing frequency at which each of these concentrations would print. Note that 1000 drops/s was the frequency limit at which the system could generate firing pulses.

Results and Discussion

The cartridge stopped producing drops after 2 minutes and did not recover at 2.5 minutes. The frequency was reduced to 33Hz and printing resumed. A series of 990 drops were printed and the results evaluated using the same scale; results were collected at the cumulative printing times 3, 3.5, 4, 4.5, and 5 minutes and are plotted in **Figure 2.5**.

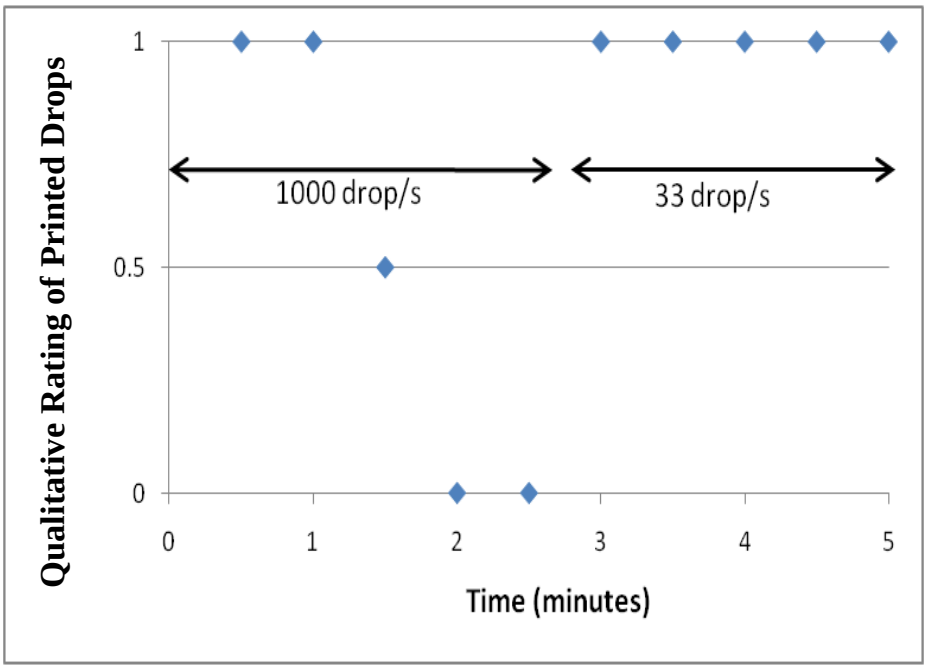

Figure 2.5: Increasing pulse frequency (reducing the period) can significantly affect the quality of printed drops. This graph represents data for one trial.

The results in **Figure 2.6** show a dramatic decrease in maximum firing frequency at 72% volume ratio of glycerol in water and that it is not possible to print at viscosities higher than 72% volume ratio of glycerol in water.

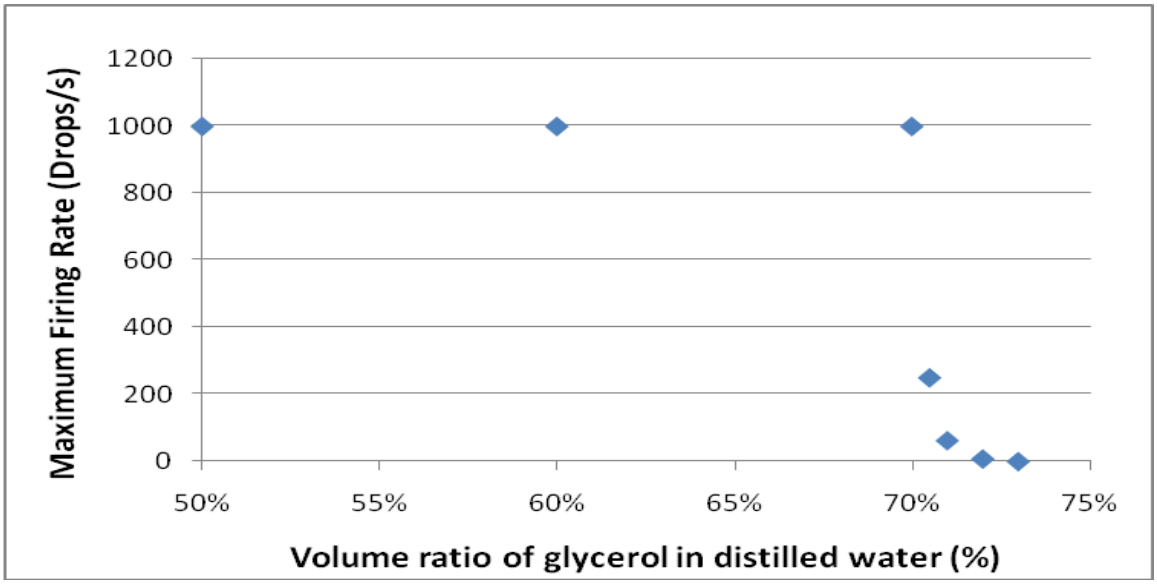

Figure 2.6: Glycerol Printing. Plot of the maximum firing rate as the viscosity of the glycerol water mixture is changed. One sample per concentration was tested.

The data indicate that the nozzle firing frequency (1/period) must be matched to viscosity. If the firing frequency is too high relative to the viscosity, drop production will cease.

Preliminary Cell Patterning

Materials and Methods

D1 cells were used to assess the capability of the printer to print high resolution single-cell patterns. Cells were suspended at 2×10^6 cells/mL in serum-free cell culture medium (DMEM, ATCC) and printed into dot or line patterns using a single, specified nozzle of the cartridge. This assessment was conducted to gain a general understanding of how well the printer could pattern cells at the single nozzle level and, qualitatively,

how many cells one could expect to be ejected within each dot of the pattern. Quantitative cell counts were attempted, but nozzle clogging due to presumed salt crystallization at the nozzle surfaces prevented the collection of this data.

High resolution dual cell patterning was achieved using D1 and 4T07 (murine non-metastatic mammary tumor) (ATCC) cells pre-labeled with green (Excitation 450 nm, Emission 517 nm) and red (Excitation 550 nm, Emission 602 nm) fluorescent CellTracker™ probes (Invitrogen), respectively. The CellTracker™ green stock solution was prepared by adding 10.76 µL dimethyl sulfoxide (DMSO) (Sigma) to the lyophilized product and diluted in 10 mL of SF-DMEM. The CellTracker™ red working solution was prepared by adding 7.29 µL DMSO to the lyophilized product and then subsequently diluting the solution with 10 mL SF-DMEM. Cells grown to confluence in a T-75 tissue culture flask (Corning Inc., Corning, NY) were washed with 1x DPBS and incubated for 45 minutes in their respective fluorescent tag solutions.

Two HP26 cartridge wells were filled with D1 and 4T07 cell suspensions at a concentration of 7.7×10^6 cells/mL in a serum-free culture medium. Alternating lines of cells were printed onto a polystyrene slide surface that was pre-soaked in a 1:1 solution of fetal bovine serum (FBS) to DMEM. Since each carriage assembly supports two cartridges, D1 and 4T07 cells could be printed simultaneously.

Results and Discussion

Figure 2.7 shows images of D1 cells printed in line patterns on the surface of a glass slide. Based on the images, it will be important to keep cells homogeneously

suspended in culture so that a more consistent number of cells will be deposited in each drop. When individual drops were printed (**Figure 2.7D**), one drop contained 6 cells while adjacent drops contained zero cells. Additionally, it will be necessary to understand the relationship between the number of cells in suspension and the average number of cells printed in each drop.

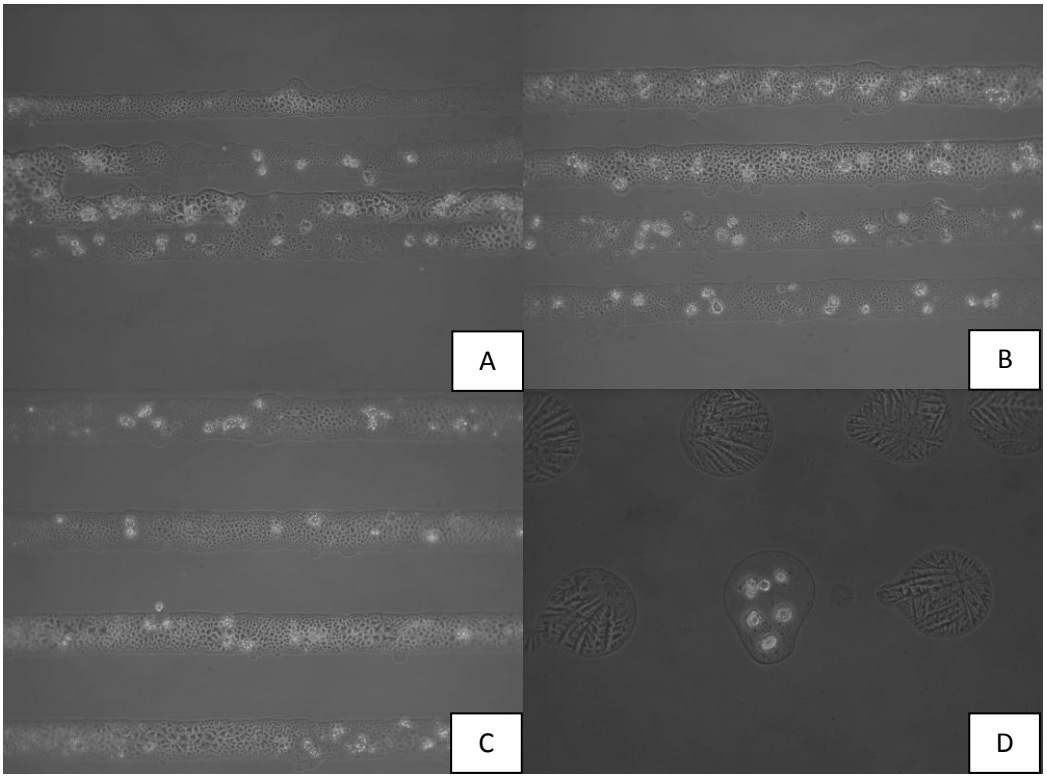

Figure 2.7: D1 cells suspended at 2×10^6 cells/mL and printed in line patterns onto a glass slide surface. A) Lines separated by 150µm. B) 200µm C) 300µm D) Some drops did not contain any cells while other drops had multiple cells. Figures A-C were captured using a 10x objective and a 20x objective was used to capture Figure D.

Figure 2.8 includes an image of the intended pattern along with the image of the actual cells on a polystyrene surface, captured immediately after printing.

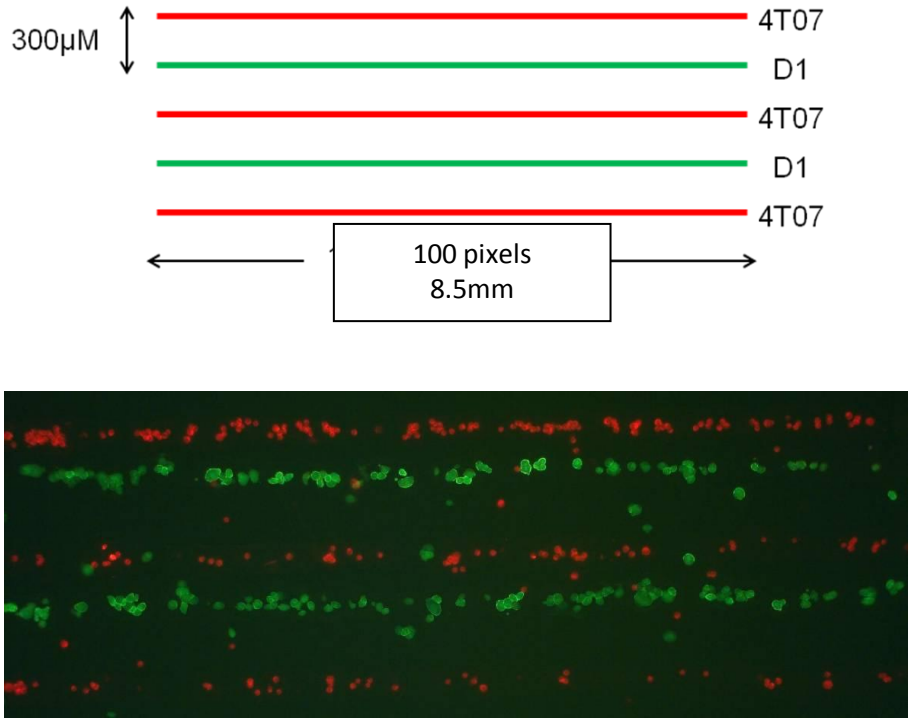

Figure 2.8: Top- Schematic showing alternating lines of 4T07 and D1 cells, depicting the intended pattern that was to be printed on a polystyrene slide surface. Bottom- actual 4T07 and D1 cells printed on a slide. Image was captured immediately after printing, using a 10x objective.

Based on the results, it will be necessary to develop a calibration system to ensure that cartridge offsets do not affect the quality of printing. Additionally, to improve current protocols, new methods of unclogging cartridge nozzles (or preventing clogging) will be investigated.

Statistics of Cell Placement

Materials and Methods

Accurate spacing of cells or cell clusters is important for developing advanced co-culture models. In the following experiment, two different patterns were used. In order to ensure that cells were deposited in their intended locations, cells were printed in these specified patterns, and the accuracy of the resulting cell locations versus their intended location was measured using a mask (**Figure 2.9**). Transparent masks that outlined the intended dimensions of Patterns A and B were created using GNU Image Manipulation Program (GIMP), and they were manually aligned to the printed cell pattern images using GIMP (**Figure 2.10**). Samples that maintained pattern definition following application of 200µL of culture medium were photographed.

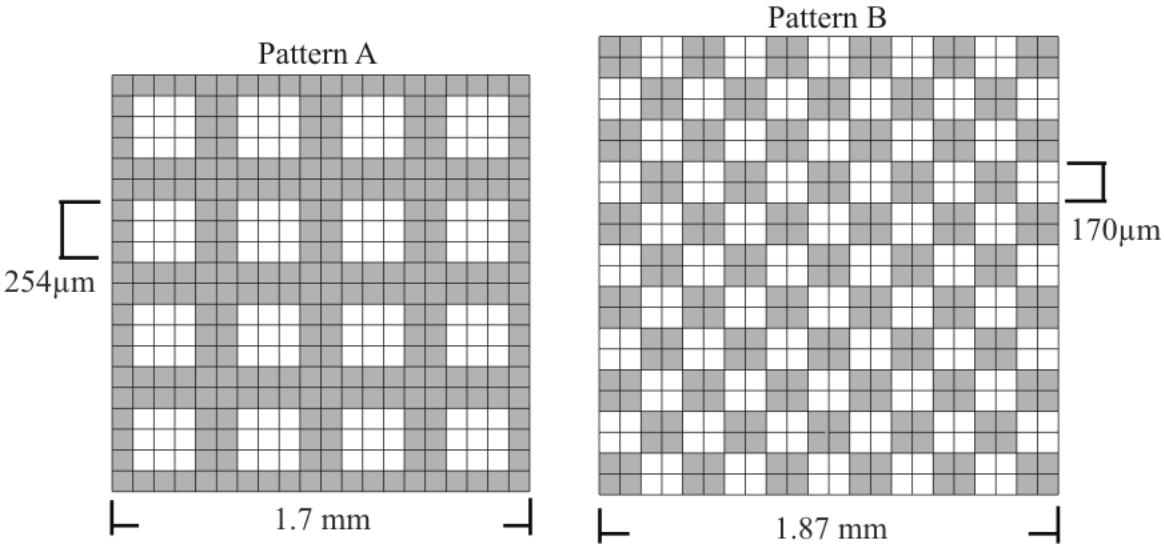

Figure 2.9: Pattern A (left) is 20 x 20 pixels square. Pattern B (right) is 22 x 22 pixels square. The D1 cells (labeled green) were correctly placed if they were located within a gray gridded area. The 4T07 cells (labeled red) were correctly placed if they were

located within a white gridded area. All cells located outside of the gridded mask were counted as incorrectly placed.

D1 murine mesenchymal stem cells were cultured according to the manufacturer's suggested protocol. Briefly, cells were maintained in DMEM containing 4 mM L-glutamine, 1.5 g/L sodium bicarbonate, and 4.5 g/L glucose (ATCC), and every 500 mL was supplemented with 50 mL FBS, 5 mL antibiotic/antimycotic (Invitrogen), and 1mL fungizone (Invitrogen). The culture medium was replaced every 48-72 hours as required, and cells were stored in an incubator (Sanyo Scientific, San Diego, CA) at 37ºC and 5% CO_2. Cells from a non-metastatic murine mammary cancer cell line, 4T07, were maintained in the culture conditions described above for D1 cells.

To prepare cell-based bio-inks for printing, D1 and 4T07 cells were suspended in serum-free DMEM (SF-DMEM) at a density two times the desired final concentration. All cell suspensions were filtered using a 40-µm sterile cell strainer (BD Falcon, Franklin Lakes, NJ). Just prior to printing, 75 µL of the cell suspension were combined with 75 µL of HBSS containing 1.06mM EDTA, and was subsequently deposited into the HP26 cartridge well (Parzel *et al.,* 2009). Thus, the resulting 150µL of bio-ink consisted of D1 or 4T07 cells suspended in 50% SF-DMEM and 50% HBSS, with a final EDTA concentration of 0.53 mM.

Cell Vu (Millennium Sciences Inc., NY, NY) gridded coverslips were coated with collagen using a modified method and aseptic techniques (Vernon *et al.,* 2005). These substrates were used as surfaces for all cell patterning studies. A 2.0 mg/mL collagen solution was prepared by combining 1.5mL collagen stock solution (3.0mg/mL -

PureCol™) (Advanced Biomatrix, San Diego, CA) with 167 µL 10x Dulbecco's phosphate buffered saline (DPBS) (Sigma), 225 µL FBS, and 358 µL DMEM; a small volume (approximately 20 µL) of 1N NaOH (Fisher Scientific, Pittsburgh, PA) was added to neutralize the solution. A 200 µL volume of solution was pipetted into each of 40 silicone rings (1/2" inner diameter) (McMaster-Carr, Atlanta, GA), where each ring was attached to a coverslip (Hausser Scientific, Horsham, PA). Collagen gels were polymerized in an incubator at 37 ºC and 5% CO_2 for at least 4 hours. The gels were then placed into a laminar flow hood (Labconco, Kansas City, MO) and allowed to dry and attach. Once dry, gel coatings were rinsed in sterile distilled water until clear and then allowed to dry in the hood. After drying, the collagen coatings were soaked overnight in a 1:1 solution of DMEM to FBS. Excess culture medium was aspirated prior to printing, and the collagen coatings were allowed to partially dry in a laminar flow hood for three minutes.

In order to differentiate between cell types in a printed pattern, D1 and 4T07 cells were labeled (methods described above) prior to printing, using green and red CellTracker™ probes, respectively.

Following incubation, D1 and 4T07 cells were suspended in SF-DMEM at an initial concentration of 1.5×10^7 cells/mL and subsequently combined with HBSS containing EDTA, as described above. The final cell solutions were comprised of 50% SF-DMEM and 50% HBSS, containing 7.7×10^6 cells/mL and 0.53 mM EDTA. To print cells in co-culture, D1 cells were pipetted into a well of the first HP26 cartridge, after which 4T07 cells were pipetted into the next cartridge well. A cartridge alignment

method was used in cooperation with a vision station (Meiji Techno America, Santa Clara, CA) to ensure pattern alignment between the two cartridges. To complete this process, a cartridge deposits one drop at a location on the stage. The stage is then moved a predetermined distance, such that the drop resides underneath the microscope, close to the camera center. An image is taken with the vision system, and the offset from the center of the drop to the camera center is determined. Before pattern creation, each nozzle was flushed (fired 100 times) in order to clear any clumps of cells that may have settled in the nozzles. The pattern was printed and the cells were placed in an incubator for 60 minutes to promote attachment.

Cells in solution will aggregate and settle over time. Cell settling is believed to be a major cause of inaccurate cell placement during printing; thus, a new pair of cartridges was inserted, filled, and recalibrated every 30 minutes in order to maintain consistent printing conditions. Twenty (20) samples were created for each of the two test patterns, 40 in total. After incubation, all samples that maintained pattern definition after being covered with 10% serum-inclusive DMEM were photographed using a Zeiss Axiovert 40 CFL microscope (Carl Zeiss Microimaging, Inc., Thornwood, NY) equipped with a 50 W Xenon lamp. The images were captured using a Zeiss AxioCam MRC 5, processed with Zeiss AxioVision LE 4.6 (Carl Zeiss Microimaging, Inc.), and merged using GNU Image Manipulation Program (GIMP).

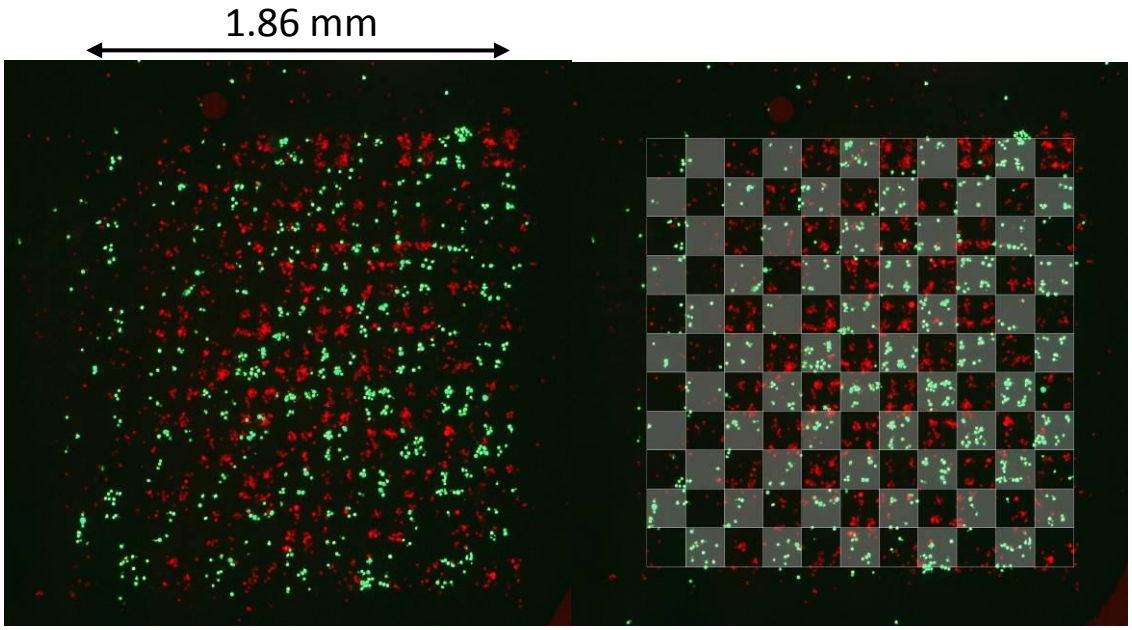

Figure 2.10: Pattern B trial 1– sample immediately after adding medium (left) and the same image masked for counting (right). Note that most incorrectly placed cells are the result of overflow from an adjacent square. 2.5x objective.

Results and Discussion

Under the microscope, samples showed good pattern definition immediately after printing following a qualitative assessment of intended cell location. After allowing time for the cells to attach to the substrate, the printed samples must be covered with medium to prepare them for incubation. The application of medium frequently disrupted the pattern and dislodged cells from the hydrated collagen substrate, rendering 80% of the 40 samples unusable. The collagen substrate used in the current experiment was associated with even lower yield from patterns printed directly onto polystyrene slides. In successful samples, the collagen enabled the cells to attach in one hour to survive the incubation preparation process. Promoting quick attachment is a key step to achieving

co-culture samples (**Figure 2.11**), since unattached cells will float away from their intended locations, disrupting sample preparation.

Of the remaining samples, 76% of all cells were placed correctly (**Table 2.1**). The addition of medium still affected the successful trials and in cases such as Trial 3 of Pattern B (**Figure 2.12**), the percentage of incorrectly located cells increased from 19.06% to 28.06%. Before the addition of medium, the sample had a total of 1751 4T07 cells, but only 951 after medium addition, a loss of 46%. Cell attachment is modulus dependent, where low modulus substrates often do not provide the appropriate rigidity for anchorage dependent cells (Ingber, 1998); hence, the 2.0 mg/mL composition of the collagen substrate may be insufficient to capture and maintain patterns reliably. The percent average placement error (± standard deviation) for all trials of pattern A and B was 19.71(±6.1)% and 26.94(±4)%, respectively (**Table 2.1**). Consistent error among trials shows the calibration algorithm worked as expected. Trial 5 of Pattern A maintained the highest level of pattern definition after medium deposition, with the lowest error of 13.31% (**Figure 2.13**).

Table 2.1: Percentage of incorrectly placed cells. Statistics showing the accuracy and precision of the system when producing the two experiment patterns, A and B.

	D1 (%)	4T07 (%)	Total (%)	# of Incorrectly Placed Cells	# of Cells in Sample
Pattern A					
Trial 1	16.94	33.74	20.48	475	2319
Trial 2	13.08	20.79	17.23	203	1178
Trial 3	17.63	36.96	27.8	456	1640
Trial 4	29.6	38.09	33.96	630	1855
Trial 5	11.86	14.66	13.31	179	1345
Pattern B					
Trial 1	20.15	23.53	22.46	479	2133
Trial 2	19.72	35.67	30.29	587	1938
Trial 3	17.97	34.31	28.06	433	1543

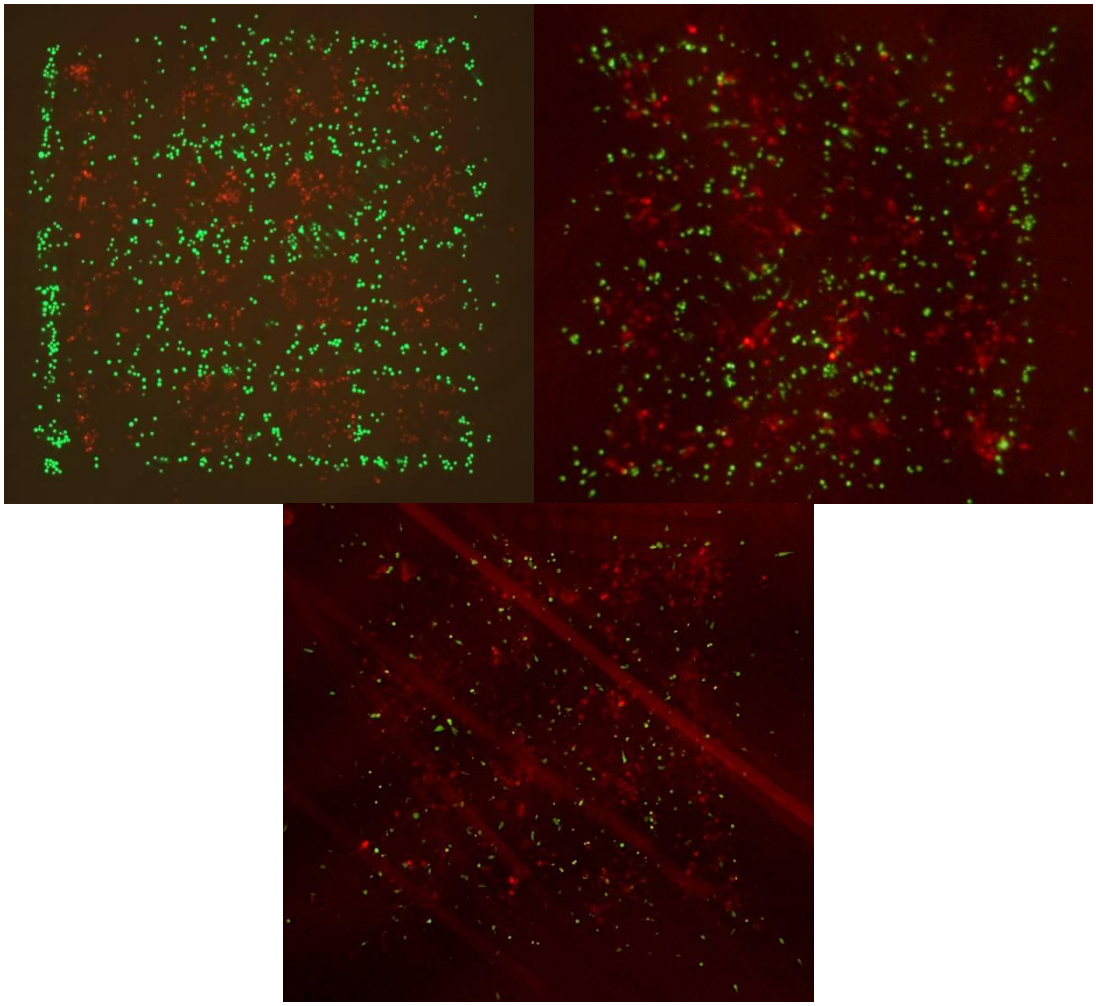

Figure 2.11: Time points 0 hrs (top left), 28 hrs (top right), and 66 hrs (bottom) of trial 4. The three time points show the migration of the cells, an indication of health after printing. Images were captured using a 2.5x objective. Note that fluorescent probes may have been fading following 66 hrs in culture.

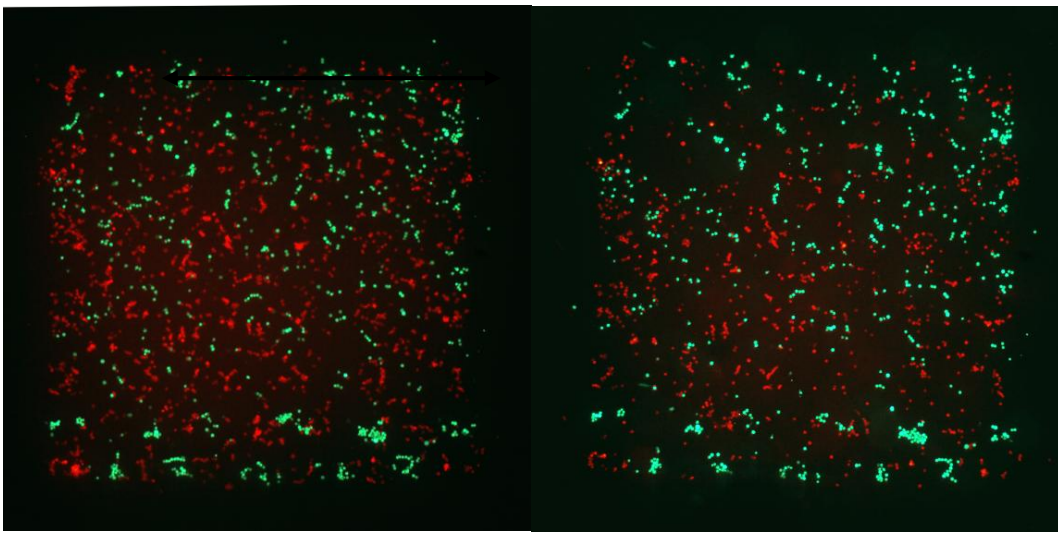

Figure 2.12: Pattern B trial 3 – sample immediately after printing (left), and immediately after being covered with medium for long term incubation (right). Though the D1 cells (green) remained intact after medium application, the population of 4T07 cells (red) was clearly diminished. Images were captured using a 2.5x objective.

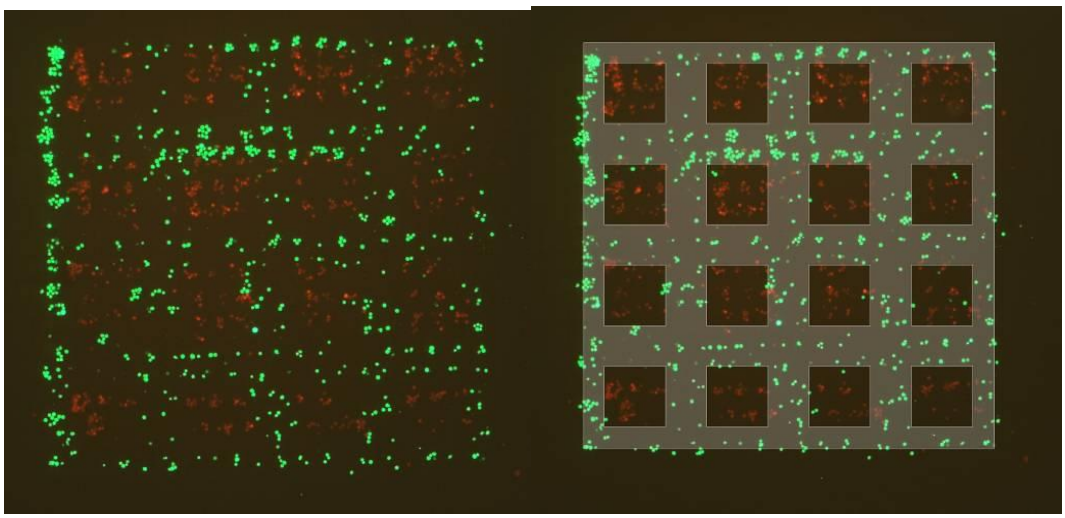

Figure 2.13: Pattern A trial 5 – original photo (left) and masked photo, used for counting (right). Images were captured using a 2.5x objective.

The increase in placement error between pattern A and B can be explained by the distribution of the drop location and drop diameter. On glass slides, drops of medium with cells can range from 200 to 250 µm in diameter. Likely, the drops do not spread as wide in the collagen substrate, but patterning cells 85 µm apart yields overlap between neighboring drops. While analyzing the patterns with the mask, it was apparent that most incorrectly located cells were located on the outer edges of correctly placed drops. Successfully cultured samples showed cells spreading, filling the gaps between their neighbors by 28 hrs (see **Figure 2.11**). Though the fluorescent dye was fading, the 66 hr time point image showed the pattern was completely destroyed; this loss of definition implies that the cells migrated from their printed location. The doubling time of each cell type likely also affected pattern definition since 4T07 cells are tumorigenic and proliferate more quickly in 2D culture.

The low ratio of successful trials was not a failure of the system to perform, but of the properties of the substrate and the liquid environment. New protocols are being researched to promote cell attachment and to hydrate cells without disturbing their location. It is anticipated that the new protocols will significantly decrease the number of unsuccessful trials due to weak cell attachment and moderately decrease the overall placement error. Optimal placement error (defined as $\geq$ 90%) would take into account cell death via the printing process, which was shown to be 8% in a previous study (Xu *et al.*, 2005), and is anticipated to be 5-10% depending on the size of the cell in suspension.

Increased sample output and better cell adhesion will continue to improve the ability to precisely pattern two or more cell types in 2D and improve studies investigating

cell migration, differentiation, and communication. The cell placement experiments demonstrate that this biofabrication system has sufficient capability to enable development of biological models that better mimic heterogeneity of natural tissue. Experiments with planar systems will provide useful data for addressing the ultimate goal of building a three-dimensional tissue fabrication system.

References

Harmon JP, Widder JA. 1988. Integrating the printhead into the HP DeskJet printer. Hewlett-Packard Journal: Technical Information from the Laboratories of Hewlett-Packard Company 39(5):62-66.

Ingber D. 1998. Cellular Basis of Mechanotransduction. Biol Bull 194(3):323-327.

Parzel CA, Hungerford B, Burg KJL. 2008. Evaluation of inkjet printing parameters on cell function. 12th Annual Engineered Tissues Workshop, Hilton Head, SC.

Parzel C, Burg T, Groff R, Pepper M, Boland T, Burg KJL. 2009a. Observations on inkjet cartridge parameters for biomaterial deposition. Trans 2009 Annual Meeting Exp Soc Biomater, San Antonio, TX.

Parzel CA, Pepper ME, Burg T, Groff R, Burg KJL. 2009b. EDTA enhances high-throughput two-dimensional bioprinting by inhibiting salt scaling and cell aggregation at the nozzle surface. Journal of Tissue Engineering and Regenerative Medicine 3:260-268.

Vernon RB, Gooden MD, Lara SL, Wright TN. 2005. Microgrooved fibrillar collagen membranes as scaffolds for cell support and alignment. Biomaterials 26(16):3131-40.

Xu T, Jin J, Gregory C, Hickman JJ, Boland T. Inkjet Printing of Viable Mammalian Cells. Biomaterials, 2005, 26(1):93-99.

CHAPTER 3

Select results in this chapter were generated by an Institute for Biological Interfaces of Engineering interdisciplinary team, including Clemson University doctoral student Matthew Pepper, and were published in the Journal of Tissue Engineering and Regenerative Medicine (Parzel et al., 2009a).

EDTA ENHANCES HIGH-THROUGHPUT TWO-DIMENSIONAL BIOPRINTING BY INHIBITING SALT SCALING AND CELL AGGREGATION AT THE NOZZLE SURFACE

Introduction

Drop-on-demand inkjet printing systems are capable of patterning a variety of cell types (e.g. primary rat hippocampal and cortical neurons, Chinese hamster ovary (CHO) cells and bovine endothelial cells) (Nakamura *et al.*, 2005; Xu *et al.*, 2005; Xu *et al.*, 2006) and biomaterials (e.g. collage and alginate) (Boland *et al.*, 2006). Based on these capabilities, inkjet systems have been proposed as microfabrication tools for organ replacement, printing multiple cell types and biomaterials in three dimensional constructs with the geometric precision to produce biological structures including vessels (Boland *et al.*, 2003; Mironov *et al.*, 2003; Wilson *et al.*, 2003).

We have proposed the use of inkjet printing for a different application - the fabrication of *in vitro* tissue test systems (Burg and Boland, 2003; Chaubey et al., 2007; Parzel *et al.*, 2008a,b). For example, the current "gold standard" for tumor modeling involves the suspension of cells within gel-like matrices, mainly matrigel (Kasper *et al.*, 2007; Sasser *et al.*, 2007); though these systems appear to be superior to traditional two-dimensional models, they lack the rigidity necessary to allow normal functioning of anchorage dependent breast cells, specifically adipocytes (Discher *et al.*, 2005; Engler *et al.*, 2004). Tissue engineering strategies may be employed in the development of *in vitro*

tissue models that are more structurally similar and therefore have enhanced potential for use in testing regimens of drug therapies and vaccines. Researchers can also employ these engineered tissue models to study the physical and chemical interactions that occur among cells and extracellular matrix (ECM) components and to better understand the progression of disease processes.

Previous *in vitro* studies have demonstrated the importance of spatial alignment of cells in culture when attempting to accurately mimic the *in vivo* microenvironment, which can include cell-cell and cell-ECM contacts in addition to physical forces and soluble factors (Wang *et al.*, 2007). Because conventional cell seeding methods (i.e. pipetting) do not allow defined cell placement within a culture system, the benefits of controlling spatial location, and therefore microenvironment, cannot be readily achieved. Conversely, microfabrication tools allow the creation of select biomaterial surface variations as well as the precise placement of cellular components (Khetani and Bhatia, 2006). Inkjet-based microfabrication, known as bioprinting, can provide a preliminary foundation for developing such *in vitro* breast tissue models. The reality is that, no matter the intended application, ink-jet printing has many logistical barriers that must be addressed in order to realize the high throughput precision fabrication of complex, 3-D tissues. For example, nozzle clogging and sustainability of printed tissue have been identified as technical limitations of high-throughput inject-based microfabrication (Khademhosseini and Langer, 2007). This chapter addresses the former limitation, and it provides an improvement for the restricted number of drops and cells that can be printed prior to clogging and printhead failure.

To address the nozzle clogging concern, the HP26 cartridge (Hewlett Packard, Palo Alto, CA) and thermal printhead, driven by custom-designed interface electronics that mimic the behavior of the HP500 series consumer inkjet printers, was employed. This thermal inkjet printhead was selected because (i) it has already been proven capable of printing viable cells and biomaterials (Roth *et al.*, 2004), (ii) it permits high throughput microfabrication by providing a large number (50) of appropriately-sized (diameter 50μm) nozzles in a small area, and (iii) is inexpensive and widely available. Before initial application of a new HP26 to printing, the cartridge is opened, the ink is drained, and the cartridge and printhead are cleaned and sterilized. The ink is replaced by a biologically relevant fluid, such as cell culture medium, or dilute hydrogel. These fluids are referred to as "bio-inks."

Inside each nozzle of a thermal inkjet printhead such as the HP26 is a small thin-film resistor. To eject a drop from the nozzle, the resistor is heated with a short, precisely timed pulse of electrical current. The heat causes the adjacent ink to evaporate and form a small bubble and, as this bubble expands, a drop of liquid ink is ejected from the nozzle. As the drop is ejected, the bubble rapidly cools and shrinks, and ink from a reservoir refills the nozzle via capillary action. This process, which occurs in less than 3μs, is illustrated in **Figure 3.1**. The process of applying current to a nozzle's thin film resistor in order to eject a drop is termed "firing" the nozzle. In previous work using the HP26 printhead to print a serum-free cell culture medium, nozzles failed, i.e. the nozzles did not eject a drop when fired, after only a relatively short amount of printing time.

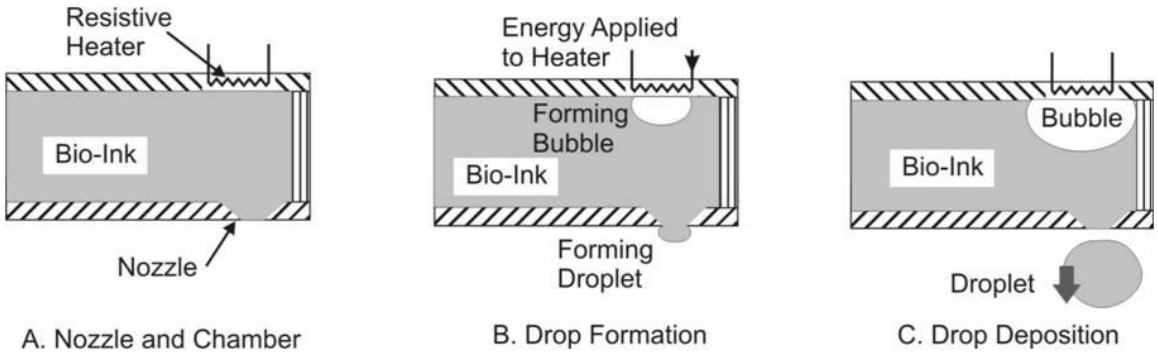

Figure 3.1: Thermal inkjet printer operation. A thin-film resistor heats the liquid print medium, causing a bubble to form. Pressure resulting from bubble formation forces the ejection of an ink drop through the nozzle. (Parzel et al., 2009a)

This failure was generally attributed to clogging by adsorbed proteins (for which reason only serum-free medium is used) and cellular components, in addition to aggregated cells. After failure, the printhead may be sonicated in a bath of warm water, which moderately restores performance of the nozzles.

In order to maintain the clinical relevance for determining cell therapy protocols, *in vitro* cultures generally have a range of at least 10^7-10^9 cells (Enderle *et al.,* 2005). Assuming one cell is ejected per drop and that there are 50 nozzles per printhead, then a nozzle should be able to eject at least one million drops before failure, in order to approach clinical relevance. Experience with printing cell cultures with the HP26 printhead, using either the custom electronics or an HP500 series printer, showed that nozzle failure occurs significantly before that lower limit. Moreover, nozzle failure was observed while printing simple salt solutions, where failure could not be attributed to adsorbed proteins and cellular components. These observations lead to an alternate explanation for nozzle failure; as fluid evaporates during firing, salt is deposited on the

print-head surface, affecting both fluid flow and drop formation, potentially resulting in degraded patterning, erratic cell ejection, or complete nozzle failure.

Materials and Methods

The experimental goals for this work were defined (i) to enable a nozzle to print at least one million cells before failure by incorporating an additive in the bio-ink, to prevent the purported salt deposits inside the printhead and (ii) to provide an improved cleaning method for the cartridge and printhead. In this study, ethylene diamine tetraacetic acid (EDTA) was used as a culture medium additive to prevent both salt scaling and cell aggregation during the bioprinting process. EDTA is a synthetic amino acid that acts as a chelating agent to trap heavy metal and mineral ions. It was hypothesized that this property of EDTA would inhibit ion crystallization, specifically crystallization of those ions which are present in commercially available cell culture media, thus preventing the degradation of printer performance. EDTA was selected for use in this study because of its already widespread use in cell culture as a calcium chelator, which can either enhance the function of trypsin or hinder the joining of cadherins among cells. All studies were performed by printing cells in two dimensions. The potential of these findings includes the construction of high-throughput clinically relevant 2-D cultures and the possible translation of these methods to facilitate creation of 3-D constructs.

EDTA Effectiveness

A procedure that rapidly fires a single nozzle was used to determine the range of concentrations of EDTA (MP Biomedicals, LLC, Solon, OH) in serum-free DMEM (SF-DMEM) that would prevent nozzle failure. A 0.5M stock solution of EDTA was diluted in Hank's Balanced Salt Solution (HBSS) (Sigma-Aldrich, St. Louis, MO) without Ca^{2+} and Mg^{2+}, and was subsequently combined with SF-DMEM to yield final EDTA concentrations of 0.27mM, 0.53mM, and 1.06mM. These concentrations are within the range typically present in commercially available trypsin solutions. Bio-inks were printed, i.e. fired, at a frequency of 1000Hz, from a single nozzle onto glass microscope slides (VWR, West Chester, PA) in successive fixed length test periods. After each period, the slide was observed for evidence of printed medium. Firing test periods for bio-inks containing EDTA were 5 minutes long, while the periods for SF-DMEM, which causes nozzles to fail much more quickly, were 1 minute. Solutions were tested at 1000 drops/second for a maximum of 25 minutes (1.5×10^6 total drops), or until the nozzle became completely clogged, whichever condition occurred first.

Samples were given qualitative scores and corresponding numerical values of yes (1, indicating a well-defined dot of medium), yes with spatter (0.5, indicating initial nozzle failure), or no (0, indicating no medium printed). Spatter within a pattern was defined as satellite drops and irregular printing that presumably result from various levels of clogging, which can cause erratic spraying of the bio-ink during ejection. **Figure 3.2** depicts a 3-line pattern printed from a single nozzle in ink, first from a clean nozzle (left) and subsequently from the same nozzle, which was partially clogged after using a 30

second printing procedure with SF-DMEM. Bio-inks were tested for a maximum of 25 minutes (1.5×10^6 total drops) or until complete nozzle failure occurred. A separate cartridge was used for each of the three trials within a control or experimental group (12 total cartridges); a maximum of five firing test periods were conducted in each individual group of a particular trial, unless the cartridge failed to print.

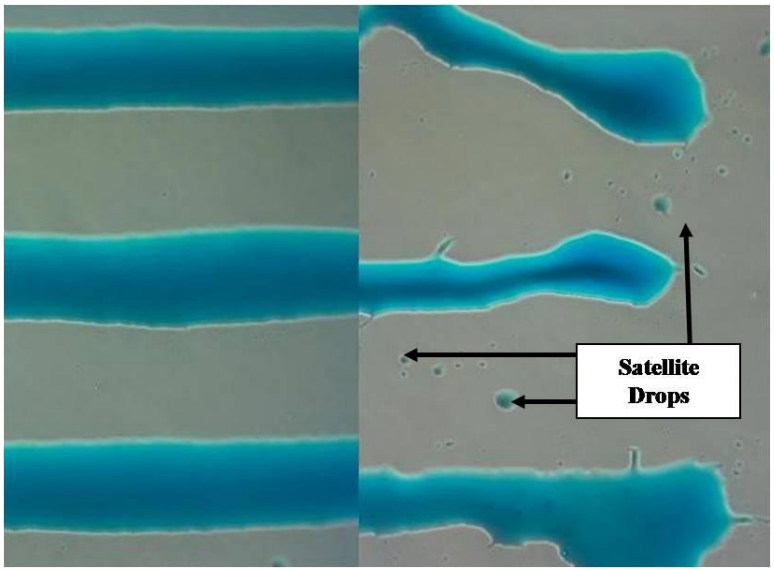

Figure 3.2: Comparison of a three line ink pattern with spatter (right) and without (left). Spatter indicates that a nozzle is in the initial stages of failure. The pattern with spatter was printed after rapidly firing SF-DMEM from the nozzle for 30 seconds. This result demonstrates how even short-term use of SFDMEM can cause significant pattern disruptions. 100x total magnification. (Parzel et al., 2009a)

The number of drops ejected during a period is estimated as the numerical score times the number of drops targeted per period.

The estimated number of drops successfully ejected from a nozzle during the test is given by:

Equation 1.

$$\#\ \text{Drops Ejected} = \#\ \text{Seconds per Test Period} \times \text{Firing Frequency} \times \sum \text{Numerical Scores}$$

Data were plotted and evaluated using a one-way analysis of variance (ANOVA) (Statistical Analysis Software, Cary NC) with a significance level of $p<0.05$ and a sample size of $n=3$.

Cell Culture

D1 murine mesenchymal stem cells (American Type Culture Collection (ATCC), Manassas, VA) were cultured according to the manufacturer's suggested protocol. Briefly, cells were maintained in DMEM containing 4mM L-glutamine, 1.5g/L sodium bicarbonate, and 4.5g/L glucose (ATCC), and 500mL were supplemented with 50mL fetal bovine serum (FBS) (Mediatech, Inc., Manassas, VA), 5mL antibiotic/antimycotic (Invitrogen Corporation, Carlsbad, CA), and 1mL fungizone (Invitrogen). The culture medium was replaced every 48-72 hours as required, and cells were stored in an incubator (Sanyo Scientific, San Diego, CA) at 37ºC and 5% CO_2. Cells from a non-metastatic murine mammary cancer cell line, 4T07, were maintained in the culture conditions described above for D1 cells.

To prepare cell-based bio-inks for printing, D1 and 4T07 cells were suspended in SF-DMEM at a density two times the desired final concentration. All cell suspensions were filtered using a 40µm sterile cell strainer (BD Falcon, Franklin Lakes, NJ). Just

prior to printing, 75µL of the cell suspension was combined with 75µL of HBSS (Sigma) containing 0.53mM, 1.06mM or 2.12mM EDTA, and was subsequently deposited into the HP26 cartridge well. Thus, the resulting 150µL of bio-ink consisted of D1 or 4T07 cells suspended in 50% SF-DMEM and 50% HBSS, with a final EDTA concentration of 0.27mM, 0.53mM, or 1.06mM.

Cell Viability and Attachment

LIVE/DEAD® Assay for Cell Viability

The viability of D1 cells printed in suspensions of the bio-inks described above was assessed qualitatively using a LIVE/DEAD® viability kit (Molecular Probes, Eugene, OR), with which live and dead cells fluoresce green and red, respectively. Additionally, cell morphology was observed to deduce whether the cells were attached to a polystyrene 24-well plate (Corning, Inc., Corning, NY). D1 cells were suspended in SF-DMEM at an initial concentration of 6×10^6 cells/mL and subsequently combined with HBSS containing EDTA. The final bio-ink solutions were comprised of 50% SF-DMEM and 50% HBSS, containing 3.0×10^6 cells/mL and 0.27mM, 0.53mM, or 1.06mM EDTA. A 100% SF-DMEM solution, devoid of EDTA, was used as a control. D1 cells were fired from a single nozzle at a rate of 1000 drops/second for 240 seconds onto a glass microscope slide, after which 2µL of the printed bio-ink was pipetted in triplicate (n=3) into individual wells of a 24-well plate. Wells were presoaked in a 50% solution of FBS in DMEM for at least 1 hour prior to the addition of cells. D1 cells were allowed to attach in an incubator at 37ºC and 5% CO_2 for 30 minutes before adding 1mL of 10%

fetal bovine serum-inclusive DMEM to each well containing cells. Cells were maintained for 24 hours, after which the LIVE/DEAD® solution was applied to the cultures, according to the manufacturer's suggested protocol. Briefly, cells were washed in 1x Dulbecco's Phosphate Buffered Saline (DPBS) (Sigma) and incubated at room temperature for 45 minutes in Live/Dead® reagent comprised of 4µM ethidium homodimer and 2µM calceinAM in DPBS. Fluorescent images of the samples were captured using an inverted microscope (Zeiss Axiovert 40 CFL microscope) (Carl Zeiss, Thornwood, NY) and Image-Pro software (Media Cybernetics, Inc., Bethesda, MD).

AlamarBlue® Metabolic Activity Assay

A quantitative AlamarBlue® assay was conducted in order to assess relative effects of various EDTA concentrations on the metabolic activity of D1 cells. D1 cells were suspended in the bio-ink solutions, including a control with no EDTA. D1 cells were suspended in SF-DMEM at an initial concentration of 6×10^6 cells/mL and subsequently combined with HBSS containing EDTA. Cells remained suspended at room temperature (to simulate actual printing conditions) for 0, 15, or 30 minutes, after which they were pipetted into 24-well plates (Corning, Inc.) at 20% confluence; a sample size of four was used for each experimental and control group. Once cells were allowed to attach for 30 minutes, 1mL of 10% fetal bovine serum-inclusive DMEM was added to each well containing cells. Cells were maintained at 37ºC and 5% CO_2, the AlamarBlue® metabolic activity assay (MP Biomedicals, LLC) was executed at both 4 and 24 hours following cell seeding. A 10% solution of AlamarBlue® dye in fresh culture medium was

prepared and added to the appropriate wells after the treated medium was aspirated. Cells were incubated at 37ºC and 5% CO_2 for 2 hours to allow a color change. Following incubation, 150μL of the culture medium from each sample was transferred in triplicate (only the mean value was reported) to a black, Costar® 96-well plate (Corning, Inc.), and the plate was read using a Fluoroskan Ascent FL fluorescent plate reader (ThermoLabsystems, Franklin, MA) with an excitation wavelength of 544nm and an emission wavelength of 590nm. Data were plotted and values within suspension time groups were analyzed using factorial ANOVA with a significance level of $p<0.05$ and a sample size of n=4. Additionally, one-way ANOVA analyses were conducted in order to identify the significance of time in suspension and subsequently compare these values to solutions effects. Again, a significance level of $p<0.05$ was selected with a sample size of n=16.

Anti-Aggregation of Tumorigenic Cells

EDTA was also tested for its ability to prevent aggregation of cells during the printing process. The 4T07 cell line (ATCC) was selected for this study because a tumorigenic cell type tends to aggregate. The 4T07 cells were suspended in SF-DMEM at an initial concentration of 1.54×10^7 cells/mL and subsequently combined with HBSS containing EDTA in concentrations described above. Final bio-ink solutions contained 7.7×10^6 cells/mL, which corresponds to approximately 1 cell/drop, estimated using a drop volume of 130pL as reported in Hewlett Packard literature (Buskirk *et al.,* 1988). Cells were printed in their respective bio-ink medium into 5x5 matrix (25 drops) patterns.

Drops were separated by 430µm to facilitate counting. Fifteen sample patterns (n=15) were printed for each of the experimental groups, along with a control group, exclusive of EDTA. Cartridges were not changed between samples in the same experimental group because, in actual printing conditions, cells suspended in a cartridge well would be allowed to settle over time. Cell counts were recorded for each of the dots printed and data were plotted as frequency histograms so that trends in changing cell counts could be deduced. Successful printing was defined as the ejection of one, two, or three cells while failure was defined as ejection of zero cells or greater than three cells. These values were selected based on the observed average number of printed cells per ejected drop.

Cartridge Cleaning

At the completion of each bioprinting procedure, the HP26 cartridges were cleaned (i.e. unclogged) using a combination of chemical soaks and sonication. This combination addressed clogging resulting from protein adsorption, cellular debris, and salt scaling. Cartridges were rinsed in distilled water to wash away any remaining bio-ink and were subsequently agitated for 15 minutes at room temperature with a chemical rust and stain remover diluted 1:1 in distilled water (Weiman Products, LLC, Gurnee, IL). The cartridges were rinsed again in distilled water and agitated for 30 minutes at room temperature with an instrument lubricant diluted 1:6 in distilled water (Weiman Products). Cartridges were then transferred to a distilled water bath and sonicated for 15 minutes.

Results

EDTA Effectiveness

Each of the bio-ink solutions was fired from a single nozzle at 1000Hz (1000 drops/sec) in successive test periods for a maximum of 25 minutes (1.5×10^6 total drops) or until the nozzle failed. A value less than 1.5×10^6 drops indicated that the nozzle failed during testing. Note that bio-inks containing 0.53mM and 1.06mM EDTA performed similarly and did not suffer nozzle failure during any of the trials. A serum-free cell culture medium with EDTA added at a concentration typically found in trypsin solutions (0.53mM), could be fired from a nozzle at a rate of 1000Hz for over 1.4 million drops without nozzle failure. Thus, reasonable levels of EDTA permit a nozzle to print over one million cells without failure. **Table 3.1** lists the qualitative scores given to high speed evacuation samples with various concentrations of EDTA added to prevent salt scaling.

Table 3.1: Corresponding numerical values calculated from qualitative data. Samples were assessed based on whether printing occurred, and qualitative scores were then given a corresponding value of yes=1, yes with spatter=0.5, and no=0. Note that bio-inks containing 0.53mM and 1.06mM EDTA did not fail during any of the trials as the maximum cumulative qualitative score was a 5.0.

		0mM EDTA	**0.27mM EDTA**	**0.53mM EDTA**	**1.06mM EDTA**
Cumulative Qualitative Score	Trial 1	2.0	3.0	5.0	5.0
	Trial 2	1.5	3.0	5.0	5.0
	Trial 3	1.0	4.0	5.0	5.0
	TOTAL	**4.5**	**10.0**	**15.0**	**15.0**

Figure 3.3 displays the approximate number of drops that could be printed before nozzle failure. Approximately 1.5×10^6 (Standard Error of the Mean, SEM = ± 0) drops could be printed with bio-inks containing 0.53mM and 1.06mM EDTA before failure occurred, while only 1.0×10^6 (SEM = ± 1×10^5) drops could be printed with 0.27mM bio-ink and only 2.0×10^5 (SEM = ± 1.7×10^4) drops with 0mM bio-ink.

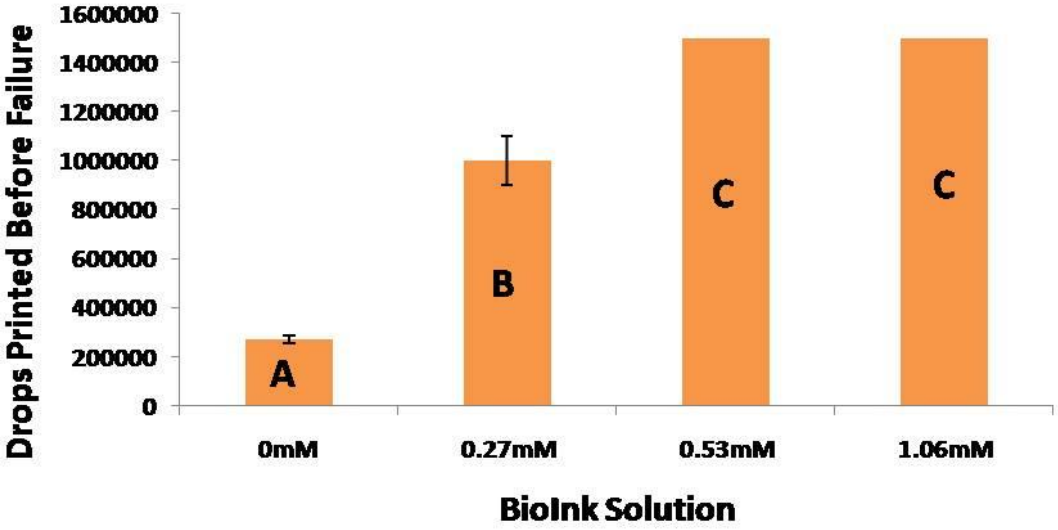

Figure 3.3: Approximate number of drops printed before failure occurred. A value less than $1.5x10^6$ indicates nozzle failure occurred. Bars with different letters are significantly different. Note that bio-inks containing 0.53mM and 1.06mM EDTA did not fail. (Parzel et al., 2009a)

Cell Viability and Attachment

LIVE/DEAD® Assay for Cell Viability

A qualitative LIVE/DEAD® assay for cell viability confirmed that the number of necrotic cells in each of the samples was negligible. **Figure 3.4** depicts D1 cells, which were suspended in bio-ink containing A) 0.53mM EDTA and B) 1.06mM EDTA, printed,

seeded in 24 wells, and maintained in culture for 24 hours. Cells in all cases looked healthy and viable, with no obvious differences between groups.

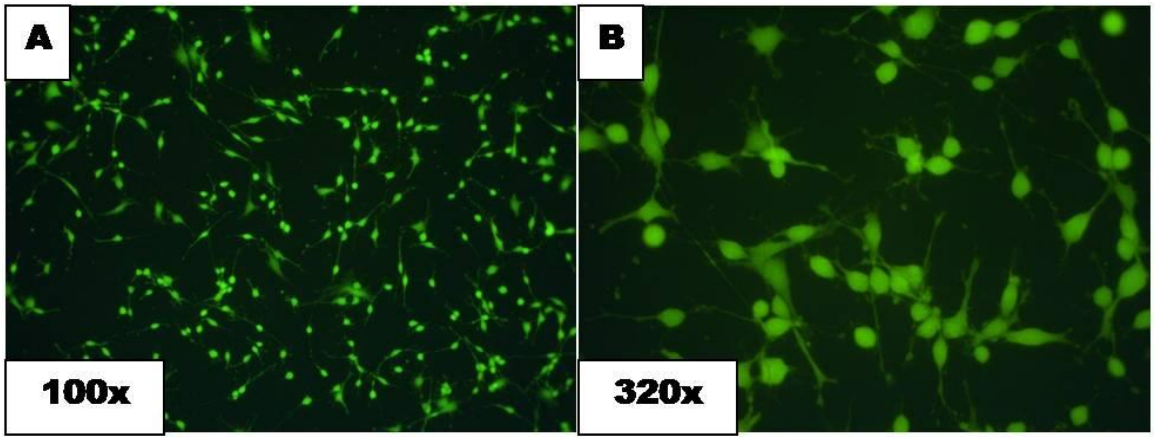

Figure 3.4-a, 3.4-b: LIVE/DEAD® assay for cell viability. D1 cells were suspended in bio-inks containing EDTA and printed using a thermal inkjet printer and HP26 cartridge. Cells were qualitatively assessed for verification of viability and attachment following 24 hours in standard culture. A)0.53mM EDTA, 100x total magnification. B) 1.06mM EDTA, 320x total magnification. Image was captured using only FITC filter. The number of dead cells visible under the rhodamine filter was non-existent or negligible. (Parzel et al., 2009a)

AlamarBlue® Metabolic Activity Assay

Figures 3.5-a and 3.5-b display absolute AlamarBlue® fluorescence values at the selected culture time points (See **Table 3.2** for averages of absolute fluorescence and the standard error of the mean). Following a 4 hour culture period, data indicated that there were statistically significant differences at the 15 and 30 minute suspension time points when cells that had been cultured in the presence of EDTA were compared to control cells. Following a 15 minute suspension time, all three EDTA concentrations were significantly different from their respective control, while at 30 minutes, only 0.53mM

and 1.06mM were significantly different from the control. Following a 24 hour culture period and 15 minutes in suspension, the effect of EDTA concentration, when compared with the control, was only significant between 0.53mM and 1.06mM. When D1 cells were kept in suspension with bio-inks for 30 minutes following 24 hour culture, the solution effects ceased. When comparing 4 and 24 hour culture times, it appears that EDTA concentration more significantly affected D1 metabolic activity following 4 hours in culture.

Table 3.2: AlamarBlue® Metabolic Activity Assay. Numerical values of absolute fluorescence followed by the standard error of the mean. Values are presented in graphical form in Figures 5-a and 5-b.

			SF-DMEM	0.27mM EDTA	0.53mM EDTA	1.06mM EDTA
4 Hour Culture Time	Absolute Fluorescence Value (SEM)	0 Minutes	1962.4 (±18.8)	1886.6 (±65.2)	1801.5 (±41.3)	1810.7 (±46.3)
		15 Minutes	1920.1 (±20.6)	1801.5 (±8.8)	1780.5 (±17.1)	1753.1 (±30.0)
		30 Minutes	1784.7 (±15.4)	1802.8 (±14.3)	1660.2 (±35.8)	1654.6 (±39.1)
24 Hour Culture Time	Absolute Fluorescence Value (SEM)	0 Minutes	4242.8 (±37.7)	4194.9 (±47.9)	4276.3 (±28.3)	4212.3 (±60.0)
		15 Minutes	3615.5 (±59.8)	3681.2 (±53.1)	3351.0 (±44.0)	3363.2 (±72.2)
		30 Minutes	3608.9 (±71.0)	3542.1 (±55.6)	3542.7 (±109.7)	3411.0 (±83.1)

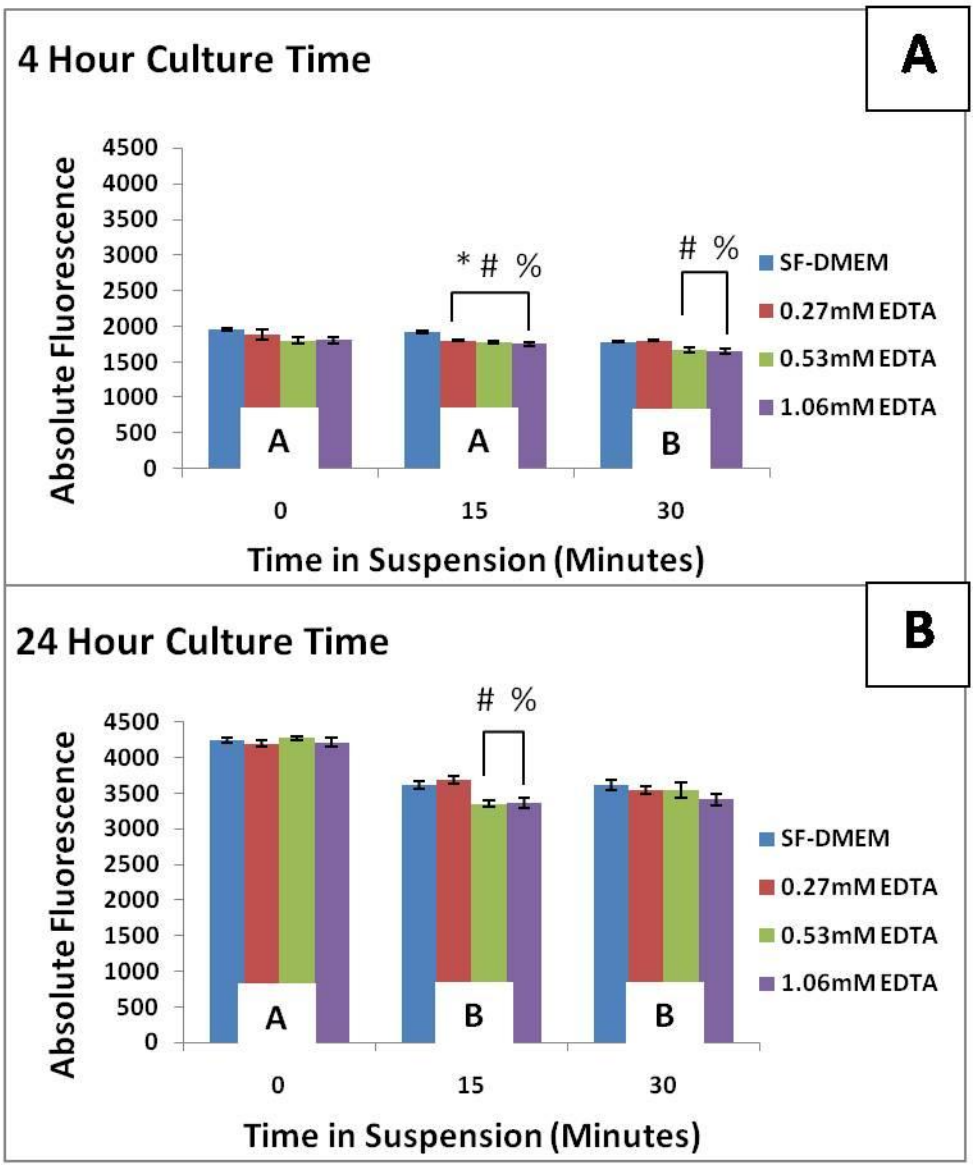

***Figure 3.5-a, 3.5-b:** AlamarBlue® metabolic activity assay of D1 cells maintained in culture for 4 and 24 hours. Cells were suspended in bio-inks containing EDTA, pipetted into 24 wells, and allowed to attach for 30 minutes. Values within groups were analyzed using factorial ANOVA with a significance level of $p<0.05$ and a sample size of $n=4$. Differences among groups were discerned following one way ANOVA with a significance level of $p<0.05$ and a sample size of $n=16$. Groups labeled with different letters are significantly different. Bars that are significantly different than their respective controls are labeled 0.27mM (*), 0.53mM (#), and 1.06mM (%). (Parzel et al., 2009a)*

Anti-Aggregation of Tumorigenic Cells

EDTA was evaluated for its effectiveness in preventing cell aggregation during the bioprinting process. Histograms are depicted in **Figures 3.6-a through 3.6-d**, which show the frequency of drops that contained a specified number of cells. Comparison of histograms indicates that a peak emerged in the lower cell-number range when 0.27mM and 0.53mM EDTA was added to the 4T07 cell suspension. The proportion of successful and unsuccessful drops printed using each of the defined bio-inks is presented in **Table 3.3**. The greatest proportion of successful drops was printed using a 4T07 cell suspension containing 0.53mM EDTA.

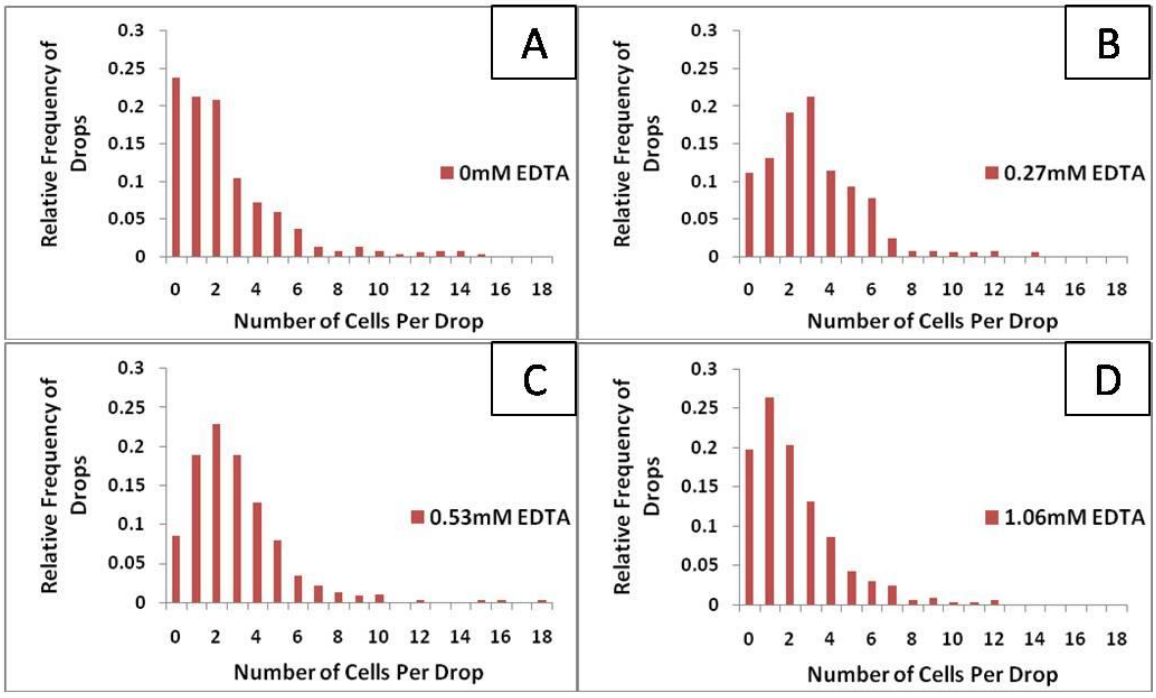

Figure 3.6-a,b,c,d: Frequency histograms illustrating the number of 4T07 cells printed per drop using the defined bio-inks. Histograms were assessed for the presence of trends that could suggest more homogeneous printing in the presence of EDTA. (Parzel et al., 2009a)

Table 3.3: Proportion of successful and unsuccessful drops printed using each of the bio-ink cell suspensions. Success was defined as 1, 2, or 3 cells per drop while failure was defined as 0 cells or greater than 3 cells per drop. The greater proportion of successful drops was printed using a 4T07 cell suspension containing 0.53mM EDTA. (Parzel et al., 2009a)

Solution	Success	Failure
0mM EDTA	197/375 = 0.53	178/375 = 0.47
0.27mM EDTA	201/375 = 0.54	174/375 = 0.46
0.53mM EDTA	228/375 = 0.61	147/375 = 0.39
1.06mM EDTA	224/375 = 0.60	151/375 = 0.40

Discussion

An average adult human organ might contain several hundred million functional units (i.e. cells of the parenchyma) in addition to supportive stromal tissue. Nozzle failure after several hundred thousand firings is thus a very serious roadblock on the path to creating tissue test systems, and an even greater impediment in engineering entire organs. The recognition of salt scaling as a new obstacle in bioprinting applications arose from our development of a high-resolution bioprinter, which we achieved by reverse engineering an HP 520C series inkjet printer and HP26 ink cartridge. Successful printing of various cellular and acellular solutions using the HP26 cartridge is described in the literature (Xu *et al.*, 2005); some, for example, DMEM, calcium chloride, and DPBS, largely contain inorganic salts, while others like fibrinogen and laminin solutions contain low concentrations of proteins. Prior to the construction of a custom bioprinting system

with which single-nozzle control could be achieved, it was hypothesized that most nozzle failure, i.e. failure to eject a drop of liquid when the nozzle is fired, occurred as a result of clogging due to high cell densities and "sticky" proteins. Cartridge failure due to salt scaling likely went unrecognized by bioprinting researchers because previous literature focused on creation of only small-scale patterns. However, when we assessed EDTA effectiveness in acellular solutions, SF-DMEM caused nozzle failure after approximately 3.0×10^5 drops. Therefore, as bioprinting procedures become more advanced and larger tissue samples are constructed, the use of SF-DMEM as a bio-ink would likely very quickly lead to large pattern disruptions and ultimately, complete nozzle failure.

EDTA is a synthetic amino acid, and it was selected for this study because of its widespread use in cell culture and *in vivo* therapeutic applications. It was hypothesized that EDTA, in concentrations that would not compromise cell viability, could prevent salt scaling by acting as a chelating agent to prevent crystallization of ions during evaporation at the printer cartridge surface. Furthermore, addition of EDTA to a cell suspension did not change the fluid viscosity, a parameter which could compromise the performance of the thermal inkjet mechanism (Sen and Darabi, 2007). The starting point for selection of EDTA concentrations was 0.53mM, which is the concentration found in commercially available trypsin solution. It was demonstrated that a concentration of 0.27mM EDTA in bio-ink reduced but did not eliminate nozzle failure within the 25 minute testing period. With increased EDTA concentrations of 0.53mM and 1.06mM, the nozzles ejected drops reliably without spatter for the entire 25 minute testing period. Through experience,

spatter was determined to be a sign of approaching failure, and as shown in **Figure 3.2**, spatter results in significant pattern disruptions.

Data generated to show the effect of EDTA on D1 cells in culture suggest that the variable indicating total amount of time in suspension has a stronger effect on metabolic activity than does solution effects. The more significant effect of EDTA concentration on D1 metabolic activity following 4 hours in culture is likely a result of slowed cell attachment in the presence of EDTA, which no longer delayed metabolic activity at the later time point, once cells had fully attached. We have demonstrated the attachment of cells and the preservation of a two-dimensional micron-scale pattern over a 5 day period (Parzel *et al.*, 2009b); thus, the presence of EDTA in the culture medium should not prevent creation of a 3D construct especially when integrin-binding materials (i.e. collagens) are introduced into the construct. It will be important to incorporate this information into the bioprinting process to ensure that, regardless of the bio-ink solution, cells should be left in solution for a minimal amount of time before being injected into the well of the printer cartridge. Future work will involve the assessment of cell viability within 3D constructs, following the addition of EDTA to a bio-ink. Regardless of the results, the prevention of salt-scaling and cell aggregation at the nozzle surface will remain an important milestone for high-throughput two-dimensional culture.

The shapes of the frequency histograms for 4T07 studies show that a peak in the low cell-number range began to form while printing with 0.27mM and 0.53mM EDTA. However, when EDTA concentration was increased to 1.06mM EDTA, the shape of the histogram began to revert back to the shape portrayed by the SF-DMEM samples. The

data further suggest that cells in toxic environments will begin to aggregate, and thus although the 1.06mM EDTA solution prevents clogging, it is not an optimal solution to achieve the most successful cell ejection frequency.

The novel cartridge cleaning protocol was implemented after observing that sonication alone was not an effective tool for unclogging nozzles. Ultrasonic cleaning methods were employed in previous studies because it was believed that clogging resulted primarily from protein adsorption and cell aggregation. The commercially available chemicals (rust remover and instrument lubricant) used in the new cleaning procedure were intended to address nozzle clogging due to salt scaling. Additionally, the instrument lubricant may help prevent contamination, as it remains bacteriostatic for approximately 1 month after use. There was a noticeable increase in the effectiveness of this cleaning procedure for unclogging nozzles when compared to sonication alone, though no formal studies have been completed to confirm these observations statistically.

The ultimate goal of this research is to apply 3D cell printing techniques toward the development of *in vitro* tissue test systems in which one can infuse heterogeneous cell populations and design an appropriate layout of biomaterial components. This tool will increase knowledge toward understanding why disease related cellular abnormalities occur (including those related to metabolic activity, migration, growth factor release, and mode of cell death) and will allow the application of therapeutic treatments to three-dimensional systems of interest. However, in order to use inkjet printing to move closer to this goal, the printer must be able to eject millions of cells out of a single nozzle without failing.

Conclusions

The salts in standard cell culture media create deposits inside a printhead, which cause the printhead to fail prematurely, well short of printing one million cells. The results presented in this chapter show that EDTA may be added to cell culture media in order to prevent nozzle failure and to facilitate the high throughput production of 3D complex tissues. The 0.53mM solution of EDTA was the best solution tested because it prevented nozzle failure for the duration of the study, had the greatest proportion of successful drops printed in the cell ejection study, and had no statistically significant toxic effects when cells were suspended in bio-ink solutions for 0 minutes and maintained in culture for 24 hours. An approximate concentration of 0.53mM EDTA in HBSS should be incorporated into all bioprinting cell suspension solutions that could trigger salt crystal formation leading to printhead failure. Far more emphasis must be placed on bioprinting details and methodologies in order for bioprinting to be a clinically relevant tool, capable of fabricating 3-D complex tissues in high throughput. The nozzle fouling that can limit the ejection of high volumes of cells is one such detail.

References

Boland T, Mironov V, Gutowska A, Roth EA, Markwald RR. 2003. Cell and organ printing 2: fusion of cell aggregates in three-dimensional gels. Anat Rec A Discov Mol Evol Biol 2:497-502.

Boland T, Xu T, Cui X. 2006. Application of inkjet printing to tissue engineering. Biotechnol J 1:910-917.

Burg KJL, Boland T. 2003. Bioengineered Devices: Minimally Invasive Tissue Engineering Composites and Cell Printing. IEEE Engineering in Medicine and Biology 22(5):84-91.

Buskirk WA, Hackleman DE, Hall ST, Kanarek PH, Low RN, Trueba KE, VanDePoll RR. 1988. Development of a high-resolution thermal inkjet printhead. Hewlett Packard Journal 55-62.

Chaubey A, Boland T, Burg TC, Burg KJL. 2007. Cell printing on 3-D matrices using a modified inkjet printer. Trans 32nd Ann Meeting Soc Biomater, Chicago, IL.

Discher DE, Janmey P, Wang YL. 2005. Tissue cells feel and respond to the stiffness of their substrate. Science 310:1139-1143.

Enderle J, Blanchard SM, Bronzino J. 2005. Introduction to Biomedical Engineering, Elsevier Inc. Burlington, MA, USA.

Engler A, Bacakova L, Newman C, Hategan A, Griffin M, Discher D. 2004. Substrate compliance versus ligand density in cell on gel responses. Biophys J 86:617-628.

Kasper G, Reule M, Tschirschmann M, Dankert N, Stout-Weider K, Lauster R, Schrock E, Mennerich D, Duda GN, Lehmann KE. 2007. Stromelysin-3 over-expression enhances tumourigenesis in MCF-7 and MDA-MB-231 breast cancer cell lines: involvement of the IGF-1 signalling pathway. BMC Cancer **7**:12.

Khademhosseini A, Langer R. 2007. Microengineered hydrogels for tissue engineering. Biomaterials 28:5087-5092.

Khetani SR, Bhatia SN. 2006. Engineering tissues for *in vitro* applications, Curr Opin Biotechnol. 17:524-531.

Mironov V, Boland T, Trusk T, Forgacs G, Markwald RR. 2003. Organ printing: computer-aided jet-based 3D tissue engineering. Trends Biotechnol 4:157-161.

Nakamura M, Kobayashi A, Takagi F, Watanabe A, Hiruma Y, Ohuchi K, Iwasaki Y, Horie M, Morita I, Takatani S. 2005. Biocompatible inkjet printing technique for designed seeding of individual living cells. Tissue Eng 11:1658-1666.

Parzel CA, Burg T, Groff R, Hill AM, Pepper M, Stripe B, Burg KJL. 2008a. High resolution inkjet printing as a tool for creating tissue test systems. Trans 2008 Fall Symposium Soc Biomater, Atlanta, GA.

Parzel CA, Hill AM, Stripe B, Burg KJL. 2008b. The modified inkjet cell printer as a tool for 3-dimensional breast tissue modeling. Fifth DoD Era of Hope Meeting, Baltimore, MD.

Parzel CA, Pepper ME, Burg T, Groff RE, Burg KJL. 2009a. EDTA enhances high-throughput 2-dimensional bioprinting by inhibiting salt scaling and cell aggregation

at the nozzle surface. Journal of Tissue Engineering and Regenerative Medicine 3(4):260-8.

Parzel CA, Pepper ME, Burg T, Groff RE, Burg KJL. 2009b. High resolution cell patterning and co-culture using a custom bioprinter. Transactions of the 2009 Symposium of the Society For Biomaterials, San Antonio, TX.

Roth EA, Xu T, Das M, Gregory C, Hickmann JJ, Boland T. 2004. Inkjet printing for high-throughput cell patterning. Biomaterials 25:3707-3715.

Sasser AK, Mundy BL, Smith KM, Studebaker AW, Axel AE, Haidet AM, Fernandez SA, Hall BM. 2007. Human bone marrow stromal cells enhance breast cancer cell growth rates in a cell line-dependent manner when evaluated in 3D tumor environments. Cancer Lett 254:255-264.

Sen, AK, Darabi, J. 2007. Droplet ejection performance of a monolithic thermal inkjet printhead. J Micromech Microeng 17:1420-1427.

Sodunke TR, Turner KK, Caldwell SA, McBride KW, Reginato MJ, Noh, HM. 2007. Micropatterns of Matrigel for three-dimensional epithelial cultures. Biomaterials 28: 4006-4016.

Wang DY, Huang YC, Chiang H, Wo AM, Huang YY. 2007. Microcontact printing of laminin on oxygen plasma activated substrates for the alignment and growth of Schwann cells. J Biomed Mater Res B Appl Biomater 80:447-453.

Wilson WC, Boland T. 2003. Cell and organ printing 1: protein and cell printers. Anat Rec A Discov Mol Evol Biol 2:491-496.

Xu T, Jin J, Gregory C, Hickman JJ, Boland T. 2005. Inkjet printing of viable mammalian cells. Biomaterials 1:93-99.

Xu T, Gregory CA, Molnar P, Cui X, Jalota S, Bhaduri SB, Boland T. 2006. Viability and electrophysiology of neural cell structures generated by the inkjet printing method. Biomaterials 19:3580-3588.

CHAPTER 4

Select results in this chapter were generated by an Institute for Biological Interfaces of Engineering interdisciplinary team, including Clemson University doctoral student Matthew Pepper, and were presented at the 2009 Annual Meeting and Exposition of the Society For Biomaterials (Parzel et al., 2009a) and at the 2009 IEEE Engineering in Medicine and Biology Society Conference (Pepper et al., 2009).

HIGH RESOLUTION CELL PATTERNING AND CO-CULTURE USING A CUSTOM BIOPRINTER

Introduction

Inkjet Bioprinting as a Tissue Engineering Tool

For almost two decades, tissue engineering has been defined as "the application of engineering methodology to the branches of life science with the goal of developing biological substitutes that restore, maintain, or improve tissue function" (Skalak, 1993). The goal of tissue engineering is to reduce the need to implant foreign, permanent materials that may cause chronic inflammatory or immunologic responses. The domain of tissue engineering has recently been expanded to include the development of *in vitro* tissue test systems, with which one can explore basic cellular behaviors, disease progression, and treatment options (Burg & Boland, 2003). A common need in almost all tissue engineering applications is the ability to position, in a reasonable timeframe, large quantities of cells and biomaterials within a three-dimensional (3D) volume.

Many approaches have been suggested to build cellular systems. Conventional cell seeding methods use static, e.g. in a well-plate, or dynamic, e.g. in a stir flask or bioreactor, loading of a volume of cells onto a biomaterial scaffold or construct. Generally, the goal is to achieve uniform cell deposition on a surface or within an open-cell volume (Xu & Burg, 2007). This approach does not allow spatial control of the

seeded cells and results in random placement of cells on the construct (Burg *et al., 2002).* Better control of cell placement is likely to benefit the construct, with designed placement of every cell being the ultimate goal. An approach that can address controlled cell and/or biomaterial placement is generally referred to as free-form fabrication or microfabrication. Many of the approaches to rapid-prototyping of mechanical components are analogous to the free-form fabrication of biological tissues. Our goal is to develop a means to precisely deposit small numbers of cells or small volumes of biomaterial.

Drop-on-demand printers have been investigated for cell deposition over the past decade. The technology used in desktop printing systems has been exploited by modifying the ink cartridges to replace the existing ink with a cell solution, i.e. a "bio-ink". To date, bioprinting work has been largely accomplished using proprietary drivers and embedded software for either Hewlett-Packard (Burg & Boland, 2002; Boland *et al.*, 2007; Mironov *et al.*, 2003; Wilson & Boland, 2003; Xu *et al.*, 2006) or Canon inkjet printers (Nakamura *et al.*, 2005; Saunders *et al.*, 2008). The main disadvantage of this approach is the limited customizability of the printed patterns and droplet firing parameters. These limits make it difficult to collect data pertinent to the printing process, such as statistics of how many cells are ejected per drop, how much energy is being delivered to each drop and how droplet firing parameters affect the bio-ink.

There has been some effort to access and optimize printing parameters to match the specifics of cell printing; most notably, Boland and coworkers describe modification of the software driver for an HP500 series printer that exposes the printing parameters in

software (Wilson & Boland, 2003). Moreover, the printer's paper feed mechanism has been modified to permit two-dimensional cell printing. This seminal work with the HP500 printer demonstrates the HP26 as a capable technology for placing cells, but use of the printer itself limits the types of substrates on which bio-ink can be printed and the types of experiments that can be conducted (Boland *et al.*, 2007). In pursuit of a core technology upon which a three-dimensional biofabrication system will be constructed, we return to a two-dimensional bioprinter. This system (**Figure 4.1**) is designed such that the droplet firing parameters may be controlled in order to print a wide variety of materials, print patterns may be changed in real time via software, and additional workstations and tools, such as computer vision and thermal processing, may be incorporated into the system.

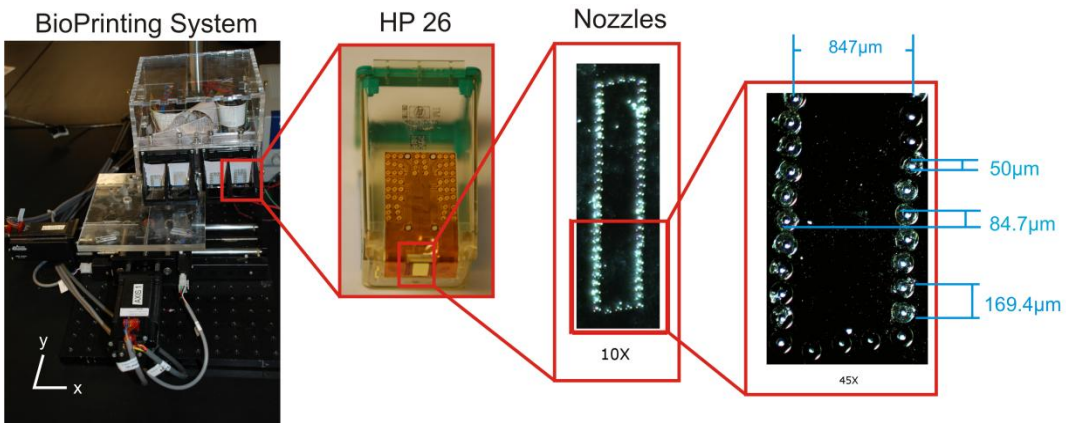

Figure 4.1: Our current Bioprinting system with print head and 2D stage, inset shows where the HP26A engages. The HP26A has a flex circuit on the back which attaches to the fifty nozzles located at the bottom of the cartridge. These fifty nozzles are arranged in two columns of twenty-five, with a vertical offset of 84.7µm and horizontal offset of 847µm. Each nozzle has a diameter of 50µm.

This chapter presents a custom bioprinting system, designed specifically to be flexible and extensible. This new bioprinting system allows expandable functionality such as ability to print multiple cell types per sample and integration of custom vision systems. Most importantly, the prototype system will serve as the basis for a 3D biofabrication system currently under development.

Cell Delivery System

The HP26 inkjet cartridge was selected as the means of cell delivery for the bioprinting system because of its proven ability to print cells. A variety of cell types have been printed with this cartridge and shown to be viable in culture after printing (Burg & Boland, 2003; Boland *et al.*, 2007; Mironov *et al.*, 2003; Wilson & Boland, 2003; Xu *et al.*, 2006; Xu *et al.*, 2005). The HP26A cartridge is easy to disassemble and

clean, is capable of a high droplet firing rate, has appropriately sized nozzles for the bioprinting application, and is widely available. In the original HP520C inkjet printer, this cartridge delivers 180,000 drops per second or 3,600 drops per nozzle per second. Thus if one cell was deposited per drop, a clinically relevant sample of ten million cells could be deposited in less than one minute.

The HP26 cartridge consists of an ink storage chamber, a print head containing the nozzles, and an electrical interconnect on the back of the cartridge (**Figure 4.1**) (May *et al.*, 1988). The nozzles in the print head are 50μm in diameter and are arranged in two vertical columns of 25 nozzles each. Within each column, the nozzles are separated vertically by 169.4μm. The cartridge's native vertical printing resolution, 300dpi, is defined by the 84.7μm spacing between a nozzle and its closest vertical neighbor in the other column. Later generations of HP inkjet cartridges provide higher vertical resolution by using smaller diameter nozzles in closer proximity. Unfortunately smaller nozzles cause damage to cells during printing, presumably due to high shear forces during drop ejection.

The HP26 is a thermal inkjet cartridge. Each nozzle contains a 30 Ω resistor, which is heated by application of a constant voltage pulse of specified duration. The rise in temperature causes a vapor bubble to form, expelling a drop of liquid from the nozzle. The electrical interconnect on the HP26 cartridge permits direct electrical connection to each of the 50 nozzle resistors. This simple interface permitted the design of custom drive electronics to address and fire individual nozzles as directed by a real-time control system. The carriage assembly is incorporated into the custom bioprinting system in

order to ensure reliable electrical and mechanical connections to the cartridge. The carriage assembly supports two cartridges, and the current printing system has two of these carriages, for a maximum of four cartridges. The purpose of this study is to demonstrate the high resolution capability of our custom bioprinter by printing mono- and co-culture patterns in 2D.

Materials and Methods

Demonstration of the 2-D Bioprinting System - Single Cell Printing

Cell Culture

D1 murine mesenchymal stem cells (American Type Culture Collection (ATCC), Manassas, VA) were cultured according to the manufacturer's suggested protocol. Briefly, cells were maintained in Dulbecco's Modified Eagle's Medium (DMEM) containing 4mM L-glutamine, 1.5g/L sodium bicarbonate, and 4.5g/L glucose (ATCC), and every 500mL was supplemented with 50mL fetal bovine serum (FBS) (Mediatech Inc., Manassas, VA), 5mL antibiotic/antimycotic (Invitrogen Corporation, Carlsbad, CA), and 1mL fungizone (Invitrogen). The culture medium was replaced every 48-72 hours as required, and cells were stored in an incubator (Sanyo Scientific, San Diego, CA) at 37ºC and 5% CO_2. Cells from a non-metastatic murine mammary cancer cell line, 4T07 (ATCC), were maintained in the culture conditions described above for D1 cells.

To prepare cell-based bio-inks for printing, D1 and 4T07 cells were suspended in serum-free DMEM (SF-DMEM) at a density two times the desired final concentration. All cell suspensions were filtered using a 40µm sterile cell strainer (BD Falcon, Franklin

Lakes, NJ). Just prior to printing, 75µL of the cell suspension was combined with 75µL of Hank's Balanced Salt Solution (HBSS) (Sigma-Aldrich, St. Louis, MO) containing 1.06mM ethylenediaminetetraacetic acid (EDTA) (MP Biomedicals, LLC, Solon, OH), and was subsequently deposited into the HP26 (Hewlett Packard, Palo Alto, CA) cartridge well (Parzel *et al.*, 2009b). Thus, the resulting 150µL of bio-ink consisted of D1 or 4T07 cells suspended in 50% SF-DMEM and 50% HBSS, with a final EDTA concentration of 0.53mM.

Preparation of Collagen Substrates

Tissue culture polystyrene microscope slides (Nalge Nunc International, Rochester, NY) were coated with collagen using a modified method and aseptic techniques (Vernon *et al.*, 2005). These substrates were used as surfaces for all cell patterning studies. A 2.0mg/mL collagen solution was prepared by combining 1.5mL collagen stock solution (3.0mg/mL - PureCol™) (Advanced Biomatrix, San Diego, CA) with 167µL 10x Dulbecco's phosphate buffered saline (DPBS), 225µL FBS, and 358µL DMEM; a small volume (approximately 20µL) of 1N NaOH was added to neutralize the solution. A volume of 200µL solution was pipetted into the center of a silicone ring (1/2" inner diameter) attached to each slide , and collagen gels were polymerized in an incubator at 37ºC and 5% CO_2 for at least 4 hours. Gel coatings were rinsed in sterile distilled water until clear and then allowed to dry in a laminar flow hood (Labconco, Kansas City, MO). Following drying, the collagen coatings were soaked overnight in a

1:1 solution of DMEM to FBS. Prior to printing, excess medium was aspirated, and collagen coatings were allowed to partially dry in a laminar flow hood for 30 seconds.

Single Cell Patterning: Mono-culture

D1 cells were suspended in SF-DMEM at an initial concentration of 1.5×10^7 cells/mL and subsequently combined with HBSS containing EDTA, as described above. The final bio-ink solution was comprised of 50% SF-DMEM and 50% HBSS, containing 7.7×10^6 cells/mL and 0.53mM EDTA. A volume of 150µL of the D1 cell suspension was pipetted into the HP26 cartridge well, which was cleaned using 70% ethanol (Pharmco-Aaper, Shelbyville, KY). The patterns were created using GNU Image Manipulation Program (GIMP) version 2.4 and then each pattern was printed onto a separate collagen coating. Following printing, D1 cells were allowed to attach in an incubator for 25 minutes, after which they were covered in 10% fetal bovine serum-inclusive DMEM. An image of each cell pattern was captured at time points 0, 24, 96, and 120 hours to show stages of cell attachment and spreading on the collagen substrates.

Demonstration of the 2-D Bioprinting System - Dual Cell Printing

Fluorescent Labeling

In order to differentiate between cell types in a printed pattern, D1 and 4T07 cells were labeled prior to printing using green (Ex. 450nm, Em. 517nm) and red (Ex. 550nm, Em. 602nm) CellTracker™ probes (Invitrogen), respectively. The CellTracker™ green stock solution was prepared by adding 10.76µL dimethyl sulfoxide (DMSO) (Sigma) to

the lyophilized product, and was then diluted in 4.3mL of SF-DMEM. The CellTracker™ red working solution was prepared by adding 7.29μL DMSO to the lyophilized product and then subsequently was diluted with 2.9mL SF-DMEM. Cells grown to confluence in a T-75 tissue culture flask (Corning Inc., Corning, NY) were washed with 1x DPBS and incubated for 45 minutes in their respective fluorescent tag solutions.

Dual Cell Patterning: Co-Culture

D1 and 4T07 cells were suspended in SF-DMEM at an initial concentration of 1.5×10^7 cells/mL and subsequently combined with HBSS containing EDTA, as described above. The final bio-ink solutions were comprised of 50% SF-DMEM and 50% HBSS, containing 7.7×10^6 cells/mL and 0.53mM EDTA. To print cells in co-culture, D1 cells were first pipetted into an HP26 cartridge well, after which a designated portion of the pattern was printed onto a collagen coating. Next, a different HP26 cartridge was used to print the remainder of the pattern using 4T07 cells. A calibration method was used to ensure pattern alignment following insertion of the second cartridge. To complete this process, a cartridge deposits one drop at a location on the stage. The stage is then moved a predetermined distance, such that the drop resides underneath the microscope, close to the camera center. An image is taken with the vision system, and the offset from the center of the drop to the camera center is determined. After printing, cells were allowed to attach in an incubator for 25 minutes, after which they were covered in 10% serum-inclusive DMEM. The samples were photographed using a Zeiss Axiovert 40 CFL

microscope (Carl Zeiss AG Oberkochen, Germany) equipped with a 50W Xenon lamp. The images were captured using an Zeiss AxioCam MRC 5, processed with Zeiss AxioVision LE 4.6 (Carl Zeiss Microimagining, Inc., Thornwood, NY), and combined using GIMP.

Results and Discussion

The pictures produced from the mono-culture cell experiment **(Figure 4.2)** demonstrate that a high resolution pattern can be successfully printed and maintained in culture for at least 120 hours. One key factor in enabling both the speed of attachment and viability of cells during the initial incubation period was the collagen substrate on which cells were printed. In earlier trials, cells printed directly onto polystyrene slides detached when culture media was applied for long-term incubation, likely because cells were printed in a serum-free medium, which is not conducive to attachment. Even the cells that did attach would not elongate or proliferate over time, as it was found that cells must be printed onto a wet substrate. The addition of a wet collagen substrate gave the cells a readily available attachment point and allowed enough moisture retention to prevent cell stress.

The D1 cells in **Figure 4.2** appear to enter a proliferative phase following 24 hours in culture. Because of cell proliferation, the pattern is no longer discernible after 96 hours. This point can be viewed as a positive result since cells responded to cues from their neighbors and covered empty spaces within the pattern. **Figure 4.3** demonstrates the creation of complex multiple-cell-type patterns. The checkered pattern shows that our

system has the capacity to fabricate tissue test systems that mirror the non-homogeneity of real tissue. In such tissue test systems, cells will be accurately patterned into a biologically meaningful architecture, after which cellular, biochemical and physical cues will provide a microenvironment to aid in the understanding of cellular behavior.

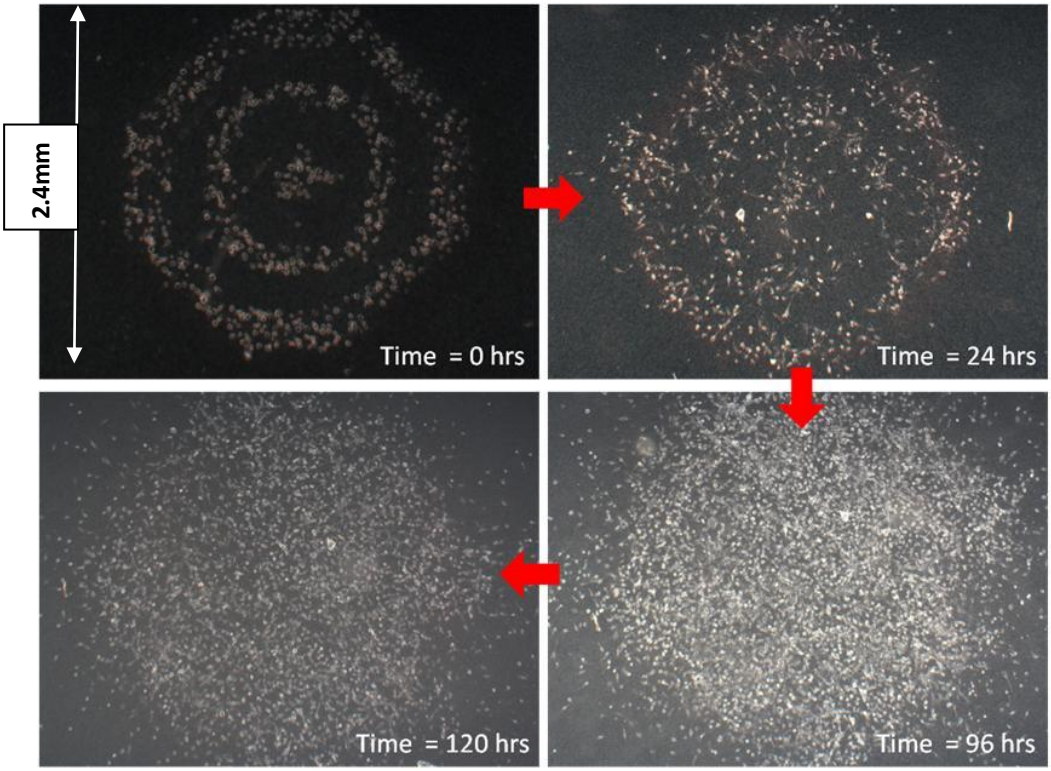

Figure 4.2: Time point observation of D1 cells printed in bullseye pattern, starting at the upper left and proceeding clockwise. Images of cells were captured from 0-120 hours to show stages of cell attachment, spreading, and proliferation on a collagen substrate. (Pepper et al., 2009)

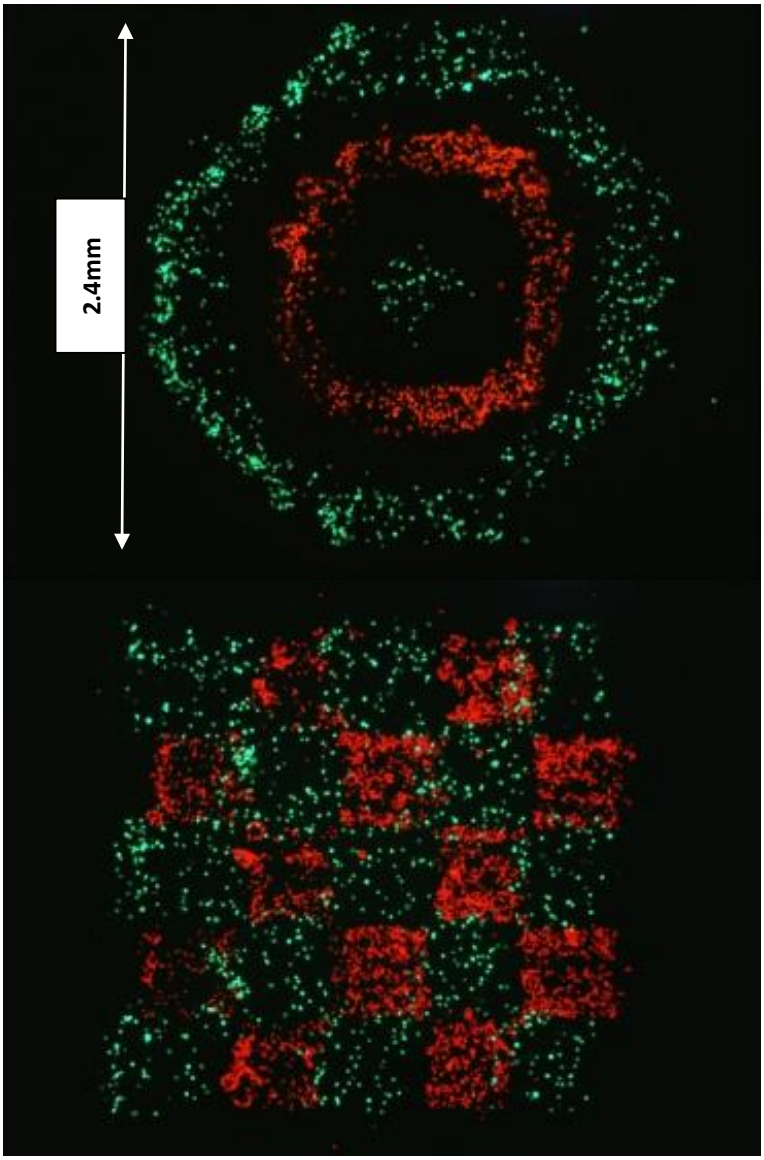

Figure 4.3: Co-culture of D1 murine mesenchymal stem cells (green) and 4T07 murine mammary tumor cells (red) printed onto collagen substrates. Images were captured using a 2.5x objective at a zero time point, immediately after printing. The cellular patterns are 2.4mm wide. (Pepper et al., 2009)

Conclusions

The capabilities of the new bioprinting system will allow further understanding and refinement of the bioprinting process, as has been demonstrated by the work

addressing nozzle clogging (Parzel *et al.*, 2009b). The ability to precisely pattern two or more cell types in two dimensions could serve as an enabling technology for investigations regarding cell migration, differentiation, and communication. Such experiments with planar systems will provide useful data for addressing our overarching goal of building a three-dimensional tissue fabrication system. The entire platform is designed to be incorporated as a subsystem of a biofabrication system capable of fabricating three dimensional tissue cultures that can be used to model biological systems.

References

Boland T, Tao X, Damon BJ, Manley B, Kesari P, Jalota S, Bhaduri S. 2007. Drop-on-demand printing of cells and materials for designer tissue constructs. Mater Sci Eng C 27(3):372-376.

Burg KJL, Delnomdedieu M, Beiler RJ, Culberson CR, Greene KG, Halberstadt CR, Holder Jr. WD, Loebsack AB, Roland WD, Johnson GA. 2002. Application of magnetic resonance microscopy to tissue engineering: A polylactide model. J Biomed Mater Res 61(3):380-390.

Burg KJL, Boland T. 2003. Minimally invasive tissue engineering composites and cell printing. IEEE Eng Med Biol 22(5):84-91.

May DJ, Lund MD, Pritchard TB, Nichols CW. 1988. Data to dots in the HP deskJet printer. Hewlett-Packard J 39(5):76-80.

Mironov V, Boland T, Trusk T, Forgacs G, Markwald RR. 2003. Organ Printing: Computer-aided jet-based 3D tissue engineering. Trends Biotechnol 21(4):157-161.

Nakamura M, Kobayashi A, Takagi F, Watanabe A, Hiruma Y, Ohuchi K, Iwasaki Y, Horie M, Morita I, Takatani S. 2005. Biocompatible inkjet printing technique for designed seeding of individual living cells. Tissue Eng 11(11-12):1658-1666.

Parzel CA, Pepper ME, Burg T, Groff RE, Burg KJL. 2009a. High resolution cell patterning and co-culture using a custom bioprinter. Trans Ann Meeting Exp Soc Biomater, San Antonio, TX.

Parzel CA, Pepper ME, Burg TC, Groff RE, Burg KJL. 2009b. EDTA enhances high-throughput two-dimensional bioprinting by inhibiting salt scaling and cell aggregation at the nozzle surface. J Tissue Eng Regen Med 3(4):260-8.

Pepper ME, Parzel CA, Burg TC, Boland T, Burg KJL, Groff RE. 2009. Design and Implementation of a two-dimensional jet bioprinter, IEEE EMBS, Minneapolis, MN.

Saunders RE, Gough JE and Derby B. 2008. Delivery of human fibroblast cells by piezoelectric drop-on-demand inkjet printing. Biomaterials 29(2):193-203.

Skalak R. 1993. Tissue engineering. Proc 15th Ann Int Conf IEEE EMBS 1112-113.

Vernon RB, Gooden MD, Lara SL, Wright TN. 2005. Microgrooved fibrillar collagen membranes as scaffolds for cell support and alignment. Biomaterials 26(16):3131-40.

Wilson Jr. WC, Boland T. 2003. Cell and organ printing 1: protein and cell printers. Anat Rec A. Discov Mol Cell Evol Biol 272(2):491-496.

Xu F, Burg KJL. 2007. Three-dimensional polymeric systems for cancer cell studies. Cytotechnol 54(3):135-43.

Xu T, Gregory CA, Molnar P, Cui X, Jalota S, Bhaduri SB, Boland T. 2006. Viability and electrophysiology of neural cell structures generated by the inkjet printing method. Biomaterials 27(19):3580-3588.

Xu T, Jin J, Gregory C, Hickman JJ, Boland T. 2005. Inkjet printing of viable mammalian cells. Biomaterials 26(1):93-99.

CHAPTER 5

Select results in this chapter were generated by an Institute for Biological Interfaces of Engineering interdisciplinary team, including Clemson University doctoral candidate Matthew Pepper, and were presented at the 2010 Annual Meeting and Exposition of the Society For Biomaterials (Pepper et al., 2010).

THERMAL INKJET PRINTING FOR PRECISION HISTOLOGICAL STAINING

Introduction

In the field of histotechnology, the driving (and often opposing) forces of efficacy, resolution, processing speed, sample volumes, and cost are informally balanced in the marketplace through the supply of and demand for new staining technologies. In this chapter, a reagent deposition system is presented that has the ability to create custom patterns and to precisely apply them to histology samples. The general staining problem can be classified into three categories: bulk, low-volume, and drop-by-drop (**Figure 5.1**). Each category is identified by the quantity of the reagent used to expose the target tissue.

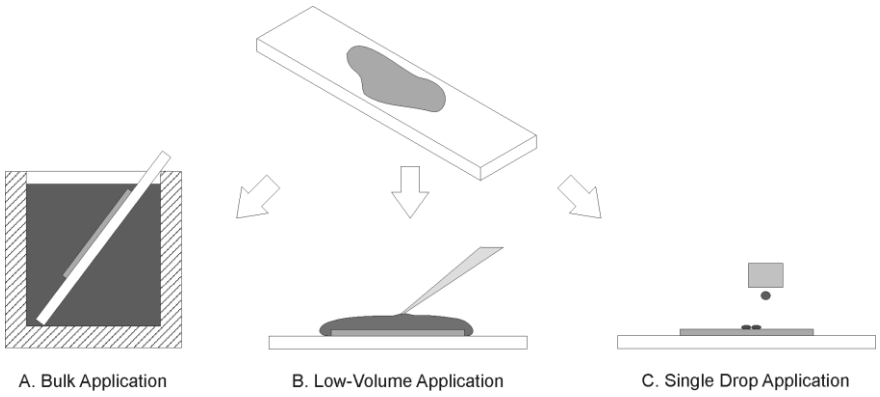

Figure 5.1: Reagent application approaches: A) Using the bulk approach, the entire tissue sample is submerged in the reagent B) In the low-volume approach, a low volume of reagent is used to cover the tissue sample C) In the single drop approach, µL or pL volumes of reagent are deposited at a desired location on the sample.

Bulk Approach

In the bulk approach, the entire tissue sample, including the sample support (e.g. a microscope slide), is exposed to a large volume of reagent (Humphreys *et al.*, 1996; Humason, 1967; Preece, 1972). In this approach, there is no discrimination in applying the reagent relative to the tissue structure. The bulk approach has the advantage that there will generally be sufficient volume of the reagent in order to support the expected staining reaction. The results of the bulk methods are well known and the standard for comparison of new methods. The bulk approach can be automated with commercially available equipment for high-throughput laboratories to provide high-volume staining with customization on a per slide basis (Titford, 2006; Neel, 1998). While these machines provide maximum efficiency and minimum reagent use, such machines are not usually found in smaller research laboratories, where protocols are executed by hand. In smaller laboratories, the most economical use of reagent is to contain it in staining jars for repeated use. Some disadvantages to this model are risk of contamination and uncertainty of the strength of the reagent (Platt, *et al.*, 2009); additionally, evaporation causes reagent waste.

Low Volume Approach

To conserve reagent and offer more staining options, lower volumes of stain can be implemented (Soma and Kamaraj, 2010; Ungaro, 2009), using precision application methodologies. One means of achieving a low-volume approach is with pipetting methods, such as shown in **Figure 5.1B**. The low-volume approach has many

advantages: 1) The amount of stain per slide can be reduced if the reagent application is limited to only the tissue, thus avoiding waste if many samples are not required 2) Fresh reagent may be supplied to each sample to avoid contamination. However, a drop-on-demand approach has the same advantages of the low volume approach but has better patterning ability and customization.

Drop-on-Demand Approach

The drop-on-demand approach described in this chapter represents a further extension of the low-volume approach and involves applying the reagent one drop at a time. The droplets are dispensed in a pattern to cover a selected section of the tissue sample or sections of multiple tissue samples. When reagents are administered one drop at a time, the user has a high level of control over usage and placement. Inkjet technology (May *et al.,* 1988*)*, used in printing applications for decades, can rapidly dispense small volumes of liquid (in the pL range). Inkjet or bubble jet printing is classified as a drop-on-demand technology, where a single droplet is formed and released at the command of the control system. The role of this technology has expanded from traditional printing of ink onto paper into a multitude of applications ranging from semiconductor manufacturing (Burns *et al.,* 2003) to cake decorating. A system that uses thermal inkjet technology to precisely pattern and deposit reagent onto tissue samples could be of great service to the histological community. A system which deposits reagent in small amounts and concurrently stains separate parts of the sample with different stains could open up new avenues and opportunities for histologic processes. For example, a

research team in New Zealand used Toludine Blue (0.12% in 1% borax) to manually stain milled sections of pig cardic atria and rat cochlea for three dimensional reconstruction (Sands *et al.,* 2006). This team indicated that their procedure would be improved if they had a more consistent and careful way to stain each section. Another evolving need involves staining certain specimens that may contain elements, such as absorbable sutures, that can be damaged during histological processing (Burg *et al.*, 1996). Only careful control of the reagent would allow exposure of the surrounding tissue without damaging the artificial element. This chapter explores a system that can meet these needs by staining tissues with uniform or complex patterns using small volumes of different reagents.

Materials and Methods

To demonstrate the efficacy of this system as a precision staining device, four experiments were performed. In the first experiment, Analine Blue (PolyScientific, Bay Shore, NY) was used to print Patterns 2 and 3 onto bovine dermal tissue; Patterns 1, 3, 4, and 5 were printed onto bovine spleen tissue. In the second experiment, Toludine Blue (Fisher Scientific, Pittsburgh, PA) was used to stain Patterns 2 and 3 (**Figure 5.2**) onto deparaffinized bovine dermal tissue. . In the third experiment fluorescent cell tracker probes were printed onto a monolayer of cells, using Patterns 2 and 3. Lastly, in the fourth experiment, primary and secondary antibodies were printed on the surface of a cell monolayer in Pattern 6 to demonstrate the value of the printer in basic immunofluroescence protocols.

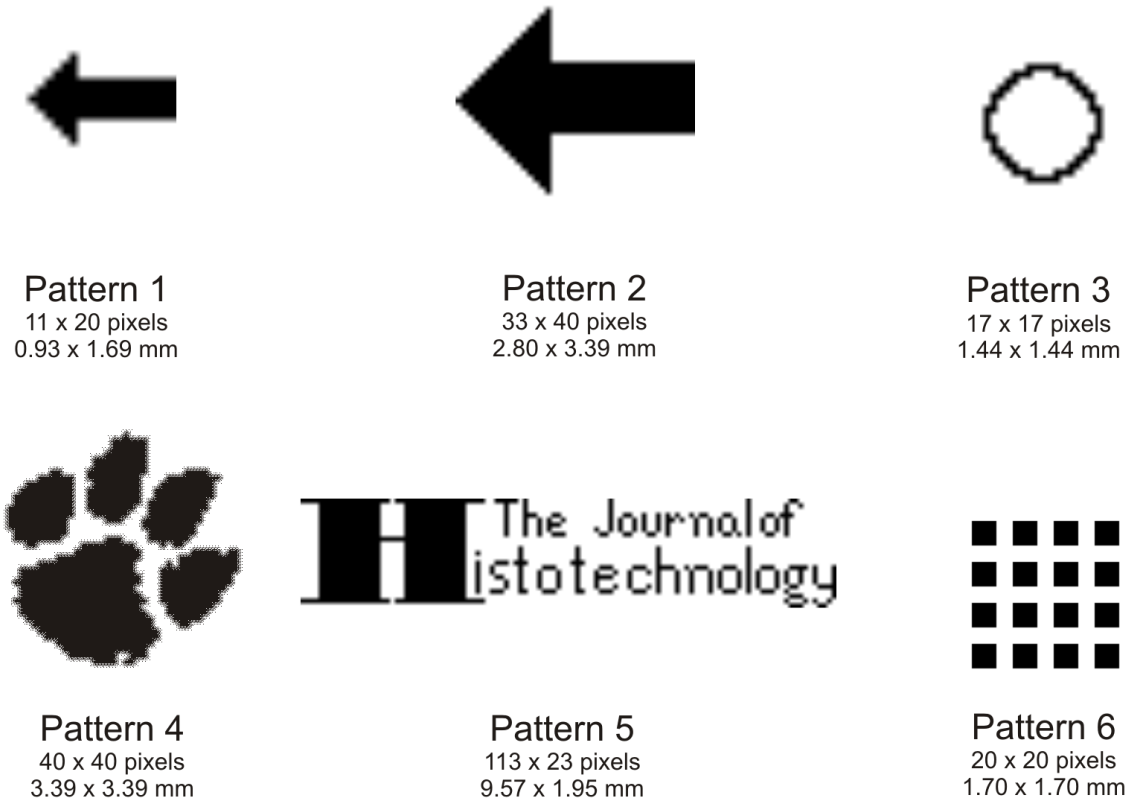

Figure 5.2: Series of six patterns that were printed using different staining reagents. Each pattern is labeled with its pixel dimensions as well as printed size (length by height).

Toludine Blue

To pattern Toludine Blue, paraffin was removed from tissue sections of 5µm thickness, and the samples were maintained in distilled water in a coplin jar. Just prior to printing, each slide with a tissue section was removed from the water and blotted dry. The Toludine Blue was strained through a 40µm filter before pipetting 150 µL of the solution into an HP26 cartridge (Hewlett Packard, Palo Alto, CA). Patterns 2 and 3 were

loaded in the software and stain was printed onto the dermal tissue. Each pattern was printed 15 times in the same location (i.e. 15 passes) to impart a significant color change on the tissue. When printing was completed, a glass coverslip (Hausser Scientific, Horsham, PA) was affixed to each sample using Permount® (Fisher) and images were captured. The pictures were captured on a Zeiss Axiovert 35 microscope (Carl Zeiss Inc., Jena, Germany) and a ProgRes C10plus 3.3 MP camera (JenOptik, Jena, Germany).

Analine Blue

Analine Blue was patterned on both bovine dermal tissue and bovine spleen tissue samples. Samples were prepared and analyzed in a similar manner as described above, however the Analine Blue only required one pass for each sample, both for dermal and spleen tissue. Patterns 2 and 3 were printed on dermal tissue samples while Patterns 1, 3, 4, and 5 were printed onto spleen tissue, then the samples were coverslipped and photographed.

Fluorescent CellTracker™ Probes

Fluorescent CellTracker™ probes (Invitrogen Corporation, Carlsbad, CA) were used to demonstrate the effectiveness in applying stain to a cell monolayer in a specified pattern using inkjet techniques. D1 murine mesenchymal stem cells (American Type Culture Collection (ATCC), Manassas, VA) were seeded onto polystyrene cell culture treated slides (Nalge Nunc International, Rochester, NY) and allowed to attach overnight. The cells were maintained in Dulbecco's Modified Eagle's Medium (DMEM) containing

4mM L-glutamine, 1.5g/L sodium bicarbonate, and 4.5g/L glucose (American Type Culture Collection (ATCC), Manassas, VA) and 500mL were supplemented with 50mL fetal bovine serium (Mediatech, Inc., Manassas, VA), 5mL antibiotic/antimycotic (Invitrogen), and 1mL fungizone (Invitrogen). Cells were maintained in an incubator (Sanyo Scientific, San Diego, CA) at 37C and 5% CO2. To complete the procedure, slides were rinsed in Dulbecco's phosphate buffered saline (DPBS) (Sigma-Aldrich, St. Louis, MO) and air-dried briefly in a sterile biosafety cabinet (Labconco, Kansas City, MO). The red and green CellTracker™ probes were prepared by diluting the lyophilized product in dimethyl sulfoxide (Sigma) to a final concentration of 10mM. A working solution was then made by diluting the stock solution in serum-free DMEM and Hank's Balanced Salt Solution containing 0.53mM ethylenediaminetetraacetic acid (EDTA) (MP Biomedicals, LLC, Solon, OH). Patterns 2 and 3 were printed in red and green tracker probes respectively onto the monolayer, and 5-8 passes of the printer were necessary to achieve a high degree of fluorescence.

Immunofluorescence Staining

The following methods were used to demonstrate the utility of the printer in augmenting basic immunofluorescence techniques. F3T3 murine fibroblasts (ATCC) were seeded at 50% confluence onto two-well glass chamber slides (Nalge Nunc International) and maintained in culture at 37°C and 5% CO_2 for 24 hours. Following incubation, cells were washed in phosphate buffered saline (PBS) (Sigma) and then fixed for 45 minutes in 10% neutral buffered formalin (VWR, West Chester, PA). Cells were

rinsed again in PBS and then permeabilized for 5 minutes with a solution of 0.2% Triton X-100 in PBS. Samples were blocked for at least 30 minutes with 10% normal goat serum (Sigma) containing 0.05% Triton X-100 (Sigma). All of these steps were performed by flooding the slides with bulk volumes of the solutions listed.

When the blocking step was complete, the chambers were removed and each slide was placed on the printing stage. The primary antibody (monoclonal anti-vimentin antibody produced in a mouse) (Sigma) was diluted 1:50 in distilled water, and 250µL of the solution was pipetted into an HP26 cartridge well. Pattern 6 (**Figure 5.2**) was printed onto each slide in three separate locations. The primary antibody solution was deposited onto each of the three locations every 77 seconds for 30 minutes. Subsequently, the slide was rinsed twice with a bulk volume of PBS without removing the slide from the stage. The secondary antibody (Alexa Fluor® 488 (Ex. 494nm, Em. 519nm) goat anti-mouse IgG (H+L)) (Invitrogen) was diluted to a concentration of 5µL/mL in water and subsequently pipetted into a separate cartridge. The secondary antibody was printed in the same three locations every 77 seconds for 15 minutes, protected from light. The slide was immediately removed from the stage and rinsed twice in PBS, then rinsed in distilled water. A separate control slide was prepared by completely covering the cell monolayer with bulk volumes of the primary and secondary antibodies and incubating the slide at room temperature for 30 minutes and 15 minutes, respectively. Slides were coverslipped with glass coverslips (Hausser Scientific) using a DAPI-containing mounting medium (Ex. 345nm, Em. 458nm) (ProLong® Gold antifade reagent with DAPI, Invitrogen) and analyzed using a The samples were photographed using a Zeiss Axiovert 40 CFL

microscope (Carl Zeiss AG Oberkochen, Germany) equipped with a 50W Xenon lamp. The images were captured using an Zeiss AxioCam MRC 5, processed with Zeiss AxioVision LE 4.6 (Carl Zeiss Microimagining, Inc., Thornwood, NY), and combined using GIMP.

Results and Discussion

The bovine dermal tissue treated with Toludine Blue stained, but only over a longer timeframe than the other staining procedures because of the number of passes required to produce a color change (**Figure 5.3**). The coarse grain of the dermal tissue, due to the presence of hair follicles, slightly affected the definition of the patterns. Since it was unclear how quickly the stain would mark the tissue, 15 passes were arbitrarily selected. The Analine Blue in 1% acetic acid stained the tissue a much darker color than the Toludine Blue, and provided dermal tissue patterns with better definition, using less reagent and allowing more critical study of staining performance. Different tissues will disperse stain differently, and future testing must be conducted with each desired tissue type and stain to ensure the desired effect.

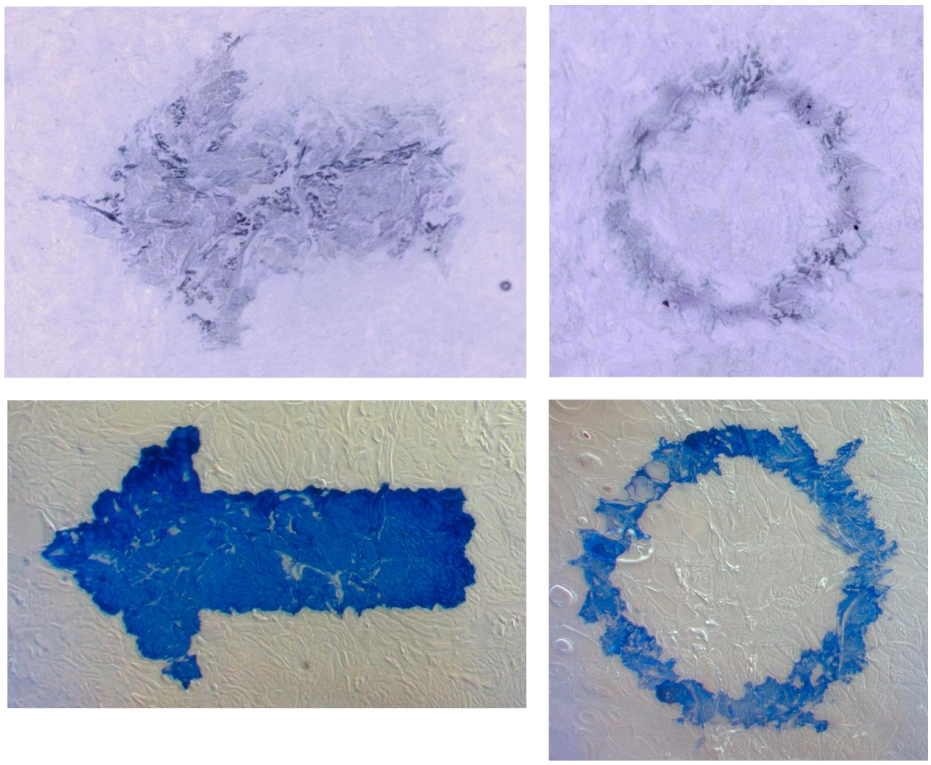

Figure 5.3: The top two images show Toluidine Blue printed onto bovine dermal tissue using 15 passes of the printer. The bottom two images show Analine Blue printed onto bovine dermal tissue in one pass. Note that each stain follows the natural texture of the tissue. Top left – pattern 2 (2.80 x 3.39mm), Bottom left – pattern 1 (0.93 x 1.69mm), Right – pattern 3 (1.44 x 1.44mm).

The spleen tissue and stem cell monolayer results more clearly demonstrated the capabilities of the system to deposit stain. In each of the results shown in **Figure 5.4**, and especially with Pattern 5, the individual drops of stain could be distinguished. Each drop of stain measured approximately 90 µm in diameter.

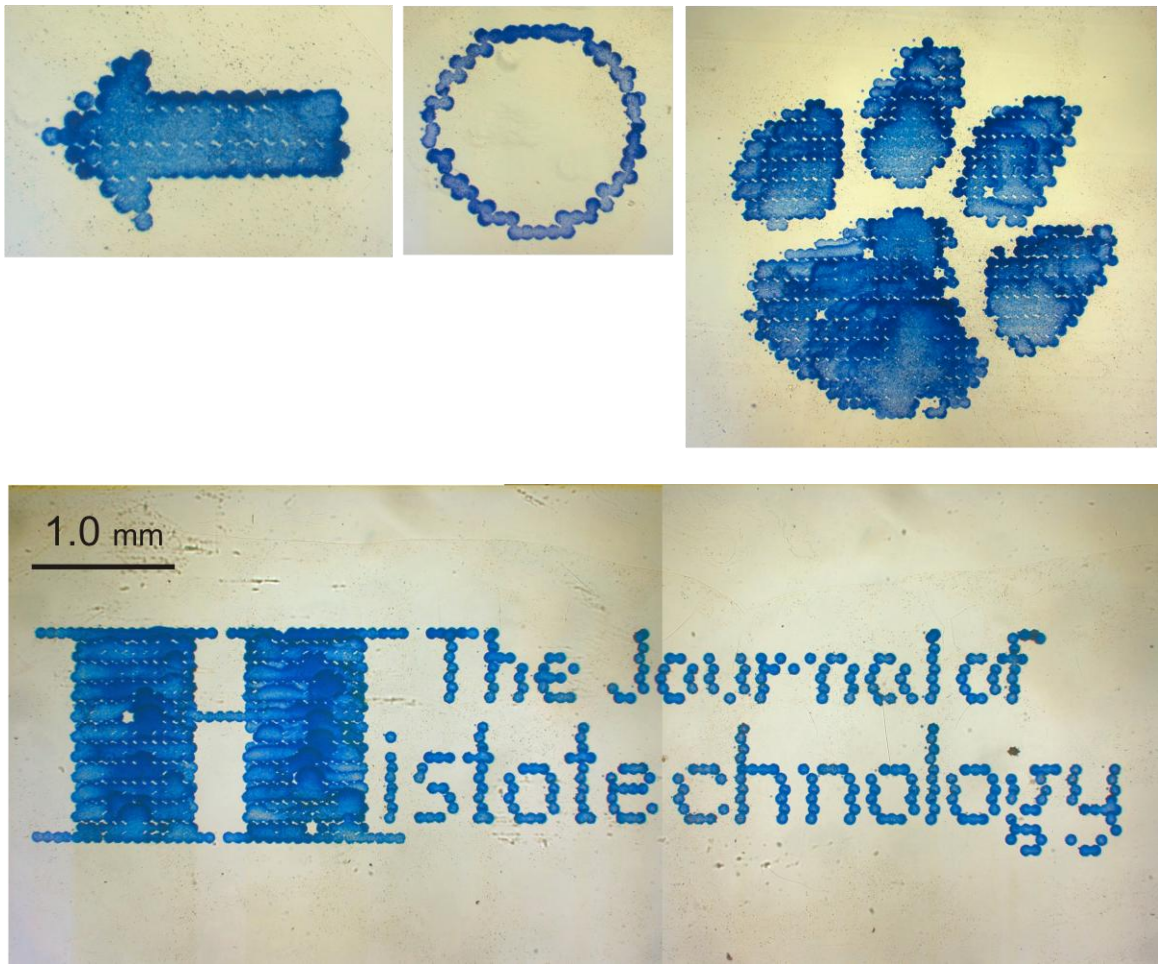

Figure 5.4: Images of bovine spleen tissue patterned with Analine Blue stain. All images are on the same scale

Figure 5.5 shows fluorescence microscopy imaging of red CellTracker™ probes printed using Pattern 2 onto a D1 cell monolayer with five passes of the printer, and Pattern 3 printed onto a D1 monolayer, using green tracker probes and eight passes of the printer. The definition of both patterns was very sharp, with the corners on Pattern 2 providing the best example.

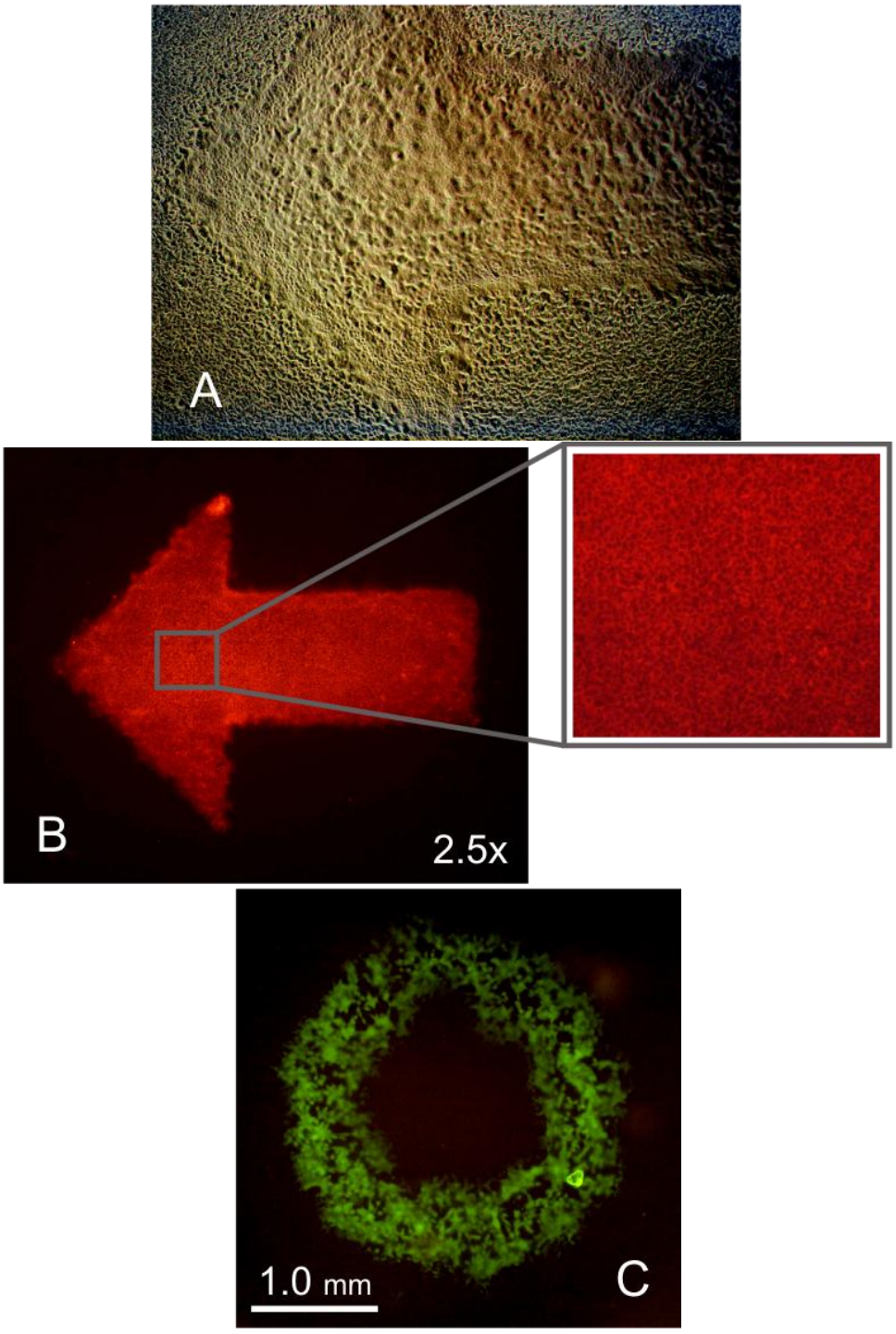

***Figure 5.5:** A) shows a monolayer of D1 mesenchymal stem cells under brightfield microscopy after staining with red fluorescent probes. B) shows the same monolayer*

under fluorescent light. C) shows a circular pattern printed onto a D1 mononlayer using a green fluorescent probe. The printer required five to eight passes to effectively stain the monolayers.

Figure 5.6 presents images of the control and experimental slides at various magnifications, showing either vimentin or nuclear staining, or a combination of both. The far left image shows the entire 4x4 pattern of squares (each square is 25 pixels) printed with the antibody stain specific to vimentin. The next image compares the control vimentin stain (top) with the printed vimentin stain (bottom) using the 10x objective. The third set of images compares the blue stained nuclei of the control (top) and experimental slides (bottom). Note that in both cases, DAPI was introduced to the whole slide in the mounting medium. Merged images depict both DAPI and vimentin in the control (top) and experimental (bottom) slides, and an enlarged section is chosen to show the details of the images. In the experimental samples, vimentin staining is only apparent in the areas of the printed pattern though nuclear staining reveals the presence of cells along the entire surface of the slide.

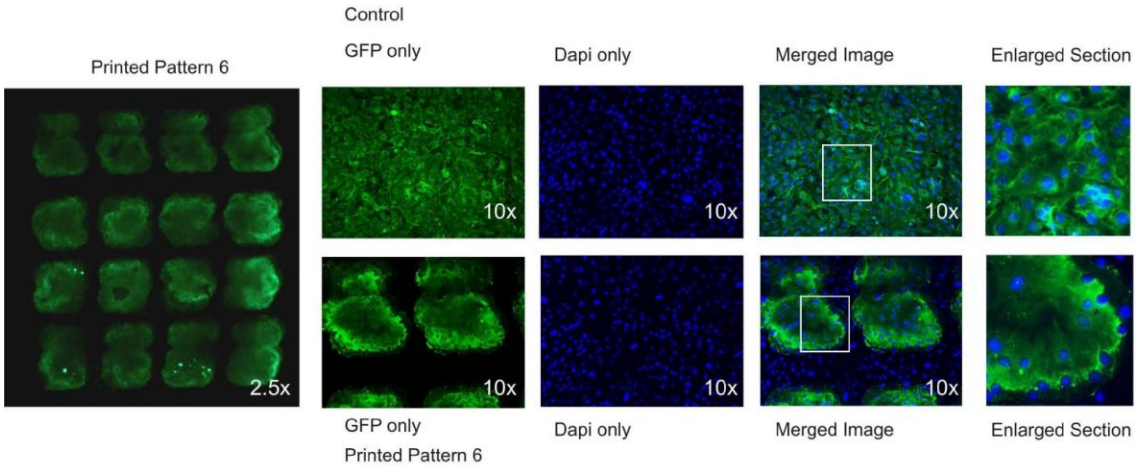

Figure 5.6: Images of the control and experimental immunofluorescence slides using various microscope objectives, showing either vimentin or nuclear staining, or a combination of both.

Conclusions

The use of a bioprinting system based on drop-on-demand thermal inkjet technology is a viable technology for depositing reagents at the picoliter scale. The ability to tailor the amount of reagent based on tissue and protocol is a key benefit of this system. Future users will need to make adjustments to their protocols, whether for staining or immunohistochemistry. The bioprinting system has the ability to deposit multiple drops in a single location and simulate multiple passes, which should simplify experiment design.

The speed and flexibility of the software allows many different potential uses. One application for this system could be in a collegiate classroom where it could help create samples for classroom use by highlighting different structures in a sample. In addition to enhancing traditional histological methods, bioprinting can also be used to stain cell monolayers, as an analysis tool following cell culture protocols. The

introduction of bioprinting techniques into cell culture assays could prove efficient and effective when working with tissue engineered constructs that are difficult to replicate in large quantities. Whether or not the protein or property is uniformly distributed, several stains can be applied to a single sample in a specified pattern, which can greatly decrease samples sizes and the amount of reagent required for cell analysis. With multiple reagent options and fine resolution patterning, histological users could label their samples precisely and economically with a minimum of configuration time.

References

Burg KJL, Jenkins L, Powers DL, Shalaby SW. 1996. Special considerations in embedding a lactide absorbable polymer. J Histotechnol 19(1):39-43.

Burns S, Cain P, Mills J, Wang J, Sirringhaus H. 2003. Inkjet printing of polymer thin-film transistor circuits. MRS Bulletin 28(11):829-834.

Humason GL. 1962. Animal Tissue Techniques, 2nd Ed. W.H. Freeman and Company, San Francisco, CA.

Humphreys TR, Nemeth A, McCrevey S, Baer SC, Goldberg LH. 1996. A pilot study comparing toluidine blue and hematoxylin and eosin staining of basal cell and squamous cell carcinoma during Mohs surgery. Dermatol Surg 22:693-697.

May DJ, Lund MD, Pritchard TB, Nichols CW. 1988. Data to dots in the HP deskJet printer. Hewlett-Packard J 39(5):76-80.

Neel TL, Moreau A, Laboisse C, Truchaud A. 1998. Comparative evaluation of automated systems in immunohistochemistry. Clinica Chimica Acta 278(2):185-192.

Pepper M, Burg TC, Groff RE, Cass CAP, Jenkins LL, Burg KJL. 2010. Precision staining of histological samples using thermal inkjet technology. Trans 2010 Ann Meeting Exp Soc Biomater, Seattle, WA.

Platt E, Sommer P, McDonald L, Bennett A, Hunt J. 2009. Tissue floaters and contaminants in the histology laboratory. Arch Pathol Lab Med 133:973-978.

Preece A. 1972. A Manual for Histologic Technicians, 3rd Ed. Little, Brown and Company, Boston, MA.

Sands G, Gerneke D, Smaill B, Grice I. 2006. Automated extended volume imaging of tissue using confocal and optical microscopy. Proc 28th IEEE EMBS Ann Int Conf,:133-136, New York City, NY.

Soma M and Kamaraj S. 2010. Detection of human papillomavirus in cervical gradings by immunohistochemistry and typing of HPV 16 and 18 in high-grades by polymerase chain reaction. Journal of Laboratory Physicians 2(1):31-36.

Titford, M. 2006. A short history of histopathology technique. The Journal of Histotechnology 29(2):99-109.

Ungaro R, Abreu MT, Fukata M. 2009. Practical techniques for detection of Toll-like Receptor-4 (TLR4) in the human intestine. Methods Mol Biol 517:1-19.

CHAPTER 6

Select results in this chapter were generated as part of an Institute for Biological Interfaces of Engineering interdisciplinary team project in collaboration with Clemson University doctoral student Matthew Pepper and were presented at the 2010 IEEE Engineering in Medicine and Biology Society Conference (Pepper et al., 2010).

EVALUATION OF PARACRINE SIGNALING BY MURINE CELLS PATTERNED USING INKJET TECHNOLOGY

Introduction

Details in Chapter 4 demonstrated that live mammalian cells can be successfully patterned into two-dimensional patterns in both mono-culture and co-culture patterns. These cells have been maintained in culture and do continue to proliferate and migrate across the surface of a Type I collagen coating over a period of 120 hours. The purpose of this proof-of-concept study was to confirm the utility of the inkjet printer for examining cell-cell interactions in 2D.

Section 1: Post-Bioprinting Processing Methods to Improve Cell Viability and Pattern Fidelity in Heterogeneous Tissue Test Systems

Most *in vitro* methods for studying cell-cell interactions, e.g. chemotactic assays (Doerr and Jones, 1996; Pennisi *et al.*, 2002; Takeda *et al.*, 2007), use uniformly random distributions of cells, whereas cell-cell interactions in native tissue occur in a highly structured, heterogeneous environment. Bioprinting can be used to create heterogeneous co-cultures with placement precision better than 100µm, i.e. within the relevant range for biological signaling (Francis and Palsson, 1997). Bioprinting thus offers the potential to generate improved *in vitro* models of cell-cell interactions that more accurately emulate *in vivo* conditions. While developing a tissue test system to study the interaction among

D1 and 4T1 cells (**Figure 6.1a**), several challenges were encountered in processing samples after bioprinting a pattern. If the application of medium is delayed, the viability of a sample is diminished (e.g. **Figure 6.1b**). Alternatively, if medium is applied directly after printing, the pattern fidelity is degraded since the cells have not had sufficient time to attach to the substrate (e.g. **Figure 6.1c**) and can be displaced from the printed location. Based on observation, the decreased viability is believed to be due to dehydration of the cells. This motivates a search for treatments to keep the cells hydrated without disturbing their intended position.

This section presents an evaluation of several post-bioprinting processing methods to maintain consistently high cell viability and pattern fidelity. Each method consists of a set of treatments applied at specific times. The treatments include application of 10% serum-inclusive Dulbecco's Modified Eagle's Medium (DMEM) using a commercial nebulizer, application of Hank's Balanced Salt Solution (HBSS) containing Mg^{2+} and Ca^{2+} via bioprinting, and application of a collagen overlay solution using a micro-pipetter. Also, attempts to print cells at higher area density is reported.

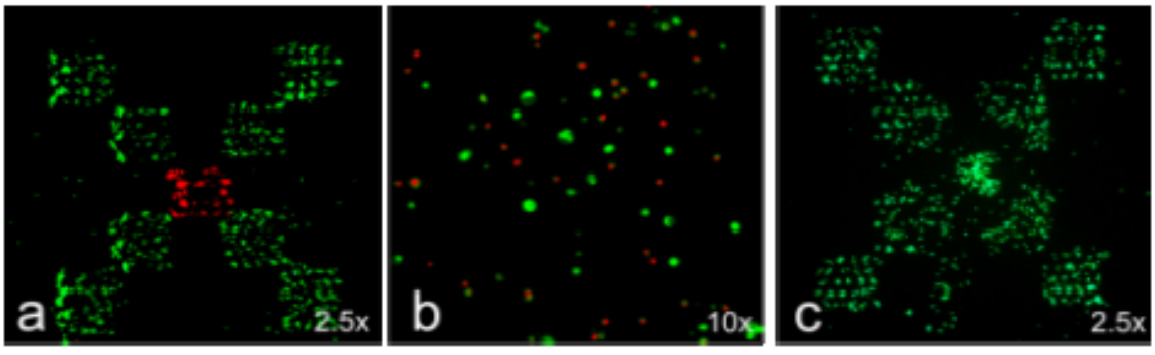

Figure 6.1: a) A printed 'X' pattern with good fidelity consisting of D1 murine mesenchymal stem cells (green) and 4T1 murine tumor cells (red), 2.5x objective b) A

LIVE/DEAD® assay of the center of the printed 'X' pattern in which viability was unexpectedly low, where red indicates dead cells and green indicates living cells, 10x objective c) A printed 'X' pattern consisting of D1 mesenchymal stem cells (green) with poor pattern fidelity, 2.5x objective.

Materials and Methods

Cell Culture

D1 murine mesenchymal stem cells (American Type Culture Collection (ATCC), Manassas, VA) were maintained in Dulbecco's Modified Eagle's Medium (DMEM) (ATCC) containing 4mM L-glutamine, 1.5g/L sodium bicarbonate, and 4.5g/L glucose; each 500mL was supplemented with 50mL fetal bovine serum (FBS; Hyclone, Logan, UT), 5mL antibiotic/antimycotic (Invitrogen, Gibco, Carlsbad, CA), and 1mL fungizone (Invitrogen), referred to as D1 maintenance medium. The culture medium was replaced every 48 to 72 hours as required, and cells were maintained in an incubator (Sanyo Scientific, San Diego, CA) at 37°C and 5% CO_2. To prepare cellular bio-inks for printing, D1s were labeled using green fluorescent CellTracker™ probes (Invitrogen), and cells were suspended in serum-free DMEM (SF-DMEM) at a density two times the desired final concentration. All cell suspensions were filtered using 40µm sterile cell strainers (BD Falcon, Franklin Lakes, NJ). Just prior to printing, 100µL of the cell suspension was combined with 100µL of Hank's Balanced Salt Solution (HBSS) (without Mg^{2+} and Ca^{2+}) (Sigma-Aldrich, St. Louis, MO) containing 1.06mM ethylenediaminetetraacetic acid (EDTA) (MP Biomedicals, LLC, Solon, OH), and was subsequently deposited into the HP26 (Hewlett Packard, Palo Alto, CA) cartridge well (Parzel *et al.*, 2009). Thus, the resulting 200µL of bio-ink consisted of D1 cells

suspended in 50% SF-DMEM and 50% HBSS, with a final EDTA concentration of 0.53mM.

Tissue Test System Fabrication

Collagen Substrate Preparation

Thin collagen gels (approximately 1mm) were used as substrates on which to print because of their ability to retain moisture (improve cell viability) and absorb printed medium to prevent cell flooding (improve pattern retention). Three collagen substrates (i.e. three samples) were prepared on a polystyrene cell culture slide (Nalg-Nunc, Rochester, NY). Accordingly, three holes were punched in a silicone (McMaster-Carr, Atlanta, GA) mask (1mm thick) using a 14mm (inner diameter) punch, and the mask was subsequently aligned with the edge of the slide (**Figure 6.2c**). The hydrophobicity of the silicone provided containment of the collagen and D1 maintenance medium, as described above.

A 2.0mg/mL collagen solution was prepared by combining 6mL collagen stock solution (3.0mg/mL - PureCol™) (Advanced Biomatrix, San Diego, CA) with 668µL 10x Dulbecco's Phosphate Buffered Saline (DPBS) (Sigma), 900µL FBS, and 1.4mL SF-DMEM; a small volume (approximately 80µL) of 1N NaOH (Fisher Scientific, Pittsburgh, PA) was added to neutralize the solution. A volume of 200µL of the collagen solution was pipetted into each 14mm sample well, and the collagen gels were polymerized in an incubator at 37°C and 5% CO_2 for at least 4 hours. Following incubation, the gels were soaked in sterile distilled water for 1 hour and then covered

with a 1:1 solution of FBS to SF-DMEM for at least 1 hour to promote cell attachment. Just prior to printing, the FBS/SF-DMEM solution was carefully aspirated so that no macroscopic traces of liquid remained on the surface.

Method Investigation

This experiment consisted of 12 slides, in which two repetitions of four methods and two controls were tested. A pattern was printed in each sample area using an HP26 inkjet cartridge based bioprinter (Pepper *et al.*, 2009). The printed pattern (**Figure 6.2a**) consisted of nine squares of five pixels by five pixels (≈ 400µm by 400µm) arranged in an 'X' pattern (≈ 2mm by 2mm). The area of a pixel generally represents the area covered by a single drop, however, using a recently added feature of the bioprinter, the pattern was printed with a density of four, i.e. a nozzle fires four drops while passing over a pattern pixel. Additionally, the patterns were printed on the sample three times, providing a total of 12 fired drops for each pixel in the pattern. Table 1 describes the four post-bioprinting methods that were investigated. Each method consists of a sequence of treatments. Each column in the table represents the number of minutes after printing at which a treatment was applied. Between treatments, each slide was kept in an incubator at 37°C and 5% CO_2.

Table 6.1: Post-bioprinting processing methods.

	0 min.	30 min.	60 min.	120 min.
Method 1			Nebulizer	Medium
Method 2			Collagen	Medium
Method 3		Nebulizer	Collagen	Medium
Method 4	HBSS		Collagen	Medium
Control 1	Medium			
Control 2	Collagen		Medium	

In the nebulizer treatment, C-Flex® tubing (Cole-Parmer, Vernon Hills, Illinois) was attached to the output of the medicine cup of an Omron NEC-25 ComAir XLT desktop nebulizer (Omron Healthcare, Inc., Bannockburn, IL) and the tube was held approximately 3cm above each sample. The medicine cup was filled with 6mL of D1 maintenance medium. Each sample of each treated slide was exposed to a mist of D1 maintenance medium for approximately 10 seconds. In the collagen treatment, 50µL of 2.0mg/mL collagen solution (described previously) was slowly pipetted on top of each sample. In the HBSS treatment, a separate printer cartridge was used to apply HBSS over the already-printed sample (**Figure 6.2b**). In all methods and controls, the last treatment was a careful application of 250µL of D1 maintenance medium. Each sample was imaged immediately after adding D1 maintenance medium and then again 24 hours later. The images were taken with a Zeiss Axiovert 40 CFL microscope (Carl Zeiss, Oberkochen, Germany) equipped with a 50W xenon lamp. The images were captured using a Zeiss AxioCam MRC 5, processed with Zeiss AxioVision LE 4.6 (Carl Zeiss Microimaging, Inc., Thornwood, NY), and combined using GIMP. Printed samples were

evaluated for viability using a LIVE/DEAD® viability assay (Invitrogen), causing live and dead cells to fluoresce green and red, respectively.

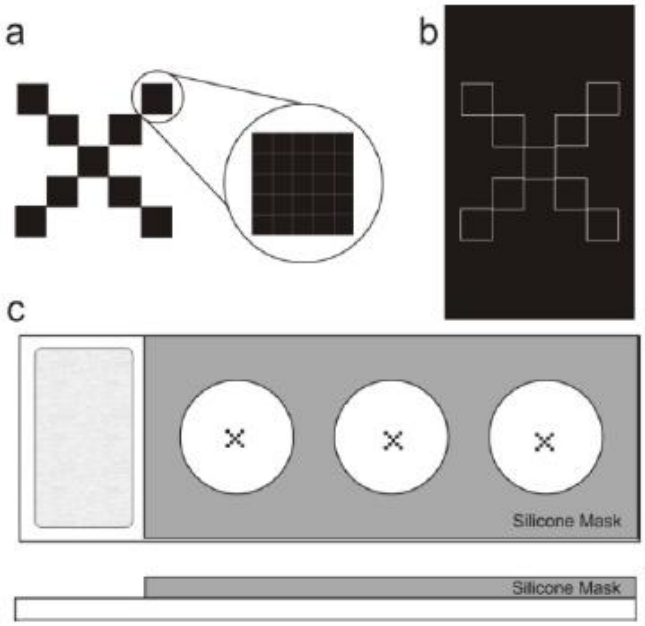

Figure 6.2: a) Shows the printed 'X' pattern used for all samples in this study, with the upper right square enlarged to show its construction from 5x5 pixels b) The black square represents the HBSS pattern printed over the 'X' pattern (represented by the white outline) in Method 4 c) A depiction of each slide, the sample mask, and the location of the printed 'X' pattern.

Results and Discussion

In both controls, a liquid was applied to the sample immediately after bioprinting. Since the cells did not have time to attach to the substrate, the control samples showed (following a qualitative assessment under the microscope) poor pattern fidelity (**Figures 6.3e,f**) but good viability (**Figures 6.3p,q**), as expected. From this result, we conclude

that D1 cells are consistently viable when printed and immediately hydrated with medium or collagen. The viability of the collagen-overlay control method (**Figure 6.3q**) showed fewer dead cells than the medium-only control (**Figure 6.3p**), perhaps because the anchorage-dependent D1 cells prefer the added surface area provided by the collagen overlay. Interestingly, the collagen overlay control maintained reasonable pattern fidelity, indicating that the higher viscosity collagen does not disturb the cells as much as D1 maintenance medium when applied (i.e. the collagen does not flow as quickly over the surface of the pattern).

The nebulizer treatment was introduced to provide a noncontact method of hydrating the cells. Immediately after applying medium, samples created using Method 1 (**Figure 6.3a**), in which the nebulizer treatment was applied after 60 minutes, appeared to have slightly poorer fidelity than samples created using Methods 2-4 (**Figures 6.3b-d**).

The HBSS treatment is another noncontact method of hydrating the cells. In Method 4, the treatment is applied immediately after printing the cells. Surprisingly, the treatment does not decrease pattern fidelity, even though the cells have not had time to attach. The collagen substrate likely absorbs the applied liquid volume within a sufficiently short time.

Methods 2-4 all include the application of a collagen overlay. After 24 hours, the patterns for samples created by these methods (**Figures 6.3h-j**) are more distinct than patterns created by Method 1 (**Figure 6.3g**). This increased pattern retention is likely due to the collagen overlay restricting cell migration.

Samples created with Method 4 (**Figure 6.3j**) retain the pattern most distinctly at 24 hours in comparison to all the other methods. This can be explained by the HBSS applied in Method 4, which contains calcium and magnesium ions, known to promote attachment.

From the LIVE/DEAD® assay at 24 hours, the viability of samples created with all four methods is similar to that of the controls (**Figures 6.3m-q**). From previous experiments without these post-bioprinting treatments for increasing hydration, viability was markedly lower.

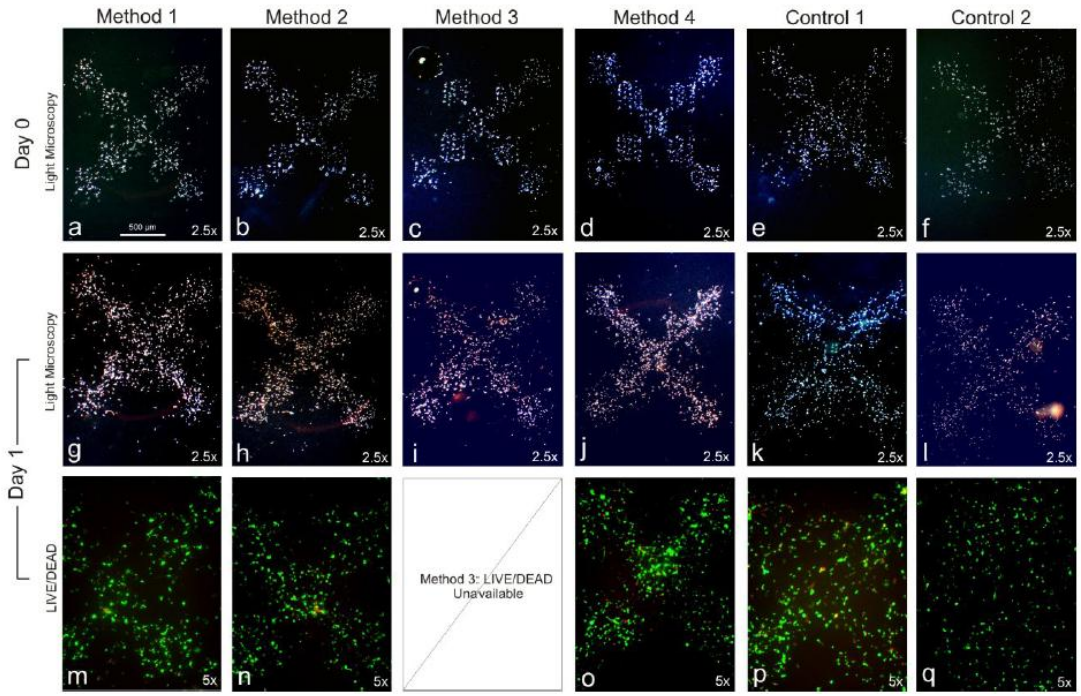

Figure 6.3: This image shows the results of all Methods and Controls for Days 0 and 1 (a to f). All samples were imaged immediately after D1 maintenance medium was applied. Twenty-four hours later, all samples were imaged again (g to l). On Day 1, m, n, and o show the LIVE/DEAD® results of patterns created using Methods 1, 2, and 4, respectively. Additionally, on Day 1 (m-q), all samples, except Method 3, were analyzed using a LIVE/DEAD® viability kit. Note how pictures n and o, which both showcase

the collagen overlay results, reflect the original pattern. Photos p and q correspond with the LIVE/DEAD® results of Controls 1 and 2. All images were captured using a 2.5x objective.

Based on these results, Method 4 was chosen as the best option for meeting the requirements of high cell viability and pattern fidelity. From a processing viewpoint, the samples are easier to fabricate because HBSS can be applied directly by the bioprinting system. However, additional quantitative studies will be necessary to ensure that this method also provides superior cell viability and pattern retention. Both HBSS and the collagen overlay promote good cell attachment, helping the pattern to remain intact over time. The collagen overlay also produces a natural signaling environment for the cells, forcing signals to diffuse through the hydrogel rather than travel via convection through media. Future studies will quantitatively assess printed samples processed using Method 4; similar to masking studies (statistics of cell placement) described in Chapter 1, individual cells will be counted in each square of the 'X' pattern so that post-processing cell viability and cell location can be better understood.

All of the experiments reported in this paper were printed with three passes with a density of four. That is, the same pattern was printed over the same spot three times and, during each pass, each pixel in the image was commanded to receive four drops from the bioprinter. The densities and passes are used to apply a higher number of cells within a given sample area, for example in order to print cells with a distribution close to confluence. In a separate set of experiments, printing at densities 4, 8, and 12 was evaluated. In density printing, the total number of drops for a given pixel is increased

from 1 to 4, 8, or 12, but that same pixel is filled (printed) in the same fixed amount of time. Thus, the frequency with which drops were fired increased with density, giving 11.4 kHz, 22.9 kHz, and 34.3 kHz respectively. The patterns printed at these different densities seemed to have approximately the same number of cells (**Figures 6.4a-c**). In fact, while printing these patterns, the average number of cells per drop decreased as the firing rate increased (**Figure 6.4d**). In **Figure 6.4e**, the different frequencies correspond to the different densities; ideally there should be 1, 4, 8, and 12 cells per pixel as the frequency (density) increases. Comparing to previous results printed at Density 1 (Parzel *et al.*, 2009), it appears that the number of cells deposited when printing a single drop in a pixel is approximately the same as deposited when printing a cluster of 4, 8, or 12 drops in a pixel. It is likely that, when printing at high speed, the cartridge nozzle does not have sufficient time to refill, so only one drop is ejected, followed by a corresponding number of misfires. Thus, achieving significantly higher cell densities in a sample cannot be achieved by merely increasing the firing frequency.

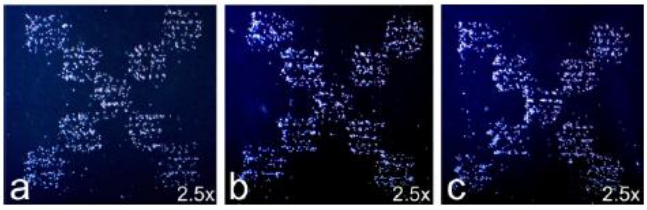

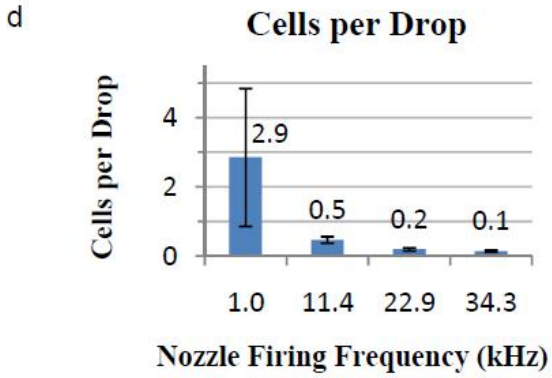

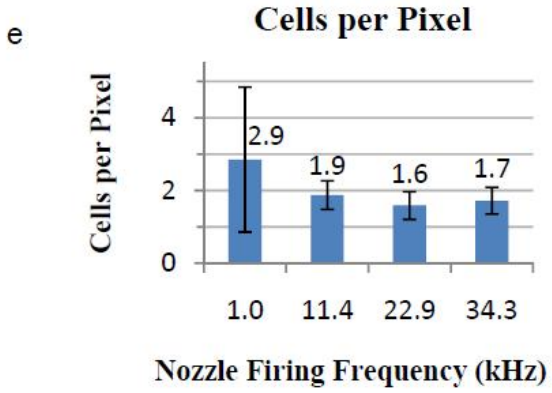

Figure 6.4: ***a-c) Correspond to the 'X' pattern printed at 4, 8, and 12 density, respectively. The patterns appear almost identical, with the number of cells in each image (a. 1033, b. 972, c. 944) being similar as well. Cells per drop (d) displays the average number of cells per drop based on the number of cells deposited at a specific nozzle firing frequency. Cells per pixel (e) shows the number of cells deposited in a pixel at a specific nozzle firing frequency. The frequencies of 11.4, 22.8, and 34.2 kHz correspond to the system firing 4, 8, or 12 drops per pixel.***

Section 2: Fabrication of Two-Dimensional Test Systems to Observe Cancer-Stromal Cell Interactions

Previous work in our lab has demonstrated the effect of 4T1 (murine metastatic mammary cancer cells) conditioned media on the differentiation capacity of D1 cells (Xu *et al.*, 2009). Differentiation of D1 cells cultured in polystyrene well plates was initiated with an adipogenic cocktail. Subsequently, the culture medium was replaced with 4T1 conditioned media (4T1-CM) for 6 days. Analysis of cultures showed a significant decrease in the amount of lipid accumulation and values of triglyceride when D1 cells in 4T1-CM were compared with the controls (D1 cells in standard DMEM). As a next step, the printer was used as a patterning tool, to analyze the effect of distance between 4T1 and D1 cells on the adipogenic differentiation capacity of D1 cells.

Materials and Methods

Cell Culture

D1 murine mesenchymal stem cells were cultured according to the manufacturer's suggested protocol, as described previously. Murine metastatic mammary tumor cells (4T1) were cultured and maintained in conditions identical to those of D1 cells. When adipogenic differentiation was initiated in various bioprinted samples, an adipocyte differentiation-inducing cocktail was introduced to the culture; this cocktail was prepared by supplementing 10mL of D1 maintenance medium with 1mL of 5mM 3-isobutyl-1-methylxanthine (IBMX) (Sigma), 1mg insulin (Sigma), and 2µL dexamethasone (Sigma) (diluted to 1mg/mL in 100% ethanol).

Assessing Viability of Bioprinted Samples Induced to Differentiate

Mono-culture 'X' patterns (two slides with three patterns per slide) were printed using D1 cells, as previously described, processed using Method 4, and images were captured immediately (using equipment described above) as Day 0. Following 1 day in culture, Slide 1 (3 samples) was tested for viability using a LIVE/DEAD® viability assay. A light microscopy image of Slide 2 was captured at Day 1, and then D1 maintenance medium was supplemented with an adipogenic cocktail for two of the three samples. Following an additional 24 hours in culture, Slide 2 was assessed using a LIVE/DEAD® assay. The LIVE/DEAD® solution was prepared according to the manufacturers's suggested protocol and applied to each gel for 45 minutes. Gels were rinsed twice in PBS (Sigma) for 10 minutes and images were taken using a Zeiss Axiovert 40 CFL microscope as described previously.

Evaluation of Cell-Cell Interaction in Two-Dimensional Test Systems

Mono- and co-culture 'X' patterns were printed (six slides per condition with three samples per slide) using D1 and 4T1 cells, as previously described, processed using Method 4, and images were captured immediately as Day 0. Following printing, samples

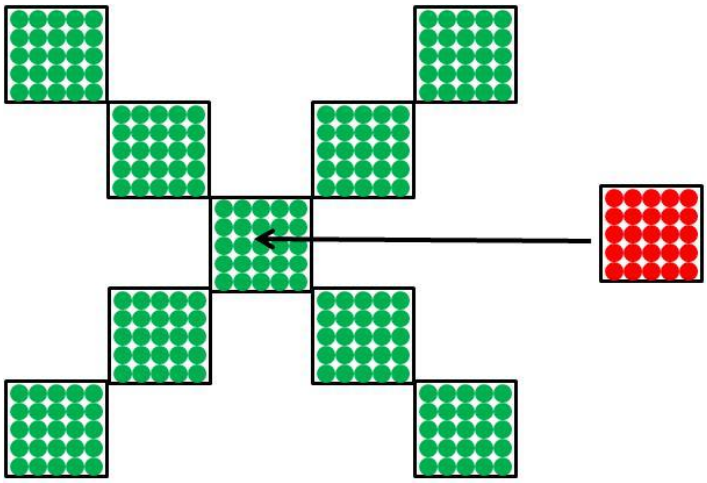

Figure 6.5: Image depicting the pattern into which D1 (green) and 4T1 (red) cells were printed. The center square contains 4T1 cells in the co-culture patterns while only D1 cells are used in the mono-culture patterns.

were covered with 250µL of bulk D1/4T1 maintenance medium and allowed to incubate for 24 hours at 37°C and 5% CO_2. Following the 1 day incubation period, images of all samples were captured as Day 1, and D1/4T1 maintenance medium was supplemented with adipogenic differentiation-inducing cocktail for an additional 1, 3, or 5 days. At each time point, a slide from each group (i.e. mono- or co-culture) was fixed in 10% neutral buffered formalin for 20 minutes, rinsed twice in PBS for 10 minutes, and stored in PBS at 4°C until staining commenced.

An immunofluorescence (IF) stain for PCNA (proliferating cell nuclear antigen) (PCNA goat polyclonal IgG, Santa Cruz Biotechnology, Inc., Santa Cruz, CA; Alexa Fluor 568 donkey anti-goat IgG (H+L), Invitrogen) was applied to each sample to better understand how the presence of 4T1 cells affected the D1 cell cycle. The protocol for this stain was adapted from previous work by others (Lee *et al.*, 2007) and is outlined in **Table 2**. Note that a negative control substituting PBS for the primary antibody was used

for one sample on all slides. All samples were counterstained with a 3μM DAPI solution (Invitrogen) in PBS for 10 minutes. Following staining, samples were imaged using an inverted fluorescence microscope described previously; nine images (per fluorescence filter set) were captured per pattern using a 10x objective and merged using Adobe Photoshop Elements (Adobe Systems Incorporated, San Jose, CA).

Table 2. Protocol for immunofluorescence staining of D1 and 4T1 cells cultured in a 3D Type I collagen gel.

PROCESS	TIME
Fix samples with 10% NBF (VWR)	20 minutes
Rinse samples with PBS-Glycine (100mM) (98%, Sigma)	3 x 10 minutes
Block samples with IF blocking solution: 10% goat serum (Sigma), 1% rabbit $F(ab')_2$ anti-bovine IgG (MP Biomedicals, LLC) in IF buffer	60 minutes
Incubate samples in primary antibody at 4°C, diluted 1:200 in IF buffer	Overnight
Rinse samples with PBS	3 x 20 minutes
Incubate samples in secondary antibody at room temperature, protected from light, and diluted 1:200 in IF buffer	45 minutes
Rinse samples with IF buffer, protected from light	1 x 20 minutes
Rinse samples with PBS, protected from light	2 x 10 minutes
Counterstain with DAPI at room temperature, protected from light	10 minutes
Rinse samples with PBS, protected from light	10 minutes

Results and Discussion

Assessing Viability of Bioprinted Samples Induced to Differentiate

Qualitative results of the LIVE/DEAD® assay (**Figure 6.6**) showed that cells appeared mostly viable at Day 2, following 24 hrs in an adipogenic cocktail, as they did

at Day 1, after 24 hours in D1 maintenance medium. There was a negligible number of dead cells after 1 and 2 days in culture, and selected images are representative of all samples. Light microscopy images of Day 0 and Day 1 samples are also provided in **Figure 6.6.** It was necessary to allow printed cells to attach to the collagen substrates for 24 hours in D1 maintenance medium because cell viability was poor when cells were printed and immediately cultured in an adipogenic cocktail (data not shown). The poor viability is likely because the adipogenic cocktail promotes differentiation of cells, and the culture environment does not allow cell attachment to the collagen substrate. In an adipogenic cocktail, the cells become rounded and the expression of integrin-binding proteins is likely altered.

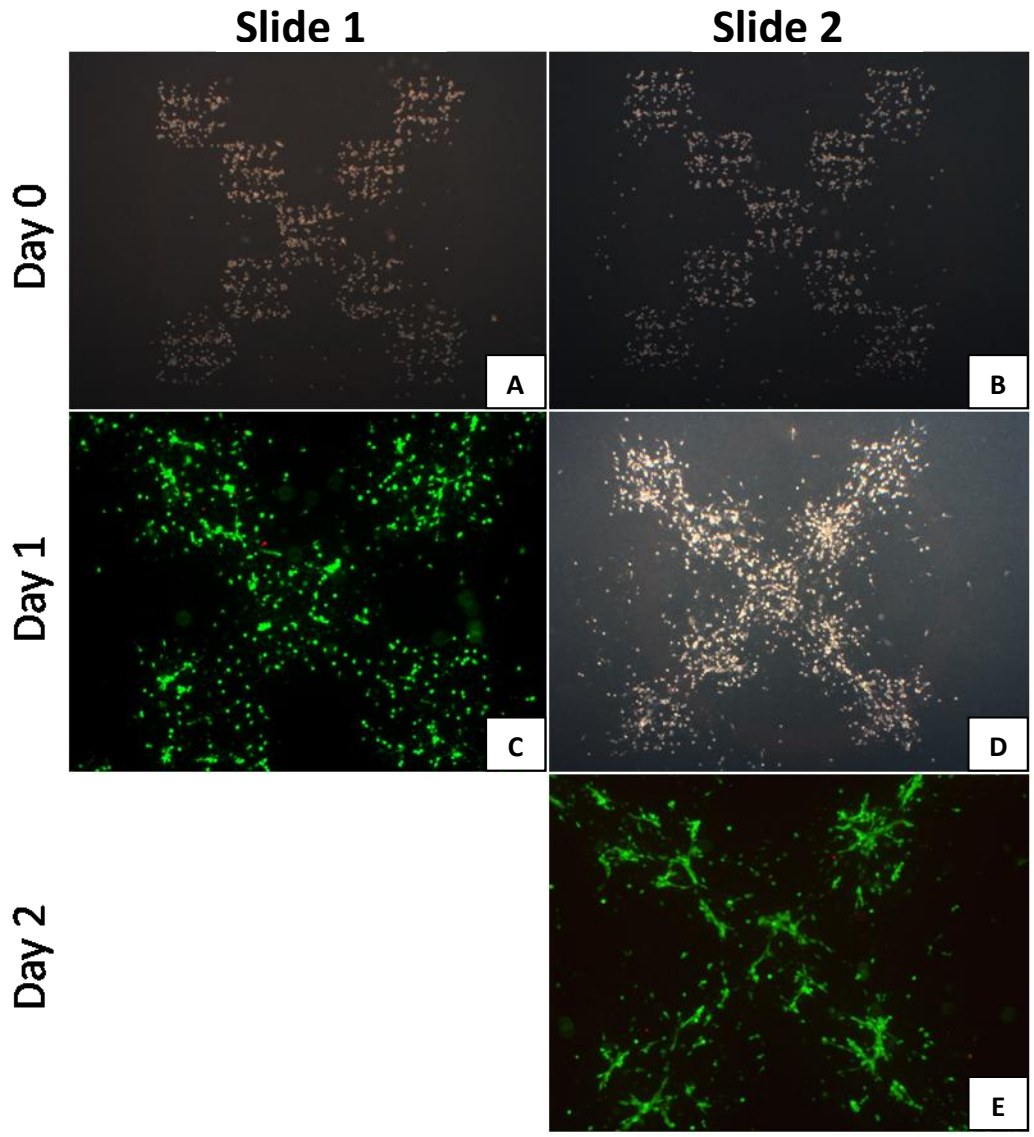

Figure 6.6: LIVE/DEAD® cell viability assay after D1 cells were printed in an 'X' pattern and cultured for 1 or 2 days. A and B) D1 cells (2.5x objective) immediately following Method 4 processing C) LIVE/DEAD® images of D1 cells (5x objective) after they were maintained for 24 hours in D1 maintenance medium D) Light microscopy image of D1 cells (2.5x objective) after they were maintained for 24 hours in D1 maintenance medium E) LIVE/DEAD® assay of D1 cells (5x objective) after they were maintained for an additional 24 hours in an adipogenic cocktail.

Evaluation of Cell-Cell Interaction in Two-Dimensional Test Systems

The immunofluorescence stain for PCNA and DAPI counterstain results are shown in **Figure 6.7A-E**. The patterns on Slides 3, 5, and 6 were printed only with D1 cells, while the patterns on Slides 10 and 11 were printed using both D1 and 4T1 cells. Slides 6 and 11 were cultured for 1 day, Slides 5 and 10 were cultured for 3 days, and Slide 3 was cultured for 5 days. There are no results for a co-culture slide maintained for 5 days. There is an even distribution of red and blue stained cells in the Slide 6 (D1 only, Day 1) sample (**A**), which means that the number of proliferating cells in the sample is consistent throughout the pattern. After 3 and 5 days in culture (**B, C**) most of the proliferating cells in mono-culture patterns were apparent within large clusters of cells, with additional red staining at the outskirts of these clusters diminishing with increased time in culture. Because cells are being maintained in an adipogenic cocktail, it is possible that they are being prompted to enter a differentiation pathway (i.e. they will be less likely to proliferate), though further analysis of gene expression profiles will be necessary to better understand the state of the cell. There is potential for this quantitative assessment to be achieved with the use of laser capture microdissection technology, whereby individual cell clusters can be harvested from a printed pattern. When cells were printed in co-culture patterns, the distribution of red and blue stained cells after 1 day in culture was relatively consistent throughout the pattern, similar to what was seen in the mono-culture pattern. However, after 3 days in culture, more red-stained proliferating cells were apparent in the outermost squares of the pattern, farthest away from 4T1 cells. Further analysis of cell phenotype will enable better understanding of the

relationship between cancer and stromal cells, and how tumor signals may affect adipogenic differentiation.

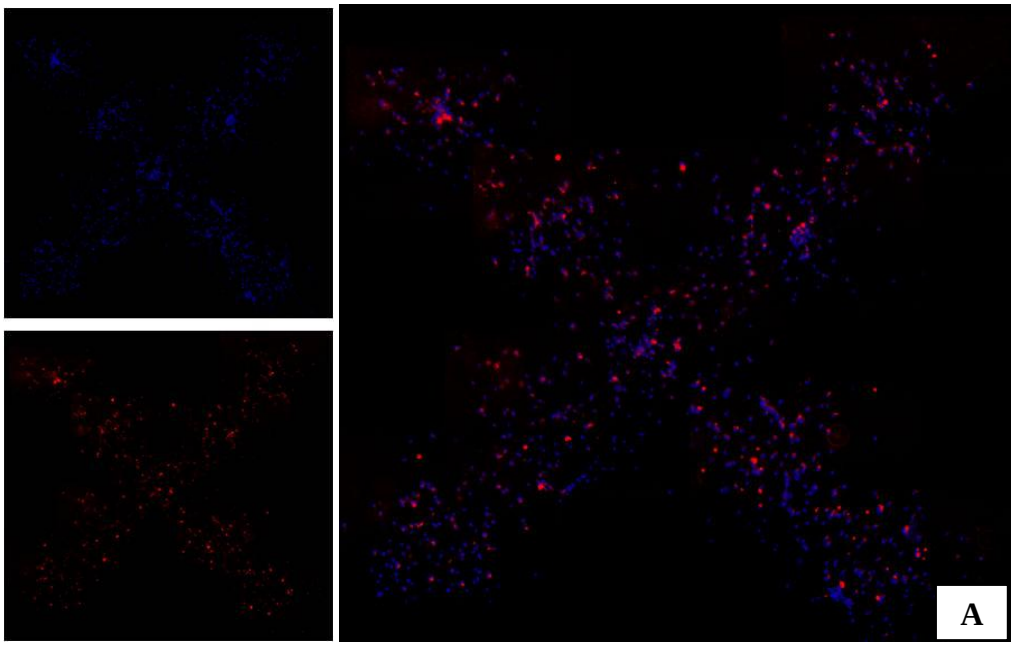

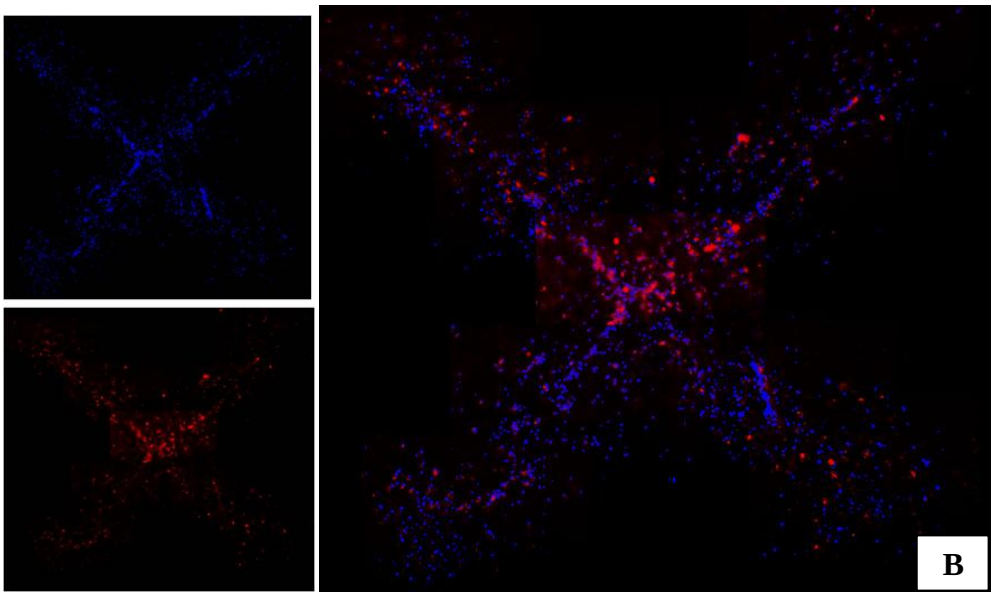

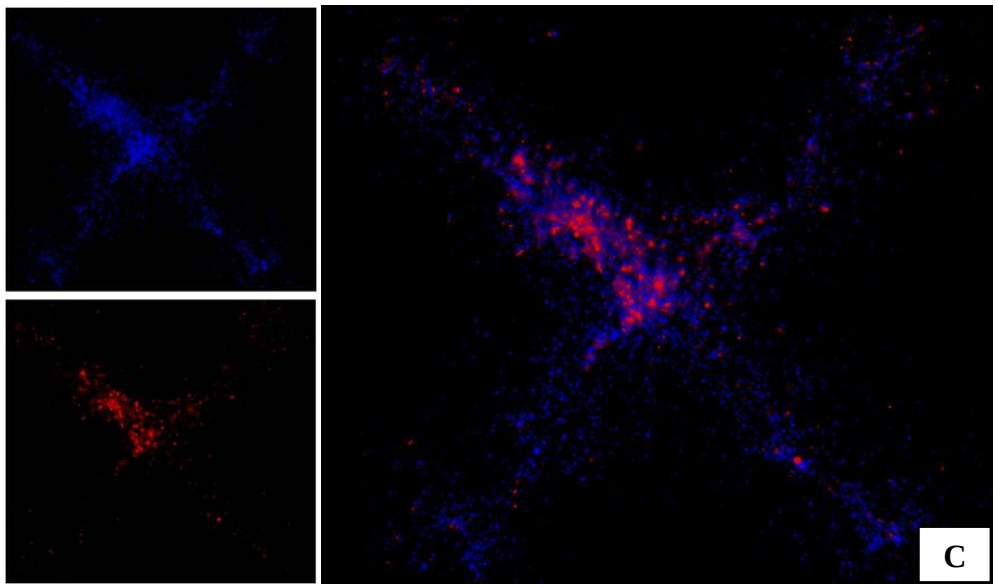
C

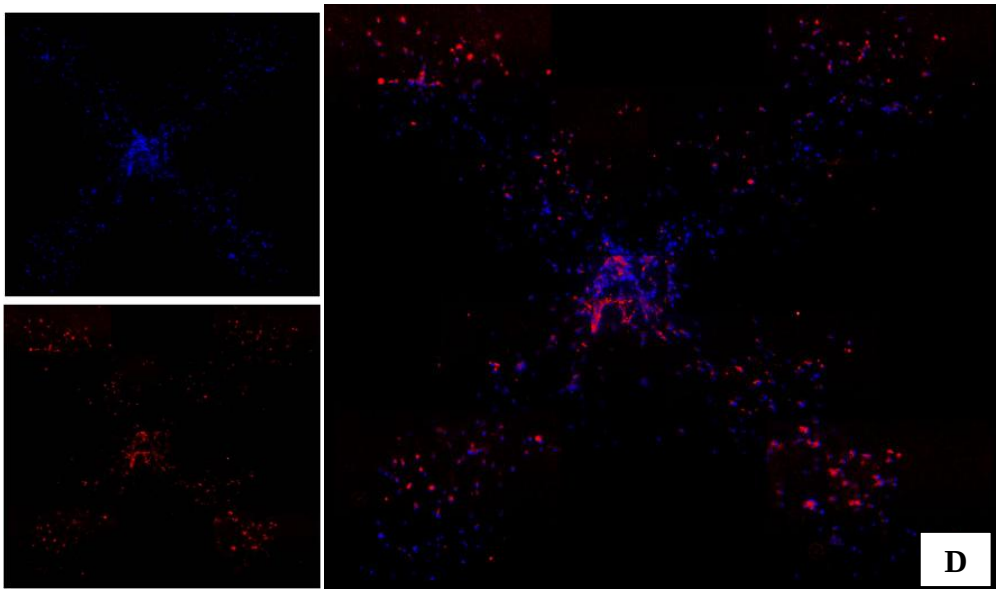
D

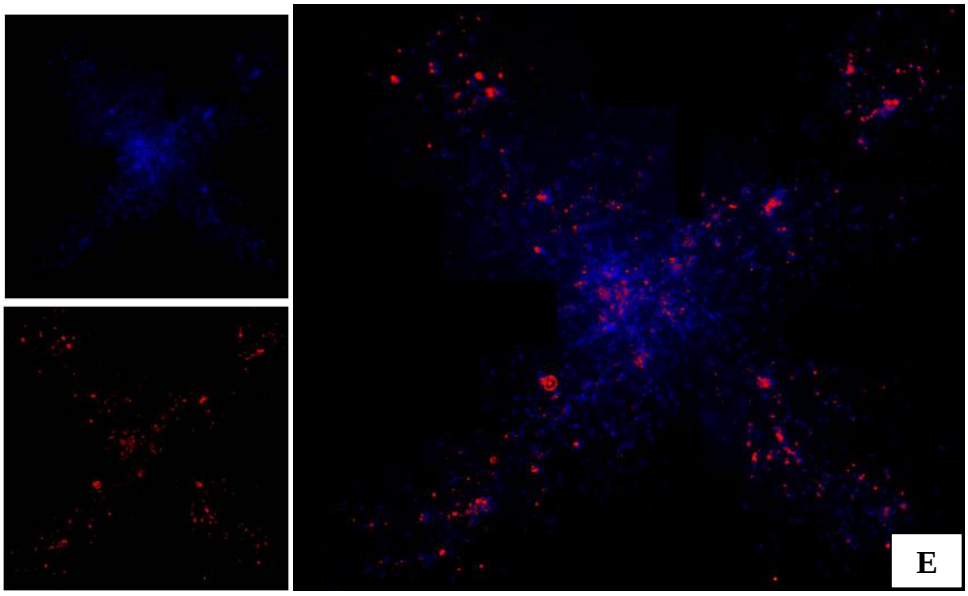

Figure 6.7: Immunofluorescence stain for PCNA (red) and DAPI counterstain (blue) of printed mono- and co-culture samples after 1, 3, or 5 days in culture. The printed pattern is approximately 2mm^2. A)Slide 6, D1 only, Day 1, B)Slide 5, D1 only, Day 3, C)Slide 3, D1 only, Day 5, D)Slide 11, D1 and 4T1, Day 1 and E)Slide 10, D1 and 4T1, Day 3. Nine images (per fluorescence filter set) were captured per pattern using a 10x objective and merged using Adobe Photoshop Elements.

Conclusions

Based on the experimental results, to generate heterogeneous tissue test systems, cells should be treated with HBSS immediately after bioprinting, of the overlaid with collagen, and finally maintained with D1 medium. The combination of HBSS and collagen promotes cell attachment and limits migration. The collagen substrate absorbs comparatively large amounts of liquid while keeping the pattern intact, allowing cells to be printed at higher densities. A frequency must be found, presumably between 1 and 11 kHz, in which multiple fully formed drops containing cells can be fired from the nozzle. Alternatively, cell densities can be increased by printing additional passes of the same

pattern. With the selected processing method, the current bioprinting system can pattern heterogeneous co-cultures with high fidelity and viability. Additionally, staining methods can provide initial insight into cellular relationships and effects of microenvironmental factors; however, quantitative methods of protein and gene analysis will be necessary to glean optimal information from tissue test systems. Overall, these heterogeneous co-cultures will serve as the basis for developing tissue test systems to model cell-cell interactions in breast tumors.

References

Doerr M, Jones J. 1996. The roles of integrins and extracellular matrix proteins in the insulin-like growth factor I-stimulated chemotaxis of human breast cancer cells. J Biol Chem 271(5):2443-2447.

Francis K, Palsson BO. 1997. Effective intercellular communication distances are determined by the relative time constants for cyto/chemokine secretion and diffusion. Proc Natl Acad Sci USA 94:12258-12262.

Lee GY, Kenny PA, Lee EH, Bissell MJ. 2007. Three-dimensional culture models of normal and malignant breast epithelial cells. Nature Methods 4(4):359-365.

Parzel CA, Pepper ME, Burg TC, Groff RE, Burg KJL. 2009. EDTA enhances high-throughput two-dimensional bioprinting by inhibiting salt scaling and cell aggregation at the nozzle surface. J Tissue Eng Regen Med, 3(4):260-268.

Pennisi P, Barr V, Nunez N, Stannard B, Roith D. 2002. Reduced expression of insulin-like growth factor I receptors in MCF-7 breast cancer cells leads to a more metastatic phenotype. Cancer Research 62:6529-6537.

Pepper ME, Parzel CA, Burg T, Burg KJL, Groff RE. 2009. Design and implementation of a two-dimensional bioprinter. Conf Proc IEEE Eng Med Biol Soc. 6001-6005.

Takeda K, Sasaki A, Ha H, Seung H, Firtel R. 2007. Role of Phosphatidylinositol 3-Kinases in chemotaxis in Dictyostelium. J Biol Chem 282(16):11874-11884.

CHAPTER 7

USING BIOMATERIAL STIFFNESS TO TUNE THE BREAST TISSUE TEST SYSTEM

Introduction

Research has shown that stromal cells are subject to various environmental signals that inform cellular behavior. For example, it was demonstrated that rat stromal cells differentiated into adipocytes or endothelial cells, according to cues from the surrounding hormones and extracellular matrix (ECM) (Zangani *et al.*, 1999). Cells maintained a fibroblast-like phenotype when cultured on plastic, differentiated into mature adipocytes when cultured in an adipogenic cocktail, and formed capillary-like networks when grown on a layer of reconstituted basement membrane. In 2008, Krause and associates demonstrated that a traditional three-dimensional mammary acini model could be more closely related to native tissue by homogeneously distributing and co-culturing MCF-10A human mammary epithelial cells with primary human fibroblasts obtained from reduction mammoplasty. This novel culture system was developed in an effort to better understand stromal-epithelial interactions in the mammary tissue and the overall effect on tissue development (Krause *et al*, 2008). However, in this model system the fibroblasts resided in a relatively compliant collagen gel environment (1mg/mL) of fixed stiffness.

Thus, we hypothesized that if adipocytes (differentiated D1 murine mesenchymal stem cells) were cultured on rigid beads prior to embedding them in a Type I collagen

gel, the effect of the adipocytes on the behavior of normal murine mammary epithelial cells (NMuMG) would differ when compared to the effect of adipocytes cultured directly in a collagen gel. That is, we recognized the anchorage-dependent nature of stromal cells and proposed using biomaterial stiffness as a "tuning" variable with which to modulate stromal cell behavior, using co-culture studies in 3D tissue test systems by way of proof of principle. Although bead chemistry, bead radius of curvature, and collagen concentration all affect cell function, stiffness of the culture environment is a major and readily modulated factor. We further hypothesized that differences in cell behavior due to biomaterial stiffness could be partially attributed to the altered production and/or secretion of matrix metalloproteinases (MMPs) by adipocytes, since the culture environment will ultimately have an effect on phenotypic gene expression and subsequent protein production. MMPs are considerably important in the promotion of ductal extension and branching *in vivo*. This study investigated the relationship between adipocytes and normal mammary epithelial cells in 3D environments of varied stiffness.

Materials and Methods

Cell Culture

D1 murine mesenchymal stem cells (American Type Culture Collection (ATCC), Manassas, VA) were maintained in Dulbecco's Modified Eagle's Medium (DMEM) (ATCC) containing 4mM L-glutamine, 1.5g/L sodium bicarbonate, and 4.5g/L glucose; each 500mL was supplemented with 50mL fetal bovine serum (FBS; Hyclone, Logan, UT), 5mL antibiotic/antimycotic (Invitrogen, Gibco, Carlsbad, CA), and 1mL fungizone

(Invitrogen), referred to as D1 maintenance medium. Normal murine mammary gland cells (NMuMG) were cultured in D1 maintenance medium containing 10µg/mL insulin. The culture medium was replaced every 48 to 72 hours as required, and cells were maintained in an incubator at 37°C and 5% CO_2. For 3D gel-based experiments, DMEM with 10% FBS, supplemented with hydrocortisone (1µg/ml) (Lonza, Walkersville, MD), insulin (10µg/ml) (Sigma-Aldrich, St. Louis, MO) and epidermal growth factor (5ng/ml) (Sigma) was used (Swamydas *et al.*, 2010) and will be referred to as 3D culture medium. Adipogenic differentiation of D1 cells was induced with an adipogenic cocktail; this cocktail was prepared by supplementing 10mL of D1 maintenance medium with 1mL of 5mM 3-isobutyl-1-methylxanthine (IBMX) (Sigma), 1mg insulin (Sigma), and 2µL dexamethasone (Sigma) (diluted to 1mg/mL in 100% ethanol).

Stir Flask Culture

D1 cells were seeded onto Type I collagen-coated polystyrene beads (Solohill Engineering, Inc., Ann Arbor, MI) for use in 3D gel-based cultures. Approximately 4 grams of dehydrated beads were steam autoclaved at 121°C for 45 minutes. Beads were then rinsed in sterile phosphate buffered saline (PBS) and pre-soaked in D1 maintenance medium until use, for at least 1 hour. A large (250mL capacity) stir flask (Wheaton, Millville, NJ) was autoclaved, coated with Sigmacote (Sigma), and rinsed twice with sterile PBS. Following stir flask preparation, 4 grams of beads were combined with 4×10^7 D1 cells and 200mL of D1 maintenance medium. Cell-bead suspensions were maintained in the stir flask for 5 days at 37°C and 5% CO_2 , using a rotation speed of

approximately 60rpm. Following 5 days in culture, D1 maintenance medium was replaced with an adipocyte differentiation-inducing cocktail and cultured for an additional 5 days.

3D Cell Seeding

Three-dimensional gel-based cultures were constructed in polystyrene 12-well plates. To begin, each well was covered with 600µL of 1.5mg/mL Type I collagen solution prepared by diluting PureCol® (3.0mg/mL bovine collagen) (Advanced Biomatrix, San Diego, CA) in phosphate buffered saline (PBS), FBS, and DMEM, and neutralized with 1N NaOH (Vernon *et al.*, 2005). The collagen layers were incubated for at least 4 hours at 37ºC and 5% CO_2, after which they were rinsed for 1 hour in sterile distilled water and then soaked in 3D culture medium until use. Four types of 3D culture models were seeded and cultured for up to 10 days. Cultures contained D1 cells alone or a co-culture of NMuMG and D1 (30:70) cells:

1. Adipo D1 cells were cultured to confluence in a polystyrene culture flask for 5 days and maintained in an adipogenic cocktail for an additional 5 days. After 10 total days in culture, D1 cells were dissociated from the flask and suspended in Type I collagen (1.5mg/mL) at 2×10^5 cells/mL. Subsequently, 1mL of the collagen-cell suspension was pipetted on top of the first gelled collagen layer of 6 wells (3 samples × 2 time points) and gelled in an incubator for 90 minutes at 37ºC and 5% CO_2. Following gelation, each sample was covered with 2mL of 3D

culture medium. Note that for these and subsequent sample types, an additional volume of cell suspension (i.e. more than 6mL) was prepared to compensate for the potential loss in volume of the collagen solution, as it tends to stick to the inner surfaces of tubes and pipettes during solution preparation.

2. Bead Adipo – D1 cells were cultured on collagen-coated polystyrene beads (described above) for 5 days in D1 maintenance medium followed by an additional 5 days in an adipogenic cocktail. After 10 days in culture, 0.8mL beads were suspended in 9mL (approximately 2×10^5 cells per mL, cell number as approximated using a PicoGreen® assay) of Type I collagen (1.5mg/mL); 1mL of the collagen-bead suspension was pipetted on top of the first gelled collagen layer of 6 wells (3 samples × 2 time points) and gelled in an incubator for 90 minutes at 37ºC and 5% CO_2. Following gelation, each sample was covered with 2mL of 3D culture medium.

3. Adipo_NMuMG – D1 cells were cultured to confluence in a polystyrene culture flask for 5 days and maintained in an adipogenic cocktail for an additional 5 days. After 10 total days in culture, D1 cells were dissociated from the flask and suspended in Type I collagen (1.5mg/mL) at 1.4×10^5 cells/mL. NMuMG cells were added to the suspension at 3×10^4 cells/mL. Subsequently, 1mL of the collagen-cell suspension was pipetted on top of the first gelled collagen layer of 6 wells (3 samples × 2 time points) and gelled in an incubator for 90 minutes at

37ºC and 5% CO_2. Following gelation, each sample was covered with 2mL of 3D culture medium.

4. Bead Adipo_NmuMG – D1 cells were cultured on collagen-coated polystyrene beads (described above) for 5 days in D1 maintenance medium followed by an additional 5 days in an adipogenic cocktail. After 10 total days in culture, 0.8mL beads were suspended in 9mL (approximately 2×10^5 cells per mL based on PicoGreen® results) of Type I collagen (1.5mg/mL); subsequently NmuMG cells were suspended at 3×10^4 cells/mL in the bead-gel suspension; 1mL of the collagen-bead-cell suspension was pipetted on top of the first gelled collagen layer of 6 wells (3 samples × 2 time points) and gelled in an incubator for 90 minutes at 37ºC and 5% CO_2. Following gelation, each sample was covered with 2mL of 3D culture medium.

Following 5 and/or 10 days in culture, 3D test systems were imaged using both light (Zeiss Axiovert 40 CFL microscope; Carl Zeiss, Oberkochen, Germany) and confocal (Olympus 1X2-UCB; Center Valley, PA) microscopy. Prior to confocal microscopy, cells were labeled with a LIVE/DEAD® Assay for Cell Viability, and samples were imaged using a 20x long-working-distance objective.

PicoGreen® Assay

A Quant-iT™ PicoGreen® dsDNA assay kit (Invitrogen) was used to quantify the amount of double-stranded DNA in a sample, and therefore estimate cell number. This kit provides a fluorescent nucleic acid stain that targets double-stranded DNA; its excitation and emission wavelengths are 480nm and 520nm, respectively. This method was employed to estimate the number of cells attached to a given volume of beads in stir flask culture and to estimate the final number of cells residing in 3D collagen-based constructs following 10 days in culture. To generate a standard curve for D1 cell number, D1 cells were dissociated from a tissue culture polystyrene flask, and a pellet resulting from centrifugation was resuspended at 2.0×10^5 cells/mL in 1× TE buffer (10mM Tris-HCl, 1mM EDTA, pH 7.5). Known numbers of cells in TE buffer, from 0 – 2×10^5, were pipetted into separate 2mL microcentrifuge tubes (1mL total volume), and cells were subjected to 3 freeze-thaw cycles. Then, 1mL of the Quant-iT™ PicoGreen® reagent diluted (1:200) with 1X TE buffer was added to each sample. **Table 7.1** displays the volume of TE buffer, cell suspension, and PicoGreen® reagent required for each cell count.

Table 7.1: Required volumes of reagents for PicoGreen Assay.

Cell Number	Volume of 1X TE Buffer (µL)	Volume of Cells Suspended at 2.0×10^5 cells/mL in 1X TE Buffer (µL)	Volume of PicoGreen® Reagent (µL)
0	1000	0	1000
20,000	900	100	1000
40,000	800	200	1000
60,000	700	300	1000
80,000	600	400	1000
100,000	500	500	1000
120,000	400	600	1000
140,000	300	700	1000
160,000	200	800	1000
180,000	100	900	1000
200,000	0	1000	1000

After 5 minutes of incubation, fluorescence intensity values of the samples were read with a Synergy™ Multimode Microplate Reader (BioTek® Instruments, Inc., Winooski, VT). Excitation and emission values used for reading were 480 nm and 520 nm, respectively. All samples were tested in triplicate and results are reported as the calculated mean of n=3 samples.

The final number of cells residing in 3D collagen-based constructs following 10 days in culture was determined, using a modification of the manufacturer's protocol. First, 3D constructs were removed from the 12-well plates and placed in individual 5mL centrifuge tubes. The collagen gels were digested for approximately 2 hours with a 1.5mg/mL (250units/mg) Type I collagenase (Worthington Biochemical Corporation, Lakewood, NJ) solution in PBS, with intermittent vortexing to assist in disintegrating the

bulk gel. Following digestion, samples were centrifuged at 1000 rpm for 5 minutes and cells were resuspended in 1mL of 1X TE buffer. The rest of the protocol was identical to that used to create a standard curve, as described above.

LIVE/DEAD® Assay for Cell Viability

Cells seeded in each 3D mono- and co-culture model were analyzed after 10 days in culture. These systems were imaged using confocal microscopy. The LIVE/DEAD® solution was prepared by adding 20µL of 2mM EthD-1 stock reagent (fluoresces red in the presence of necrotic cells) and 5µL of 4mM calcein AM stock reagent (fluoresces green in the presence of live cells) to 10mL of PBS and vortexing. Cellular gels were covered with the LIVE/DEAD® solution and incubated for 45 minutes, protected from light.

Oil-Red-O Stain for Lipid

A quantitative analysis of lipid production by D1 cells seeded in a 12-well polystyrene culture plate or on Type I collagen coated polystyrene beads was performed using an Oil-Red-O stain (Sigma) for lipid following 5 days of culture in an adipogenic cocktail. This assay was conducted to ensure that most of the cells differentiated and began producing lipid prior to being embedded in a 3D collagen gel-based culture. An Oil-Red-O stock solution was prepared by dissolving 0.5g powder concentrate in 100mL isopropanol and filtering. A working solution was prepared by combining 60mL stock solution with 40mL distilled water and filtering. Cells fixed in 10% neutral buffered

formalin were rinsed with distilled water, and the Oil-Red-O working solution was added to each well containing cells or containing cellular beads that had previously been removed from a stir flask. Cells were incubated at room temperature for 15 minutes and then rinsed with distilled water three times. Lipid produced by the cells appeared red after staining.

Immunofluorescence Staining for Vimentin

Cells were labeled for vimentin using immunofluorescence techniques. D1 cells that were cultured on beads or in a polystyrene 12-well plate for 10 days (5 days in D1 maintenance medium and 5 days in an adipogenic cocktail) were assessed prior to seeding in 3D cultures. Additionally, cells seeded in each 3D mono- and co-culture system were stained after 10 days in culture. To stain embedded cells, gels were fixed in neutral buffered formalin for 20 minutes, then removed from the culture well and transferred to a Petri dish. The top and bottom collagen layers were separated using forceps, and the top layer was discarded leaving cells and/or beads on top of the lower collagen layer; using this method, the staining reagents were not required to penetrate the top collagen layer, and cells could be directly stained.

Staining was performed after fixation of cells, using 10% neutral buffered formalin. The staining procedure is detailed in **Table 7.2.**

Table 7.2: Protocol for vimentin immunofluorescence staining.

PROCESS	TIME
Fix samples with 10% NBF	20 minutes
Rinse samples with PBS	3 x 5 minutes
Block samples 10% goat serum, diluted in PBS	30 minutes
Incubate samples in primary antibody at room temperature, diluted 1:200 in PBS	90 minutes
Rinse samples with PBS	3 x 5 minutes
Incubate samples in secondary antibody at room temperature, protected from light, and diluted 1:200 in PBS	45 minutes
Rinse samples with PBS, protected from light	3 x 5 minutes
Counterstain with DAPI at room temperature, protected from light	10 minutes
Rinse samples with PBS, protected from light	5 minutes

Mouse Total MMP-9 Detection

A Quantikine® mouse total MMP-9 kit (R&D Systems, Minneapolis, MN) was used to determine levels of MMP-9 in Day 9 samples. Fresh 3D culture medium was added to well at Day 7, and cultures were maintained for an additional 2 days. Media samples were collected and stored at -80ºC until use. The manufacturer's suggested protocol was used to implement the ELISA kit. Solutions for a standard curve were prepared by first reconstituting the mouse MMP-9 (total) Standard with 2.0mL of Calibrator Diluent RD5-10 to produce a stock solution of 5ng/mL. The standard was maintained for a minimum of 15 minutes with gentle agitation to ensure complete reconstitution. The 5ng/mL standard served as the highest standard value, and a 2-fold dilution series was prepared using Calibrator Diluent, as shown in **Figure 7.1** (R&D Systems, Inc., 2010).

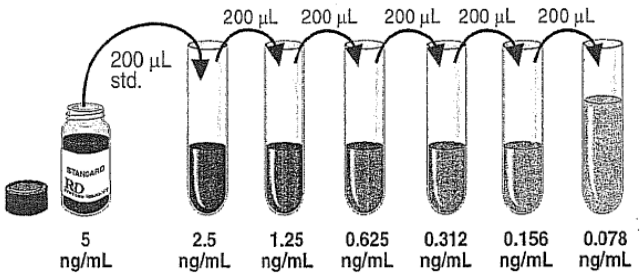

Figure 7.1: Total MMP-9 standard solution dilution series.

Following preparation of standard solutions, 50µL of Assay Diluent RD1-34 was added to each well. Then, 50µL of Standard, Control (provided in the kit), or culture medium sample was added to each well. The plate was covered with an adhesive strip and incubated at room temperature for 2 hours. Each well was aspirated and rinsed 4 times with Wash Buffer (provided in the kit), after which 100µL of Mouse MMP-9 (total) Conjugate (provided in the kit) was added to each well. The plate was incubated for 2 hours at room temperature, then washed four times with Wash Buffer. Subsequently, 100µL of Substrate Solution (provided in the kit) was added to each well, and the plate was incubated at room temperature for 30 minutes, protected from light. Stop Solution (provided in the kit) was added to each well (100µL), and the optical density of each well was read using a Synergy™ Multimode Microplate Reader set to 450nm with the correction wavelength set to 540nm.

Results

Cell Culture

Figure 7.2 depicts preconfluent NMuMG cells in addition to D1 cells that were cultured to confluence for 5 days and maintained in an adipogenic cocktail for an additional 5 days. Both cell types were cultured in a standard tissue culture polystyrene cell culture flask (T-75). These images were taken to illustrate cell morphology on the day that cells were dissociated and cultured in a 3D collagen gel environment.

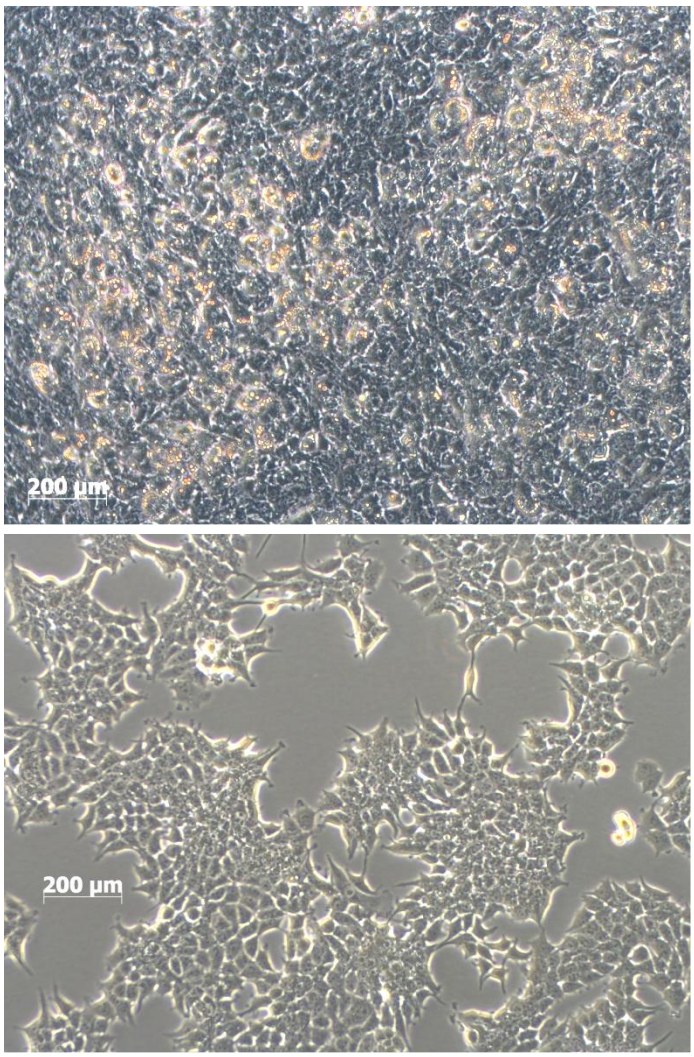

Figure 7.2: Morphology of D1 cells cultured in an adipogenic cocktail for 5 days (top) and preconfluent NMuMG cells (bottom). Both cell types were cultured in a polystyrene culture flask and were imaged using a 10x objective.

PicoGreen® Assay

The standard curve of double-stranded DNA (dsDNA) harvested from D1 cells is depicted in **Figure 7.3**, and has a resultant R^2 value of .9455.

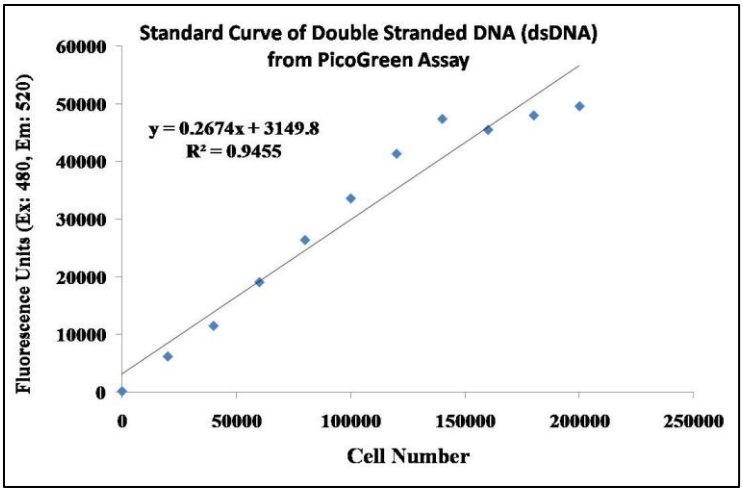

Figure 7.3: Standard curve of double-stranded DNA obtained from known D1 cell numbers.

Table 7.3 contains values for average fluorescence units and corresponding average cell number, which is based on the dsDNA standard curve. Approximately 1.77×10^5 cells were attached to 0.1mL beads, which were removed from the stir flask on the same day 3D cultures were fabricated. Additionally, PicoGreen® data shows that, following 10 days in culture, approximately 3.31×10^5 cells resided in Adipo cultures, 3.47×10^5 cells in Bead Adipo cultures, 2.85×10^5 cells in Adipo_NMuMG cultures, and 3.06×10^5 cells in Bead Adipo_NMuMG cultures.

Table 7.3: Average fluorescence units and corresponding average cell number for PicoGreen® samples.

Sample Type	Average Fluorescence Units	Average Cell Number
0.1mL beads (from stir flask)	50429	1.77×10^5
Adipo – Day 10	88954	3.31×10^5
Bead Adipo – Day 10	96059	3.47×10^5
Adipo_NMuMG – Day 10	79388	2.85×10^5
Bead Adipo_NMuMG – Day 10	85054	3.06×10^5

Oil-Red-O Stain for Lipid and Vimentin Immunofluorescence Stain

The Oil-Red-O stain for lipid that was conducted on D1 cells that had been seeded in a polystyrene culture flask or on collagen coated polystyrene beads for 10 total days (5 days in D1 maintenance medium and 5 days in an adipogenic cocktail) (**Figures 7.4)** showed significant lipid staining (red color) in both conditions. It appeared that approximately half of the cells cultured in a flask were producing lipid at this time point; cells that were visible on the surface of beads and bridging beads were also producing lipid, although the extent of lipid production is difficult to see on the 3D substrates. Cells grown in a culture flask for 10 days also showed some evidence of vimentin staining (**Figure 7.5A**), which appears bright green, although vimentin staining was much more apparent in cells grown on beads (**Figure 7.5 C**). The DAPI counterstain appears as blue-stained nuclei (**Figures 7.5A, C**), and light microscopy images of both conditions are depicted in **Figures 7.5B, D**.

Red-stained lipid is also apparent in the 3D test systems following 10 days in culture (**Figure 7.6E-H**). The Bead Adipo (**F**) and Bead Adipo_NMuMG (**H**) samples

were similar in that most of the red staining was seen along the surface of the beads with little to no staining among cells growing in the gel between beads. Approximately half of the population of cells in the Adipo sample (**E)** stained (similar to pre-seeding results), although unlike D1 cells in 10 days of flask culture, lipid vacuoles were large and red staining was dense. Finally, the Adipo_NMuMG sample showed red-stained lipid only within the NMuMG cell clusters. Little to no staining was apparent between cell clusters, among D1 cells growing within the gel. When assessing the vimentin staining of 3D cultures, the Adipo sample showed very little fluorescent green staining (**Figure 7.6A** (fluorescence and corresponding light microscopy images shown for all samples)) while a significant amount of vimentin staining is apparent in the Bead Adipo sample (**Figure 7.6B**). Vimentin staining was seen only at the edges of NMuMG cell clusters in the Adipo_NMuMG sample (**Figure 7.6C**), but not within D1 cells growing in the collagen gel between clusters. Finally, the Bead Adipo_NMuMG sample (**Figure 7.6D**) showed vimentin staining along the surface of the beads and at the edges of NMuMG cell clusters, but not within D1 cells growing in the collagen gel between beads.

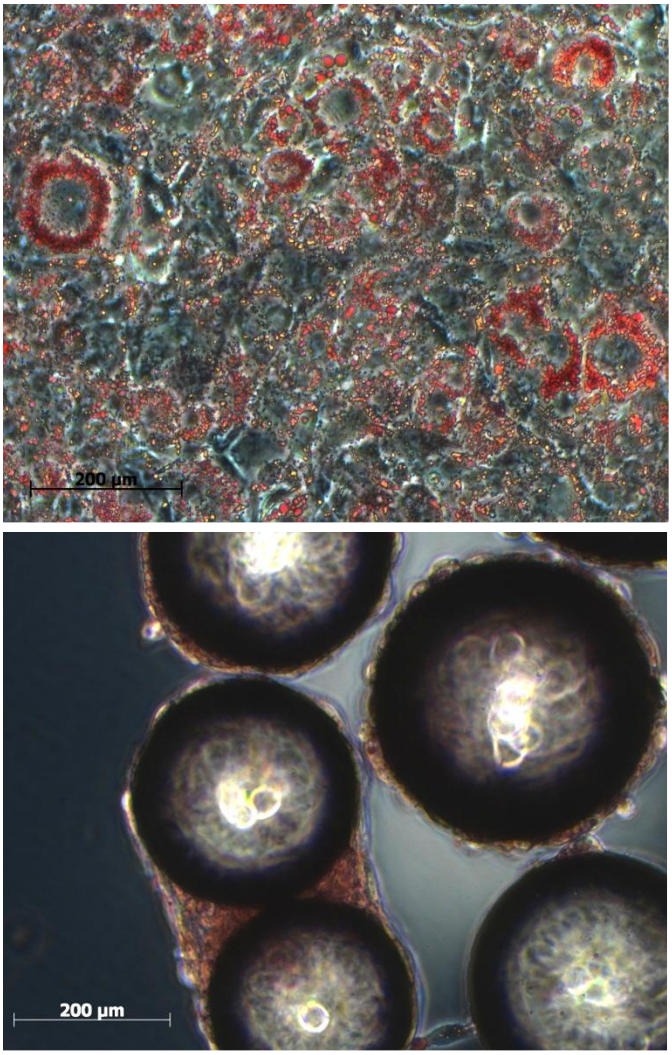

Figure 7.4: Oil-Red-O stains lipid red. Lipid was produced by D1 cells seeded on tissue culture polystyrene (top) and on Type I collagen coated polystyrene beads (bottom) following 5 days of culture in an adipogenic cocktail. Images captured using a 20x objective.

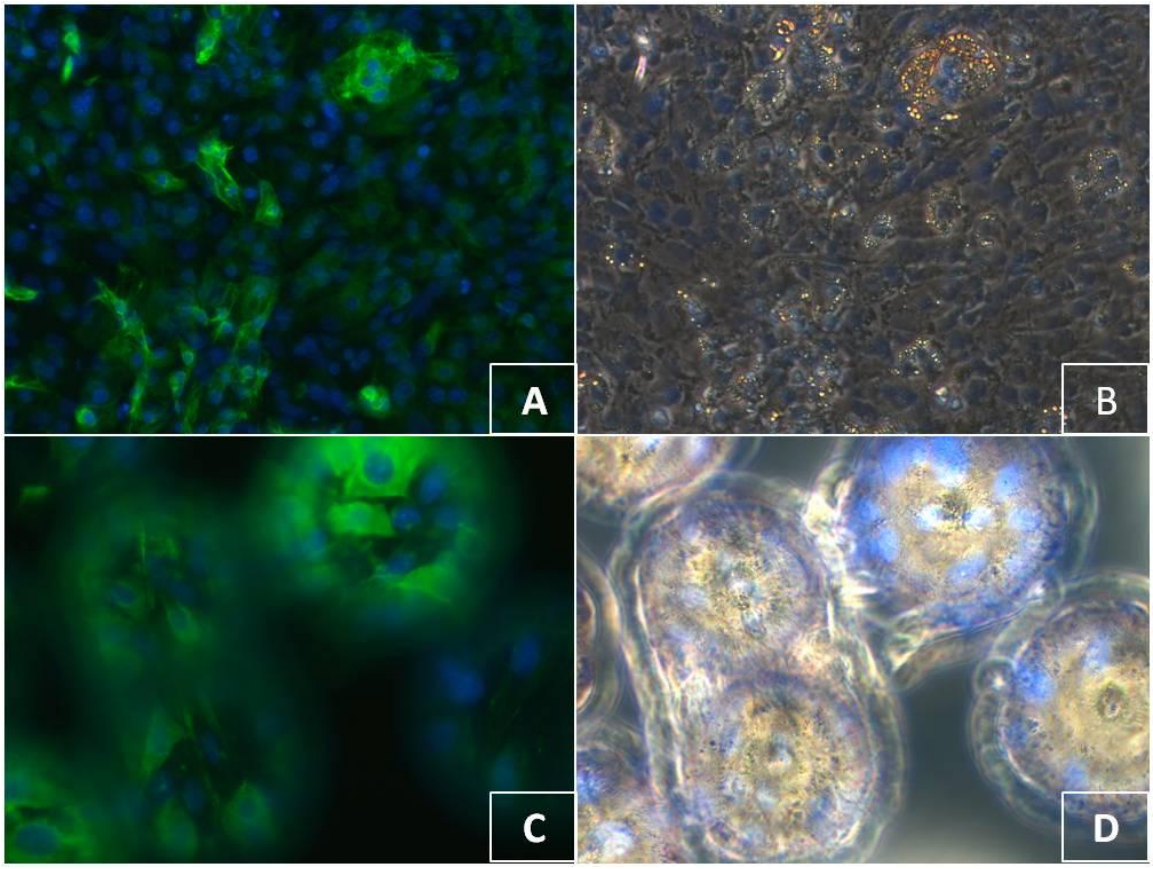

Figure 7.5: Immunofluorescence stain for vimentin and corresponding light microscopy images. A,C) Vimentin staining appears green while DAPI counterstaining appears blue and B,D) corresponding light microscopy images following 5 days of culture in an adipogenic cocktail. Images captured using a 20x objective.

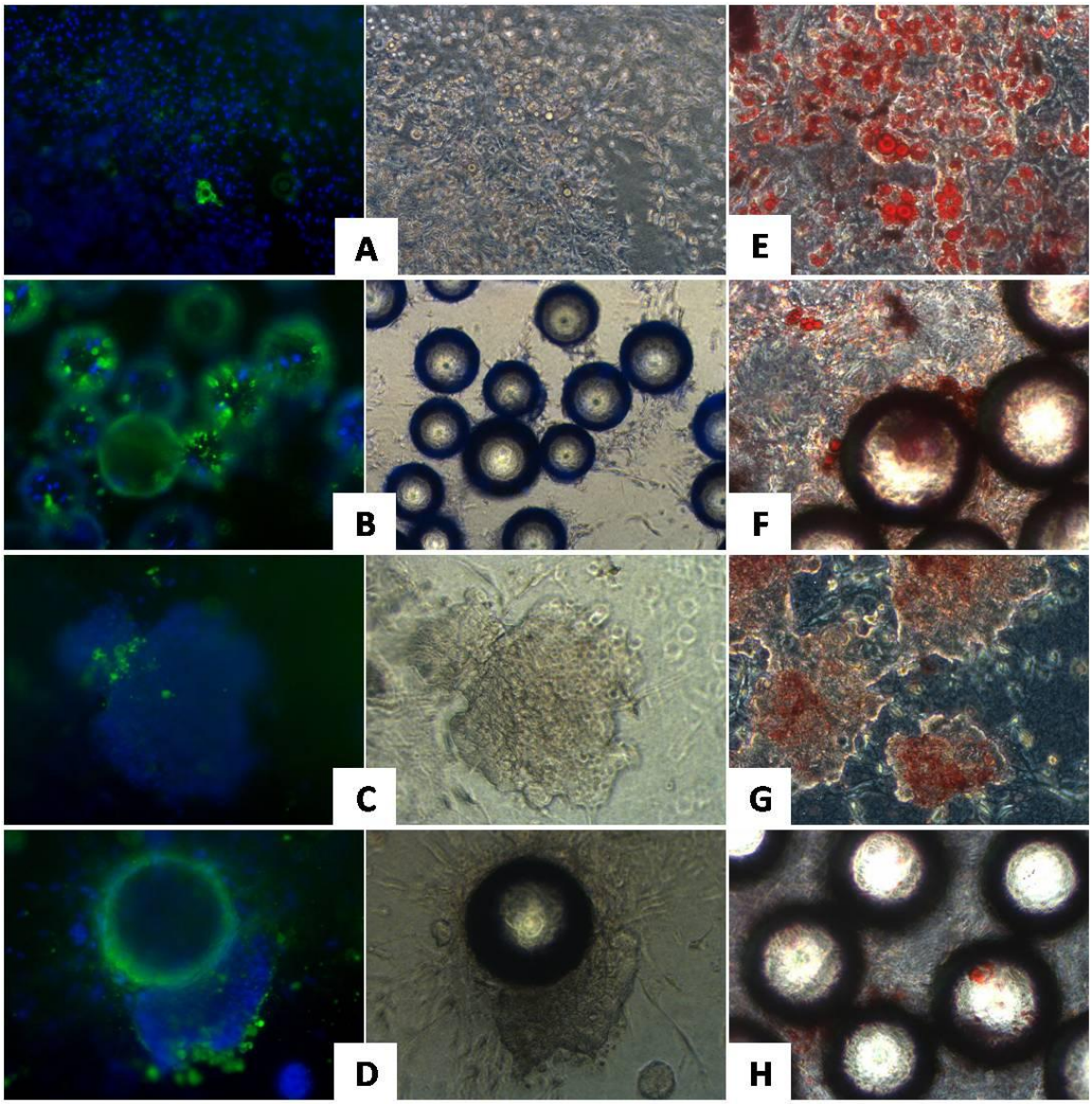

Figure 7.6: Three-dimensional gel-based models cultured for 10 days. Vimentin staining and corresponding light microscopy of A) D1 cells suspended in Type I collagen (Adipo), B) D1 cells seeded on beads and suspended in Type I collagen (Bead Adipo), C) D1 and NMuMG cells suspended in Type I collagen (Adipo_NMuMG) and D) D1 cells seeded on beads and suspended in Type I collagen with NMuMG cells (Bead Adipo_NMuMG). Images E-H) Oil-Red-O stains lipid red. Images A and B were captured using a 10x objective while images C-H were captured using a 20x objective.

3D Cell Seeding

Light microscopy images of 3D test systems on Days 3, 5, and 10 are depicted in **Figure 7.7**. When D1 cells were suspended in Type I collagen (Adipo), they were preconfluent and retained a fibroblast-like morphology with only few lipid-containing cells on Day 3. By Days 5 and 10, the D1 continued to become rounded, and more lipid-producing cells were prevalent. When D1 cells were seeded on beads prior to suspension in Type I collagen (Bead Adipo), the cells growing between beads retained a fibroblast-like morphology throughout the 10 day culture period. The morphology of cells attached to beads is difficult to visualize with this technique. When D1 cells were suspended in co-culture with NMuMG cells (Adipo_NMuMG), the D1 cells appeared to retain a fibroblast-like morphology (few or no lipid producing cells) throughout the 10-day culture period. NMuMG cells formed clusters, and these clusters continued to grow larger throughout the culture period. Lastly, when D1 cells were cultured on beads and then suspended in co-culture with NMuMG cells (Bead Adipo_NMuMG), the NMuMG clusters became less apparent. Additionally, the D1 cells that grew between beads appeared to retain a fibroblast-like morphology.

Confocal images of 3D gel samples (**Figure 7.8**) show that most cells remained viable after 10 days in culture. In the 3D reconstruction of the Adipo_NMuMG sample (**right side**), dead cells can be seen in the center of the NMuMG cell cluster.

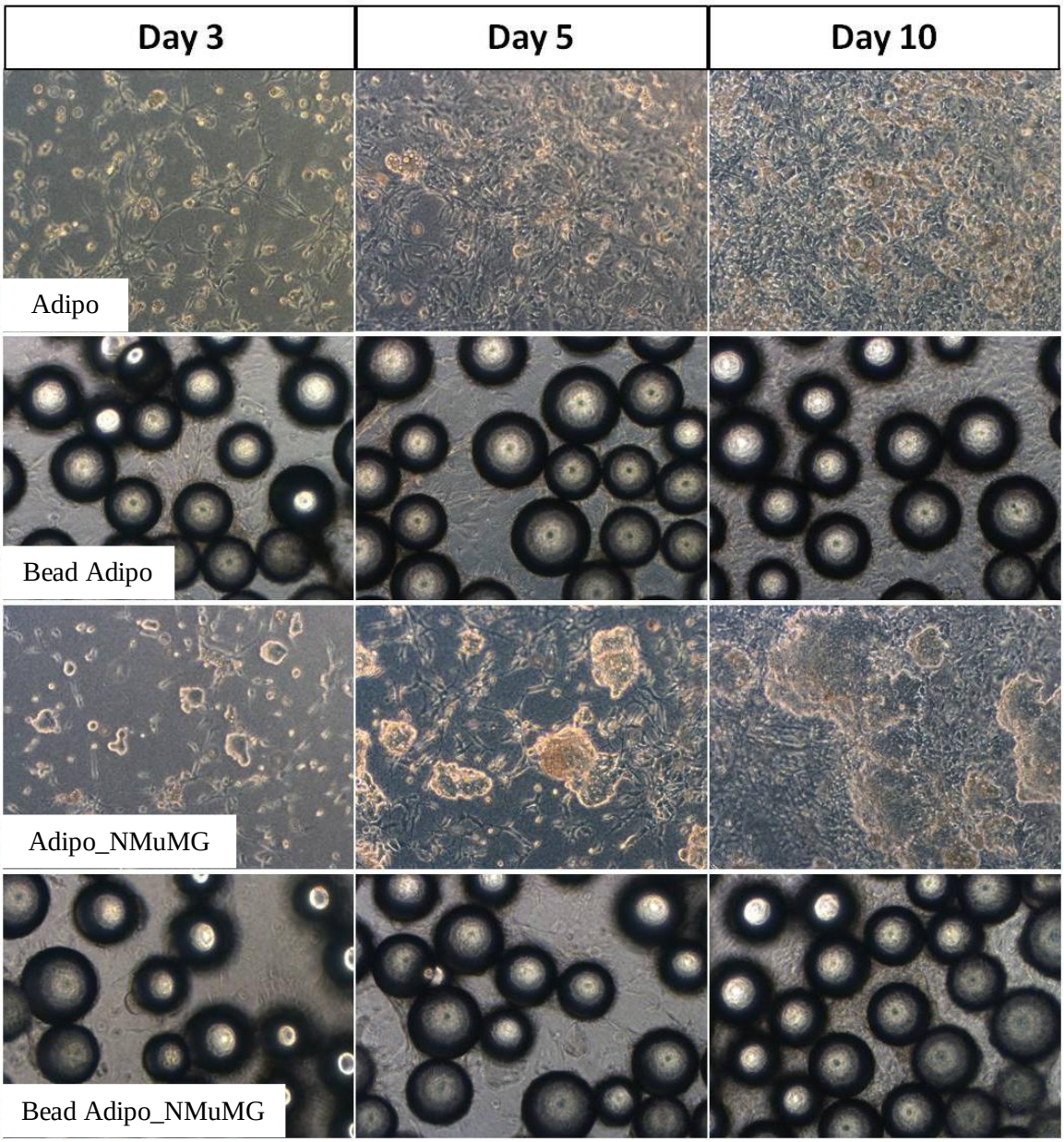

Figure 7.7: Light microscopy images of 3D gel-based cultures. Images captured using a 10x objective.

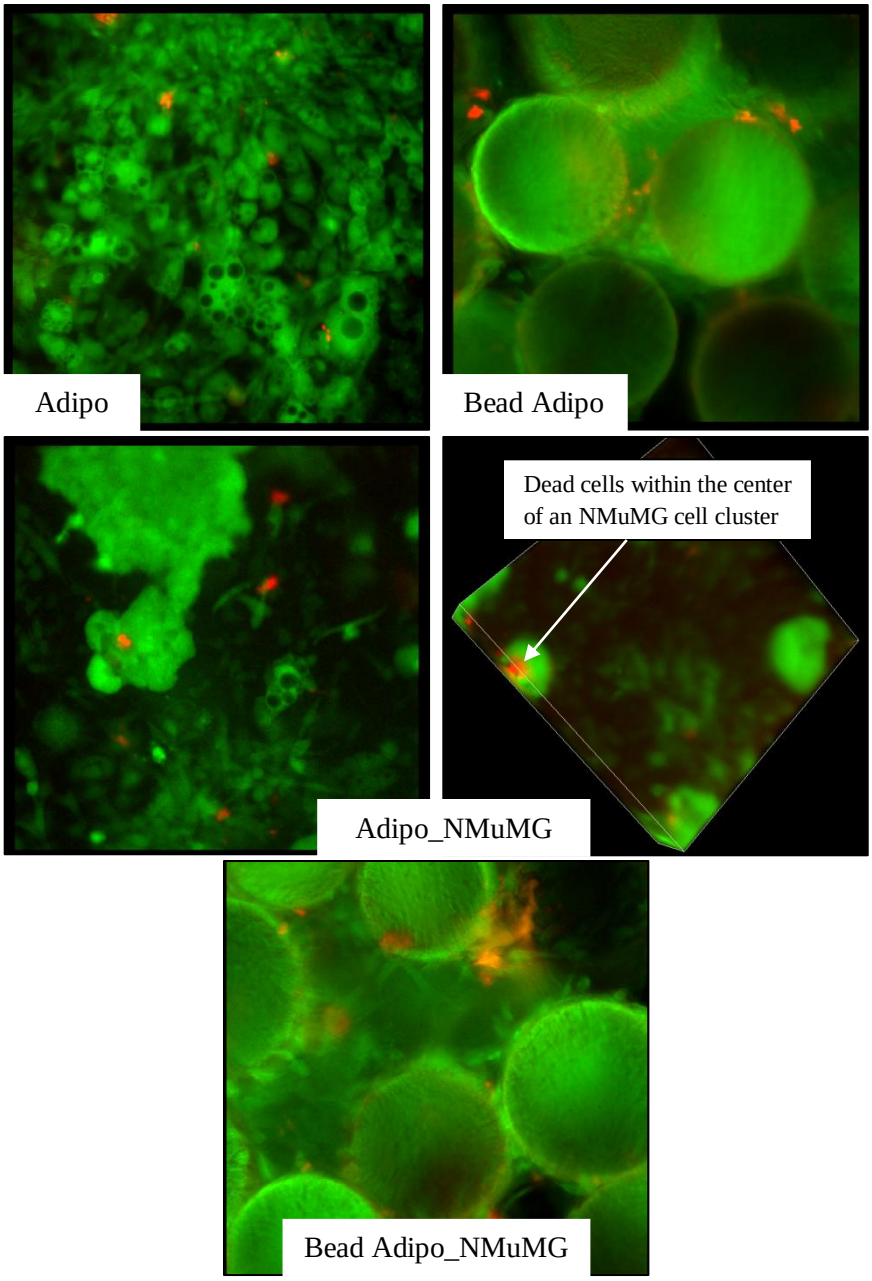

Figure 7.8: Confocal microscopy images of 3D gel-based cultures following 10 days in culture. Images captured using a 20x long-working-distance objective.

Mouse Total MMP-9 Detection

The standard curve of Total MMP-9 determined with a standard solution is depicted in **Figure 7.9**, and had a resultant R^2 value of .9988.

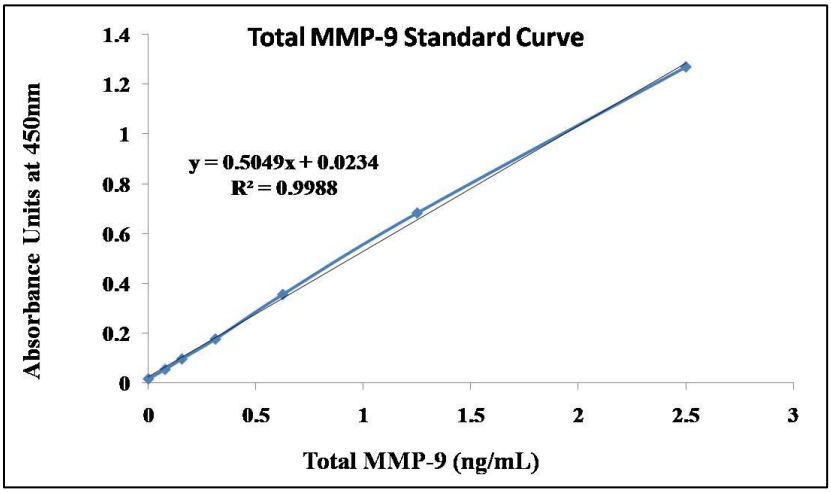

Figure 7.9: Total MMP-9 standard curve obtained by reading known concentrations of a mouse MMP-9 standard solution at 450nm.

Total MMP-9 detected from 3D culture media samples using ELISA is depicted graphically in **Figure 7.10**. Adipo samples had the highest levels of total MMP-9 in media samples at 0.108ng/mL and Bead Adipo samples had the lowest levels at 0.013ng/mL. Adipo_NMuMG and Bead Adipo_NMuMG samples had similar levels of total MMP-9 at 0.047 and 0.039ng/mL, respectively.

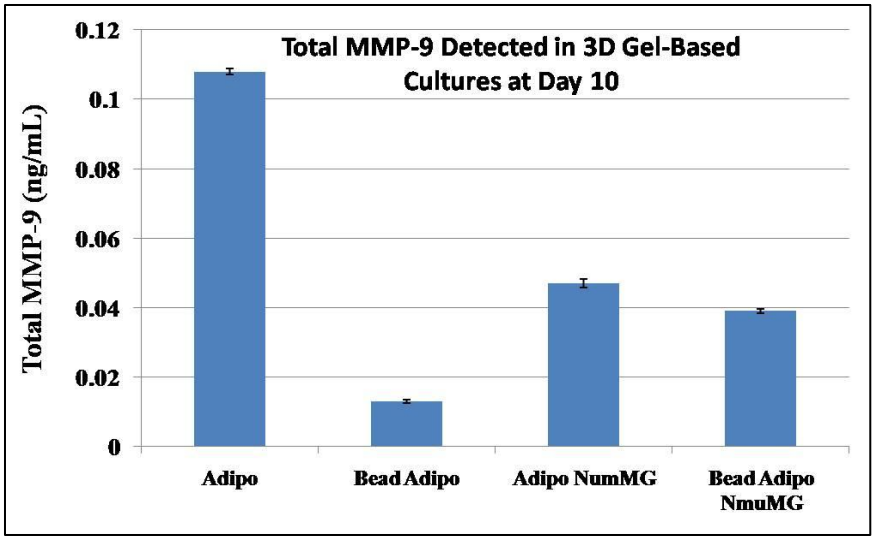

Figure 7.10: Total MMP-9 detected in 3D gel-based cultures at Day 10. Absorbance values were read at 450nm and compared to the total MMP-9 standard curve.

Discussion

Adipogenic differentiation of mesenchymal stem cells (D1s) in a 2D culture flask, prior to seeding in 3D cultures, was confirmed by observing cell morphology and lipid production via Oil-Red-O staining techniques. Though lipid staining in 3D gel-based cultures was also apparent, it will be important in future studies to better understand the resultant composition of fatty acids in each culture environment. Furthermore, in order to maintain the adipocyte phenotype, the bead-based culture systems may prove to be a more favorable option, not only because they provide a rigid surface for the anchorage-dependent cells, but because they do not require dissociation of cells for seeding in gels; when cells are dissociated from a polystyrene flask, it is likely that some of the cells will revert back to a proliferative phenotype instead of continuing down the adipogenic pathway. It has been shown that mature adipocytes are capable of both dedifferentiation

to proliferative fibroblast-like cells (Matsumoto *et al.*, 2008) and transdifferentiation into other mesenchymal cell lineages (Song and Tuan, 2004). Following observation of Adipo mono-cultures, it appears that the ratio of cells forming lipid droplets did not increase over the 10 day culture period; roughly half of the cells were lipid-producing prior to cell seeding and this remained constant over the 10 day-culture period, although lipid did become more dense in the cells committed to the adipocyte phenotype. Based on this information, it is likely that we would see few cells achieve an adipocyte phenotype if cells were seeded in an undifferentiated state, i.e. without being maintained in an adipogenic cocktail for 5 days.

Additionally, following analysis of lipid content in 3D culture systems, it appeared that NMuMG cells inhibited the differentiation of D1 cells located in the gel-based portion of the culture, when comparing the Adipo samples to the Adipo_NMuMG samples; lipid staining was only apparent within the NMuMG cell clusters of co-cultures. Previous *in vitro* studies in our lab have demonstrated that NMuMG conditioned media does not inhibit the differentiation of D1 cells through the adipogenic pathway (Yang *et al.* 2007), however these studies were conducted on 2D polystyrene culture surfaces rather than in a 3D Type I collagen gel environment. The stiffness of the flask may have provided a signaling mechanism to overcome the inhibitory effects of the NMuMG cells. For example, it has been discussed by Gospodarowicz and associates (1978) that cell shape as it relates to its attachment substrate via integrin-ligand binding plays a major role in the determination of cellular growth and behavior. Cells also have the ability to transduce mechanical forces into biochemical signals via the arrangement of the

cytoskeleton, which ultimately follows the interaction of integrins and ligands (Wozniak *et al.* 2003). In the body, local alterations in the extracellular matrix may be responsible for controlling this mechanism.

Therefore, a potential explanation for the production of lipid within an NMuMG cell cluster is that the cluster provides a more stiff microenvironment compared to the relatively compliant Type I collagen gel. Increased stiffness could result from, for example, increased cell density and ECM production, the expression of tight junctions among NMuMG cells, and/or the expression of E-cadherins, which provide tension. Similarly, though minimal lipid staining was apparent in Bead Adipo_NMuMG samples within the collagen gel environment, cells seeded on beads did stain red after 10 days in culture, likely due to the stiff nature of the bead surfaces.

While NMuMG cells appeared to inhibit the differentiation of D1 cells in Adipo-NMuMG samples, the NMuMG cell proliferation appeared to be inhibited in Bead Adipo-NMuMG samples, as there appeared to be far fewer NMuMG cell clusters. Additional studies investigating D1 cell culture environments and the ultimate effect on NMuMG cell behavior with respect to lipid content will be necessary.

Prior to seeding D1 cells in 3D systems, the immunofluorescence (IF) stain for vimentin showed far fewer green-stained cells in the culture flask, when compared to cells cultured on beads. Vimentin is an intermediate filament protein that can reorganize to form cage-like structures around lipid droplets. It has been shown that the disruption of the vimentin intermediate filament system during adipose conversion can inhibit lipid droplet accumulation (Lieber and Evans, 1996). This (IF) stain was used as a marker to

assess whether the applied culture condition (bead vs. 3D gel) had an effect on vimentin organization; it has been suggested that vimentin may play a significant role in the maintenance of cell homeostasis and integrity and that vimentin may induce pro-MMP-2 synthesis (Blain *et al.,* 2006*).*

Based on vimentin staining results, the expression of vimentin does appear to be positively correlated with microenvironmental stiffness, (i.e. green staining was present at the surface of beads and within NmuMG cell clusters but not within the Type I collagen gel). There also appears to be a positive correlation between the expression of vimentin and the accumulation of lipid droplets. Wang (2002), when addressing the mechanical role of vimentin, discussed work demonstrating that vimentin intermediate filaments possess tensional stresses and that cell-cell interactions decrease in the absence of vimentin-positive cells. This phenonenon could ultimately prove to have an effect on the phenotypic maintenace of adipose cells.

When assessing total MMP-9 content of 3D test system media samples following 10 days of culture it was found that the Adipo samples had the highest concentration while Bead Adipo samples had the lowest concentration. Additionally, based on PicoGreen® results for ds-DNA content of 3D test systems, Adipo samples and Bead Adipo samples were relatively close in average corresponding cell number with 3.31×10^5 and 3.47×10^5 cells, respectively, meaning that the total MMP-9 content was higher in Adipo samples even after normalizing to cell number. Previous studies (Karamichos *et al.,* 2009; Hadjipanayi *et al.,* 2009) have shown that fibroblasts will preferentially migrate to a more stiff environment within 3D collagen gel environments. Since cell migration

through the ECM also implies the concurrent secretion of MMPs, this helps explain why the Adipo samples had the highest levels of total MMP-9. This is extremely important when designing a tissue test system since MMP activity can ultimately have an effect on mammary epithelial cell morphogenesis and oncogenesis (Montesano *et al.,* 2007; Chabottaux *et al.,* 2007). Specifically, an influx in MMP activity could result in aberrant migration of epithelial cells.

Finally, it is important to note that this study was intended to run a course of 10 days, although ELISA media samples were harvested at Day 9 because several of the gel samples were already beginning to lift from the culture well surfaces. Future studies may, in addition to native ECM proteins, incorporate additional materials that are not as susceptible to cellular remodeling (e.g. agarose) so that cell behavior can be assessed over longer periods of time.

Conclusions

These *in vitro* culture models are well-suited for the study of normal and malignant mammary gland development because they can be modulated to mimic a particular *in vivo* environment. For example, not only can the stiffness of the system be modified to study changes in cell behavior, but the types and ratios of cells can be varied as well. The results do support the hypothesis that a stiffer substrate (i.e. beads) would result in altered activity of D1 cells, e.g. inducing differentiation. Furthermore, the addition of the beads to a standard 3D Type I collagen gel culture does appear to provide a more favorable microenvironment for the D1 cells, particularly in co-culture with

NMuMG cells, since NMuMG cells only inhibited differentiation of D1s located in the gel environment. Future studies should investigate the bulk stiffness and micro-stiffness (i.e. stiffness of the cellular microenvironment) of 3D gel-based cultures to allow a better understanding of mechanical influences on normal and malignant breast tissue development.

References

Blain EJ, Gilbert SJ, Hayes AJ, Duance VC. 2006. Disassembly of the vimentin cytoskeleton disrupts articular cartilage chondrocyte homeostasis. matrix biology 25:398-408.

Chabottaux V, Noel A. 2007. Breast cancer progression: insights into multifaceted matrix metalloproteinases. Clin Exp Metastasis 24(8):647-56.

Gospodarowicz D, Greenburg G, Birdwell CR. 1978. Determination of cellular shape by the extracellular matrix and its correlation with the control of cellular growth. Cancer Res 38(11 Pt 2):4155-71.

Hadjiipanayi E, Mudera V, Brown RA. 2009. Guiding cell migration in 3D: A collagen matrix with graded directional stiffness. Cell Motility and the Cytoskeleton 66:121-128.

Karamichos D, Lakshman N, Petroll WM. 2009. An experimental model for assessing fibroblast migration in 3D collagen matrices. Cell Motility and the Cytoskeleton 66:1-9.

Krause S, Maffini MV, Soto AM, Sonnenschein C. 2008. A Novel 3D *In Vitro* Culture Model to Study Stromal-Epithelial Interactions in the Mammary Gland. Tissue Eng Part C Methods 14(3):261-71.

Lieber JG, Evans RM. 1996. Disruption of the vimentin intermediate filament system during adipose conversion of 3T3-L1 cells inhibits lipid droplet accumulation. J Cell Sci 13(1):3047-3058.

Matsumoto T, Kano K, Kondo D, Fukuda N, Iribe Y, Tanaka N, MatsubaraY, Sakuma T, Satomi A, Otaki M, Ryu J, Mugishima H. 2008. Mature adipocyte-derived

dedifferentiated fat cells exhibit multilineage potential. J Cell Physiol 215:210-222.

Montesano R, Carrozzino F, Soulié P. 2007. Low concentrations of transforming growth factor-beta-1 induce tubulogenesis in cultured mammary epithelial cells. BMC Developmental Biology 7(7):1-16.

R&D Systems, Inc. 2010. Product Insert.

Song L, Tuan RS. 2004. Transdifferentiation potential of human mesenchymal stem cells derived from bone marrow. FASEB J 18(9):980-2.

Swamydas M, Eddy JM, Burg KJ, Dréau D. 2010. Matrix compositions and the development of breast acini and ducts in 3D culture. *In Vitro* Cell Dev Biol Anim Epub.

Vernon RB, Gooden MD, Lara SL, Wight TN. 2005. Microgrooved fibrillar collagen membranes of micron-scale and submicron thicknesses for cell support and perfusion. Biomaterials 26(10):1109-17.

Wang N, Stamenovic D. 2002. Mechanics of vimentin intermediate filaments. J Muscle Res Cell Motility 23:535-540.

Wozniak MA, Desai R, Solski PA, Der CJ, Keely PJ. 2003. ROCK-generated contractility regulates breast epithelial cell differentiation in response to the physical properties of a three-dimensional collagen matrix. J Cell Biol 163(3):583-95.

Yang CC, Ellis SE, Xu F, Burg KJL. 2007. *In vitro* regulation of adipogenesis: tunable engineered tissues. J Tissue Eng Regen Med 1:146-153.

Zengani D, Darcy KM, Masso-Welch PA, Bellamy ES, Desole MS. 1999. Multiple differentiation pathways of rat mammary stromal cells in vitro: acquistion of a fibroblast, adipocyte or endothelial phenotype is dependent on hormonal and extracellular matrix stimulation. Differentiation 64(2):91-101.

CHAPTER 8

Select results in this chapter were generated as part of an Institute for Biological Interfaces of Engineering interdisciplinary team project in collaboration with Clemson University doctoral candidate Cheryl Gomillion and were published in the Journal of Histotechnology 32(3): 107-113 (Parzel et al., 2009).

EDUCATION AND OUTREACH IN BIOENGINEERING

Effective communication of scientific ideas to the general public is necessary to inform non-scientists about important research and to engage the public and generate interest and support (Parzel et al., 2009). This chapter details four classroom modules that were developed for use in a high school classroom. The first section describes the outcome of our experiences presenting one module to local high school students after which we followed up with a pilot study to improve implementation of bioengineering demonstrations in the public arena. The final two sections describe modules that were developed but have not been rigorously tested in a classroom or public setting.

STEM CELLS AND TISSUE ENGINEERING

Introduction

As tissue engineers, a great majority of our research involves the use of adult stem cells; while presenting our research findings to students at the high school level, we quickly learned that there are great discrepancies in understanding the ethical implications of the use of stem cells. Most students, we found, were unaware that stem cells existed in their very own bodies! The idea for developing a classroom module, therefore, arose because of the many scientific and ethical misconceptions we encountered while working with local schools and presenting educational workshops.

We aim to provide a model-based activity that will more effectively communicate the basic idea of stem cells to a general population and clarify misconceptions.

Classroom Exercise

The following is a simple exercise that can be used to assist in explaining one basic tissue engineering concept that uses adult stem cells.

Isolation of Bone Marrow Stem Cells

In this exercise students will isolate stem cells from a sample of bone marrow, separating the red and white blood cells found in the marrow. The stem cells will then be differentiated (turned into a specialized cell type, e.g. a bone cell) with a chemical cocktail into cells that can be used to form a tissue engineered device for a bone, skin, or soft tissue defect. See **Figure 8.1** for a detailed explanation of tissue engineering. Concepts that will be emphasized include:

1) Stem cells are multipotent cells, meaning that they have the ability to generate multiple specialized cell types that are function and/or tissue specific.
2) Chemical cocktails provide the stimuli needed for differentiation to occur outside the body.
3) When creating a tissue engineered device, the scaffold used to support cell growth is dependent on the cell type and intended location of implantation.

The most relevant National Science Education Standards for this activity are:

> **Life Science** (NS.9-12.3; The Cell; Matter; Energy, and Organizations in Living Systems)
> **Personal and Social Perspectives** (NS.9-12.6; Personal and Community Health; Science and Technology in Local, National, and Global Challenges)

Materials and Supplies

- Empty paper towel rolls = hollow bones (depicted in **Figure 8.2)**
- Squirt bottles filled with water
- Canvas mesh with openings larger than red and white beads but smaller than the yellow, blue, and green beads = cell sorter
- Waste pans large enough to support canvas mesh
- Straight pins
- Scissors
- Stuffed animal
- Bandages
- Disposable gloves
- Safety glasses

Bone Marrow

- Snack size plastic baggies
- Yellow hair gel = bone marrow
- Small red and white beads = red and white blood cells of the bone marrow
- Larger beads in three different colors, such as yellow, blue, and green = differentiated stem cells
- Black acrylic paint = to color large beads black to represent undifferentiated stem cells in the bone marrow

Chemical Cocktails for Cell Differentiation

- Small cups/tubes with lids
- Odorless, non-toxic, non-flammable paint brush cleaner (Betterway® found at local craft stores)
- Food coloring (colors should match colors of larger beads)

One of the most widely researched areas in the field bioengineering is tissue engineering. The National Science Foundation defined tissue engineering as "…the development of biological substitutes that restore, maintain, or improve tissue function" (Skalak and Fox, 1988). The schematic in Figure 1 depicts the general concept of tissue engineering. The steps involved in tissue engineering (Langer and Vacanti, 1993) are as follows:

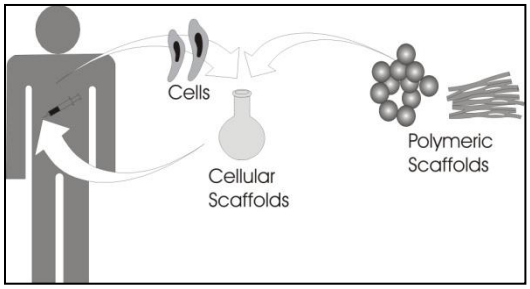

1. A sample of tissue is taken from the patient and healthy cells are isolated from the tissue.
2. The cells are grown (the cells multiply) in the laboratory.
3. Biodegradable scaffolds are fabricated in the laboratory, often in a similar anatomical shape of the injured part.
4. Cells are seeded onto scaffolds.
5. The cellular scaffolds are implanted back into the body at the site of injury or disease.
6. The healthy cells will continue to proliferate and form new tissue as the scaffold slowly degrades. The material gradually breaks down and is "absorbed" by the body and is thus removed.

The idea of using one's own cells (i.e. autologous tissue engineering) means that the body will recognize the cells as "self" and will not attempt to reject them; rather, the body will attempt to incorporate them and return the injured tissue to its natural, original shape.

A large point of public discussion has been over the use of stem cells in tissue engineering applications. Stem cells can be derived from an embryo, fetus, or adult, and they have the ability to mature (differentiate) into many of the body's function-specific cell types. Adult stem cells (ASCs) are most commonly found in the bone marrow, but it is believed that ASCs are only multipotent, meaning they do not have the potential to differentiate into any cell type in the body. Embryonic stem cells (ESCs) are derived from 3-5 day embryos. These cells are able to differentiate into all cell types found in the body, a quality described as pluripotency. Often, differentiated cells of a specific function are not available in large quantities, and thus adult stem cells are a viable option for tissue engineering methods.

	Advantages	**Disadvantages**
Adult Stem Cells	▪ No risk of transplant rejection ▪ Easily maintained in culture ▪ Self-renewing and able to divide over many generations	▪ Limited differentiation potential ▪ Limited number of cells able to be cultured while maintaining an undifferentiated state
Embryonic Stem Cells	▪ Potential to develop into any cell type ▪ Potential for treatment of degenerative diseases ▪ Ability to grow large numbers in the laboratory ▪ Self-renewing and able to proliferate for extended culture times	▪ Ethical Concerns ▪ Transplant Rejection ▪ Development of mixed cell populations following differentiation ▪ Undefined and inefficient cell culturing methods ▪ Formation of tumors

Figure 8.1: Tissue engineering scaffold preparation and the use of stem cells.

Scaffolds

- Styrofoam balls, 1” diameter (soft tissue scaffold)
- Cork stoppers (bone plug)
- Flat cork coasters (skin graft)

Safety

Note that if odorless, non-toxic paint remover is used, then the activity will be relatively harmless to students. However, good laboratory safety habits should be encouraged, included donning of the following:

- Safety glasses
- Gloves (to prevent staining of hands with food coloring)

Figure 8.2: Materials needed for the classroom exercise.

Directions: Advance Teacher Preparation

- Paint the large yellow, blue, and green beads with the black paint, being sure to keep colors separated.
- Prepare the bone marrow packets by squeezing a small amount of hair gel into a plastic baggie. Include red and white beads and one type of the painted black beads.
- Close the baggies and place the baggies inside the hollow bones. Keep track of the color of the painted beads.
- Prepare the chemical cocktails by pouring paint brush cleaner into the small cups/tubes. Add a few drops of food coloring to color the cleaner. The brush cleaner will remove the black paint from the beads to simulate cell differentiation.
- Use bandages to identify injury sites on the stuffed animal. For example, one defect could be a head or neck defect caused by removal of a cancer tumor. A soft tissue graft made with the styrofoam balls would work in this case.
- Distribute the bones filled with marrow, the cocktail, and the scaffolds to the students so that each person has a cocktail and scaffold specific to their stem cell and tissue type. The following system may be helpful:

Bead Color	**Cocktail Color**	**Location of Injury**	**Scaffold Type**	**Cell Type**
Yellow	Yellow	Head or Neck	Styrofoam Ball	Fat
Blue	Blue	Leg	Cork Stopper	Bone
Green	Green	Stomach	Flat Cork Coaster	Skin

Student Activity

The problem:

Mr. Bear was in an accident and suffered injuries to his leg, face, and abdomen.

Your job:

Isolate bone marrow stem cells that can be used to engineer new bone, fat, and skin tissue to repair his injuries.

- Remove the bone marrow packets from the bone.
- Place the canvas mesh over the waste pan.

- Cut open the marrow pouch and squeeze the gel and beads onto the top of the mesh.
- Use the squirt bottles to rinse. The red and white blood cells should go through the mesh and be collected in the pan. The larger undifferentiated stem cells should remain on top of the mesh (The cells are sorted based on their size as seen in **Figure 8.3**).

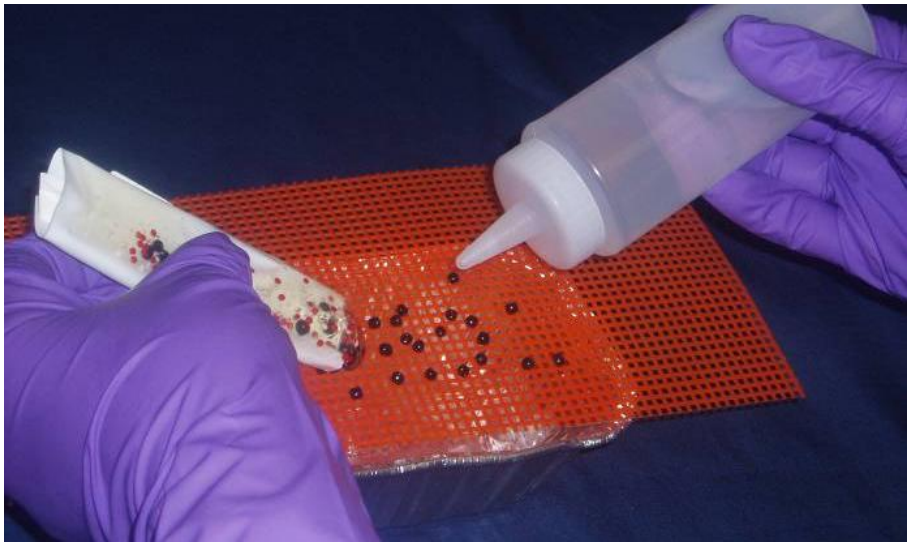

Figure 8.3: Cell sorting based on size of the cell. Smaller red and white beads (blood cells) will fall through the mesh while larger painted black beads (stem cells) will remain on top of the mesh.

- Place the remaining black stem cells into the colored chemical cocktail. Close the container and shake vigorously for 1-2 minutes. The paint should release from the beads.
- Open the container and pour the solution through the canvas mesh. Rinse with the squirt bottles to remove any foam that has formed from shaking. The color of the beads should now be revealed. (The stem cells have differentiated into multiple cell types as seen in **Figure 8.4**).

Figure 8.4: Differentiation of stem cells into specialized cells. Specimen cups contain non-toxic paint remove and food coloring (differentiation cocktail), and black paint is removed from the black painted beads (stem cells) demonstrating cell differentiation. Specialized cells include fat cells (yellow beads), bone cells (blue beads), and skin cells (green beads).

- Use straight pins to attach the beads to the scaffolds. This forms the tissue engineered device.
- The straight pins may also be used to attach the grafts to the stuffed animal's defect sites to repair its injuries (**Figure 8.5**).

Figure 8.5: Clemson Bear with multiple injuries. Here, green beads (skin cells) are attached to the flat tissue engineering scaffold. This scaffold will eventually degrade as skin cells continue to proliferate and rebuild the injured skin tissue on the abdomen.

Classroom Assessment Tools

With the assistance of a science teacher at a regional high school in the southeast, the hands-on activity was presented to a group of 51 10th grade honors biology students in two class periods. Prior to the activity, students were given a simple, anonymous pre-quiz, which included the following questions:

1) What is a stem cell?
2) Do you support stem cell research?

One day following the pre-quiz, the students were presented with slides containing general information about stem cells and tissue engineering, along with a list

of essential vocabulary words presented in **Table 8.1**. Then, students were divided into groups of four to complete the classroom activity. At the end of the week, the students were tested on class material, including information related to stem cells in tissue engineering research.

Table 8.1: Pre-activity Vocabulary Words

Adult Stem Cell (ASC)	Cells with differentiation capacity that exist in the fully developed human body, such as in the bone marrow, blood, and intestines. ASCs are believed to be multipotent.
Chemical Cocktail	A supplement added to a culture of stem cells that is intended to induce differentiation into a predetermined specialized cell type.
Differentiation	The process by which stem cells become more specialized and acquire specific functions.
Embryonic Stem Cell (ESC)	Cells with differentiation capacity that can be derived from an early stage embryo. ESCs are pluripotent.
In Vitro	Takes place inside a laboratory environment.
In Vivo	Takes place inside of a living organism such as a mouse, rat, or human.
Multipotency	The ability to differentiate into a limited number of cell types in the body. For example, a multipotent ASC from the bone marrow may be able to differentiate into fat, cartilage, and bone cells but not into liver cells.
Pluripotency	The ability to differentiate into any cell type in the body.
Scaffold	A substrate derived from natural or synthetic material that is intended to mimic tissue in the body and support cell growth while building new, healthy tissue.
Tissue Engineering	A field of study that combines techniques from engineering and biological sciences with the goal of repairing and/or replacing diseased or damaged tissue, to improve the quality of life of the patient.

Student Knowledge and Opinion

The students responded to anonymous, pre-quiz questions in a free-response format. Following, in **Table 8.2**, are selected answers from the students to the questions 1) "What is a stem cell?" and 2) "Do you support stem cell research?". The following list of quotes is not comprehensive, but the quotes are representative of the entire classroom of students. Statements that were not included are at least thematically related to the ones presented here.

Table 8.2: Student Responses to Pre-Quiz

1) "DNA they take out of babies…for cloning." 2) "I do not support stem cell research because I do not believe in cloning."
1) "Embryos in the very first stage of development." 2) "No, because embryos are babies and they are killing them."
1) "Stem cells are the cells that make parts in the human body. They can be used to reproduce parts of the body." 2) "I support cell research because it could help very many different problems…"
1) "Stem cells are unspecified cells that have the potential to become specialized." 2) "Not really. It would be great if we could reverse injuries…we need to find another way than to take another human to cure them…"
1) "I don't know." 2) "I don't know."
1) "Stem cells are cells in the body that can be used in any different area in the body." 2) "I do support stem cells, but I don't think it is right to take them from baby embryos. I think that if you can take them from your own body then it is fine."

All of the students who took the post-test received a grade of 80% or better. Questions directly assessing knowledge on stem cells included the following:

1) What is a stem cell?
2) Are fetuses and embryos the only places where stem cells are found?
3) Why is it important for people to understand stem cells?

Other questions included on the post-test gauged knowledge of tissue engineering, which is the area of research upon which the module is based. The responses to the tissue engineering related questions are not included here. Selected answers from the students to these particular questions follow in **Table 8.3**.

Table 8.3: Student Responses to Post-Test

1) "Cells that can differentiate and help research." 2) "No, brain, liver, skin." 3) "It is important because people need to know that all stem cell research does not involve harm."
1) "Stem cells are undifferentiated cells." 2) "No, also adults." 3) "…Also, many people who don't understand stem cell research and are against it because they don't really know about it."
1) "It is a specialized structure that can take on any cell role in the body." 2) "No, can be found in adults also." 3) "So they can help to not hinder the progression of new medical breakthroughs in stem cell research."
1) "An undifferentiated cell that can be embryonic or adult." 2) "No, bone marrow, brain, liver, skin, muscle, eyes." 3) "They help life go easier for people when they get really hurt or have a disease."
1) "An undifferentiated cell." 2) "No." 3) "So that they understand that it's not killing babies and what it is really used and meant for."
1) "An undifferentiated cell." 2) "No!" 3) "So we can make advancements in medicine and to also inform people that cells don't just come from embryos or fetuses."

Developing Student Understanding

Classroom lessons involving the discussion of stem cell biology and ethics are limited, largely due to the influence of state and federal education standards. The goal of this project was two-fold. First, we wanted to understand the misconceptions of high school students regarding stem cells and demonstrate the need for incorporation of a stem cell biology lesson in the high school science curriculum, due to its controversial nature in the news media. Second, we wanted to develop a classroom teaching tool that could potentially meet education standards, which would help teachers clarify the differences between human and embryonic stem cells.

According to the anonymous pre-quiz, most students fell into one of three categories when answering the question "What is a stem cell?" Students either 1) knew to some extent that stem cells have the potential to become specialized 2) believed they were deoxyribonucleic acid and/or involved in cloning or 3) simply did not know the answer. When asked about whether or not they supported stem cell research, a majority of the students made comments about cloning or harming babies. Only a few of the students alluded to the idea that stem cells could be harvested from adults. There were also some students who claimed they were against stem cell research, but they could not explain why. Following the teaching module, students who took the post-quiz showed improvement in understanding stem cell biology and why society needs to be better informed about research involving stem cells. For example, all of the students answered "no" when asked if embryos and fetuses are the only sources of stem cells and some commented on specific adult tissues where they may be located, such as the bone

marrow. Additionally, students no longer focused on cloning as an application of stem cells. When asked why it is important for people to understand stem cells, students discussed their utility in tissue replacement and saving lives, and some even mentioned the need for better understanding of stem cells so that people in society can make more informed decisions about research and medical ethics. The pre-quizzes were not graded, nor were they a direct comparison to the post-test. Therefore, data indicating an improvement in understanding is partially qualitative and observational. In order to assess the effectiveness of the stem cell demonstration on the understanding of basic stem cell biology concepts, two classes would be required. One class would serve as a control, where only traditional teacher-centered methods (a MS Powerpoint presentation) would be used to teach the class. The second class would serve as the experimental group in which both a Powerpoint presentation and the stem cell demonstration would be used. Prior to implementation of teaching methods, students in both classes would be given a pre-quiz to ensure that knowledge of stem cell biology as well as misconceptions were similar. Two weeks after implementation of teaching methods, students would be given a quiz containing questions similar to those on the pre-quiz as well as additional application questions. This would test the effect of this particular hands-on learning activity on both the retention and application of information.

Conclusions

Overall, this classroom demonstration on stem cells appeared to be very useful in helping students understand the major differences between embryonic and adult stem

cells and the applications of these cells in bioengineering research. Certainly, this material could have been presented to the class using traditional lecture-style methods. In fact, the module was introduced to the class after a slide presentation about tissue engineering and stem cells. However, because it has been shown that some students do not learn as well in a teacher-centered, passive learning environment, (Spence 2001), this tool may prove more effective in the delivery of a stem cell biology lesson.

Likely, some of the students in the classes would have fared well with only the slide presentation from which to learn about and better understand stem cell biology; however, because of the wide range of learning styles in any particular classroom, this tactile activity may help reach some of the students who require a more active learning environment. Lastly, this activity may reinforce the importance of model systems; students should realize that models are used to study concepts or objects that are, for example, too large (model of the solar system, or a globe), too small (model of cellular organelles), or just inaccessible or unsafe (model of an active volcano). With each example, students can discuss the short-comings of these classic science models. Perhaps the biggest flaw of this model is that the beads are already colored before they are painted. This aspect implies that the stem cells already have a plan before differentiation. Based on our teaching experience, we have found that most hands-on activities generate student enthusiasm and allow them to enjoy science and recall more information. Going through the process of treating the bear gave students a memorable activity showcasing how medical problems might be solved with the use of adult stem cells. Additional

assessment of this activity could lead to broader studies on active learning that may assist in reshaping the STEM curricula.

Increasing Effectiveness of Bioengineering Demos: A Pilot Study

To complete this pilot study, a module demonstrating the function of cartilage in the knee was presented at The Museum of Science Design Challenges center (Boston, MA). This module was selected because of its simplicity in material preparation, which lended itself to ease in travel and functionality in large, informal groups. The purpose of this pilot study was to better understand if the Design Challenges center would serve as an appropriate arena for future education studies and to gauge the type, scope, and limitations of possible future studies. Design Challenge activities are typically open to all museum visitors daily from 10:30am-12:30pm, and they are intended to promote the design of engineered prototypes and to demonstrate that engineering is an iterative process.

The cartilage module was implemented during a two hour timeframe following the regularly scheduled Design Challenge activity (**Figure 8.6**). Because the demonstration was not listed on the museum's schedule of activities, participants were informally recruited by museum employees. Participants were asked to begin the activity by filling out a questionnaire consisting of the following questions:

1. What is cartilage and what is its function in the body?
2. Where in the body is cartilage located?
3. Why might a patient have a need for a knee implant?
4. Please tell us your age and gender.

Figure 8.6: Design Challenges Center at the Museum of Science in Boston. Implementation of cartilage teaching module.

After completing Part 1 of the questionnaire, participants were shown a model of a knee joint containing a prosthetic knee implant and asked about their familiarity with the function of cartilage. Regardless of their written and verbal responses, the participants were then instructed how to complete the module. Participants were given a magic erase board, 2 sheets of purple foam, a wooden "knee" block, and a ruler. They were asked to place 0, 1, or 2 sheets of foam on top of the magic erase board and to drag

the wooden knee joint block from top to bottom of the foam to make a vertical line on the underlying magic erase board (**Figure 8.7**). Equal pressure was used for each trial to simulate constant body weight.

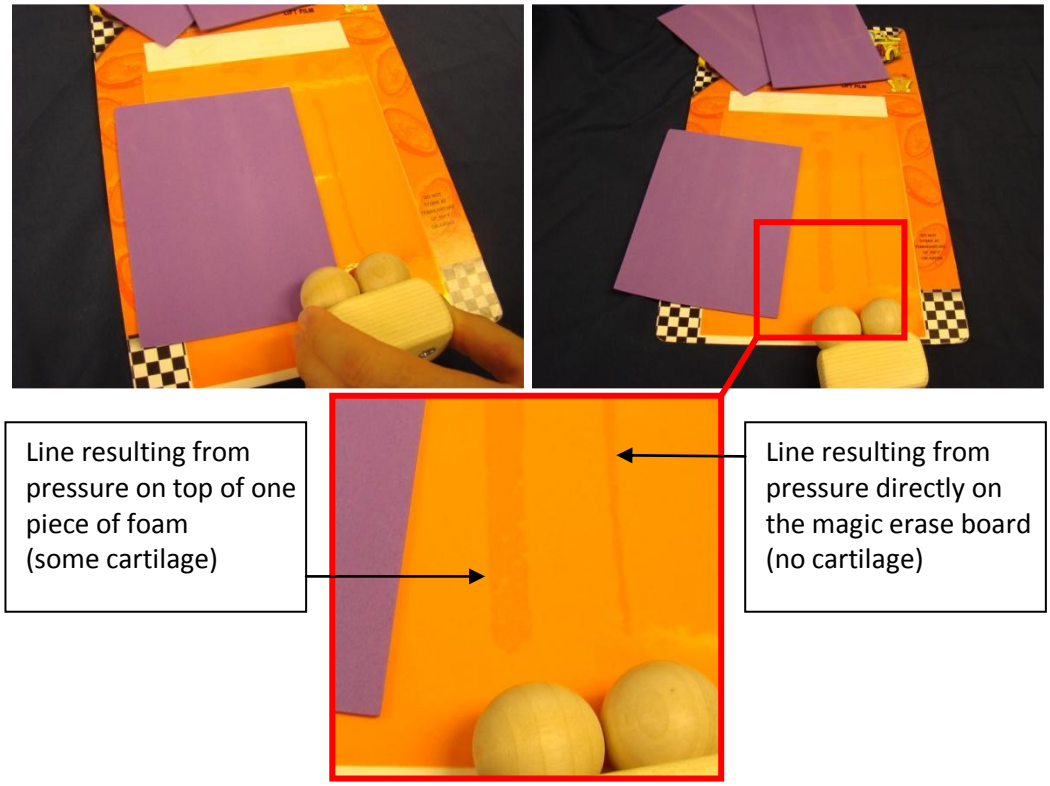

Figure 8.7: Cartilage teaching module. Wooden block represents knee joints while purple foam represents thickness of cartilage. Left side shows participant pressing knee joint over one piece of foam or directly on magic erase board (no foam). The right side shows the resultant lines. The line formed underneath the sheet of foam is much thicker, indicating that the force in that knee will have a wider area of distribution.

Participants were then asked to describe and explain the thickness of resultant lines in terms of weight distribution in the knee joint. At the end of the demonstration,

participants were asked to complete Part 2 of the questionnaire, which consisted of the following questions:

1. What is cartilage and what is its function in the body?
2. Where in the body is cartilage located?
3. Why might a patient have a need for a knee implant?
4. How does the thickness of cartilage in the knee compare to the thickness of cartilage in the shoulder? Why?

Part 2 of the questionnaire was identical to Part 1, except it included an additional question that required application of knowledge about cartilage to another area of the body.

In the two hour timeframe, 60 participants were recruited to complete the cartilage module, 50 of whom completed both Parts 1 and 2 of the questionnaire. Of those 50 participants, 43 attempted to answer the application question on Part 2 of the questionnaire. Eight of the 50 participants were male while 42 were female, and the distribution of ages is presented as a histogram in **Figure 8.8.**

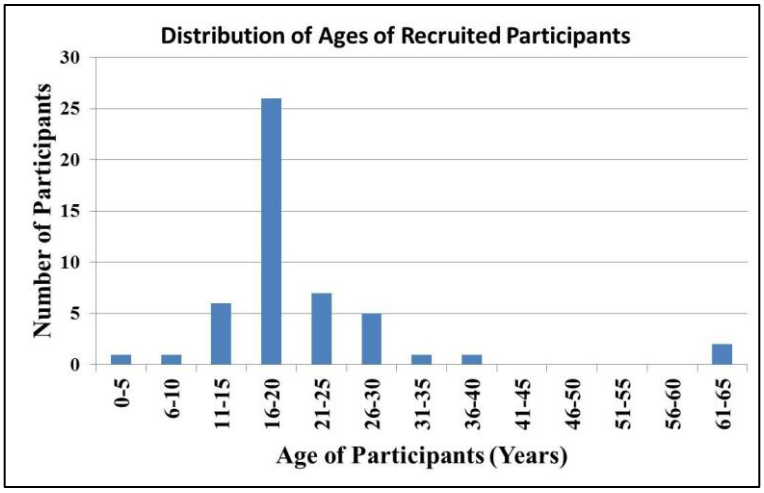

Figure 8.8: Age distribution of participants recruited to complete cartilage teaching module.

Overall, the Museum of Science Design Challenges Center did appear to be an appropriate setting for the implementation of teaching modules. There was a wide range of ages, although a majority of the participants were between the ages of 16-20. Based on the 43 answers to question 4 on Part 2 of the questionnaire (listed below), implementation of the module in a large group was not productive because most of the students appeared to be sharing answers. They were focused on getting the correct answers instead of learning from the module. This was particularly apparent when a large group (>20) of high school-aged girls participated; there was a lack of involvement, and there are several identically answered questions in the female age group 16-17 (answers 16-38 below). Because of this observation, we recommend no more than four participants to one instructor. Additionally, in this informal setting, the attention span of the participants appeared to be limited to approximately 5-10 minutes, depending on the age group. Of the 60 participants, only one person stayed behind to perform the pressure

calculations based on the equations listed in a worksheet that was distributed at the beginning of the activity.

Answers to Question 4, Part II:

1. Thicker in the knee – more weight placed on it.
2. Body weight.
3. Cartilage in the knee is thicker because it has to support more weight and is subjected to more pressure.
4. Knee cartilage would be thicker as our legs need more pressure distribution. They carry the weight of our bodies over extended periods.
5. Knee cartilage is thicker due to having more force and pressure than the shoulder.
6. It is thicker in the knee because it is a weight-bearing joint.
7. Your knees bear more weight so maybe they have more cartilage, but shoulders move in more ways so there might be more area.
8. Knee cartilage is thicker because it is weight bearing.
9. It would be thicker in the knee because the knee bears weight whereas the shoulder usually doesn't.
10. I would imagine knee is thicker because it has more wear due to supporting greater weight.
11. It's probably thicker in the knee because it has to support the weight of the body and has less stress.
12. Cartilage in the knee would be thicker because it bears more weight than the shoulder joint.
13. Thicker – needs more.
14. Thicker cartilage in knee because more force on knee than on shoulder.
15. It's thicker due to needing more surface area to support the weight constantly put on it.
16. The cartilage in your knee is thicker than on your shoulder due to the amount of weight it needs to support.
17. Knee is thicker because it must support more weight.
18. The cartilage in the knee has more pressure because less area.
19. They are softer, but it needs to be a little loose to move the two knee bones.
20. It's softer on the shoulder.
21. It's softer in the shoulder.
22. No idea, sorry – perhaps thicker to provide support.
23. Thicker in knee because more pressure in the knee.
24. More pressure, less surface area.
25. Knee less thick.
26. It is better.
27. Thicker in knee because we use it (our knees more).
28. Thicker in the knee because there is more pressure.
29. Thicker in the knee because of pressure.
30. Thicker in knee because more pressure on knee.
31. Thicker in the knee because we use our knees more.
32. Thicker in the knee because more weight and pressure there than in the shoulder.
33. It's thicker, holds the weight of your body.
34. More because you use it more.
35. It's thicker in the knee so there is less pressure in the shoulder.
36. There's more in knee than in shoulder.
37. It's thicker in the knee because there's more weight to support.
38. It's probably more thick in the knee because more pressure to put on it.
39. It is thicker because there are two bones rubbing against each other.
40. Not a lot of weight.
41. The knee is lowest so there isn't as much weight.
42. The thickness of cartilage in the knee is thicker because there is more pressure being put on your legs.

43. More in the knee.

In addition to promoting the development of an informed community of non-scientists, the implementation of teaching modules with the general public could provide a means to enhance graduate student communication skills. Graduate student communication skills are important because this population of students can help bridge the gap between K-12 and university level academic environments, ultimately enhancing science, technology, engineering, and mathematics (STEM) curricula and teaching methods (Huziak-Clark *et al.*, 2007). A study in 2005 (Andrews *et al.*, 2005) found that most graduate students were motivated to participate in outreach projects because of the opportunity to improve their teaching and communication skills. Based on these findings, a study investigating the development of graduate student communication skills will be universally valuable in the endeavor to improve STEM education.

Explore these online resources for more information:

1.Clemson University Institute for Biological Interfaces of Engineering (IBIOE): Bioengineering Learning Module
http://www.clemson.edu/centers-institutes/ibioe/tiger.html

2. Regenerative Medicine Partnership in Education
http://www.sepa.duq.edu/forms/index.html

3. Pittsburgh Tissue Engineering Initiative: Regenerative Medicine
http://www.ptei.org/section.php?pageID=5

4. National Institutes of Health (NIH) Resource for Stem Cell Research
http://stemcells.nih.gov/info/basics/

5. Stem Cells: A Primer
http://www.bioethik-diskurs.de/documents/wissensdatenbank/linksammlung/Linkliste_neu/Stem_Cells.pdf

References

Andrews E, Weaver A, Hanley D, Hovermill J, Melton G. 2005. Scientists and public outreach: participation, motivations, and impediments. J Geoscience Ed 53(3): 281-293.

Huziak-Clark T, VanHook SJ, Nurnberger-Haag J, Ballone-Duran, L. 2007 Using inquiry to improve pedagogy through K-12/university partnerships. School Sci Math 107(8): 311-324.

Langer R, Vacanti JP. 1993. Tissue engineering. Sci 260:920-926.

Parzel CA, Gomillion C, Burg KJL. 2009. Collaborating with school teachers: histology as a science and technology teaching tool, J Histotechnol 32(3):107-113.

Skalak R, Fox CF. 1988. Tissue Engineering. Alan R. Liss Inc., New York, NY.

Spence LD. 2001. The case against teaching. Change 33(6):10-19.

INFLAMMATION AND ENCAPSULATION

Introduction

The shape of a biomedical device should be carefully considered in the design process, as sharp or rough edges tend to cause chronic inflammation in surrounding tissue following implantation. During an implantation surgery, the body's inflammatory response is immediately initiated due to tissue damage and disruption of microvasculature (blood capillaries). Specific inflammatory cells called macrophages are called to the site of injury/implantation via chemical signals (chemotaxis) to engulf and digest foreign particles. Macrophages fuse to form foreign body giant cells when debris particles are too big to engulf. Over time, if a material (or biomedical device) cannot be broken down, an encapsulation response will occur; multiple layers of fibrous collagen will be deposited around the implant to completely isolate it from the surrounding host tissue. Chronic inflammation results in a foreign body response followed by formation of granulation tissue (immature tissue with many new blood vessels) and implant encapsulation. The intent of this exercise is to demonstrate that fibrous encapsulation around sharp edges of an implant is much thicker that that surrounding a smooth, uniform surface, because sharp edges are more irritating to the surrounding tissue. A higher cellular response (and thicker fibrous capsule) means the implanted device is less "biocompatible".

Classroom Exercise

The following is a simple exercise that can be used to assist in describing the response of the body to a medical implant.

Inflammation and Encapsulation

In this exercise students will wrap collagen around the implants, observing which implant allows space for granulation tissue, which will also be added as appropriate. Concepts that will be emphasized include:

1) The texture of an implant can stimulate the formation of a collagen capsule; implants with thicker capsules are considered less "biocompatible".
2) Implants made of the same material, implanted at the same site, can cause very different reactions if their shapes differ.
3) Devices are typically designed to cause minimal inflammation.
4) An implant does not have to be made from living tissue (i.e. a liver transplant) to cause a reaction in the body.
5) Inflammation is not the same process as infection. Infection only occurs if a pathogen (e.g. bacteria) is present in the tissue.

The most relevant National Science Education Standards (for Grades 9-12) for this activity are:

> **Scientific as Inquiry** (NS.9-12.1; Understandings about Scientific Inquiry; Abilities Necessary to do Scientific Inquiry)
>
> **Life Science** (NS.9-12.3; The Cell; Matter; Energy, and Organizations in Living Systems)
>
> **Science and Technology** (NS.9-12.5; Understandings about Science and Technology)
>
> **Personal and Social Perspectives** (NS.9-12.6; Personal and Community Health; Science and Technology in Local, National, and Global Challenges)

Materials and Supplies (per student)

- One wooden block cut to form pyramid (paint if desired as shown in **Figure 8.9**)
- One wooden ball (paint if desired)
- Two lengths of white rope
- Six adhesive, Velcro dots (each dot comprised of a hook and a loop disc)
- Five adhesive, Velcro dots (will need five loop discs and one hook disc)
- Sponge
- Red beads
- Safety pin

Figure 8.9: Prepared materials for demonstration. Orange ball and pyramid represent implants, white ropes represent collagen fibers, and spongy material represents immature scar tissue.

Student Activity

The problem: The Clemson Tiger needs an implantable identification tag.

Your job: Determine which tag, a sphere or a triangular block, will cause minimal disruption *in vivo*.

- Paint blocks and balls if desired.
- Attach two Velcro dot hooks to wooden ball and two Velcro dot loops to rope that is cut to fit around the ball such that the hooks and loops engage.
- Attach two Velcro dot hooks to the two parallel faces of the pyramid; attach two Velcro dot and to the rope that is cut to size.
- Prepare new blood vessels by attaching red beads to safety pin.
- Prepare granulation tissue by attaching blood vessel to sponge. Put a Velcro dot on the bottom side of the granulation tissue that will correspond to a macrophage.
- Give each student a pyramid and a ball, with corresponding ropes cut to size.
- Focusing on the top edge of the triangle, attach the loop discs of five Velcro dots to the implant top edge, simulating chemotaxis of macrophages and formation of foreign body giant cells, as seen in **Figure 8.10**.
- Attach granulation tissue to top of foreign body giant cell layer, by engaging the Velcro hook disc on the sponge with a loop disc on the pyramid.
- Engage the rope Velcro loops to the matching pyramid Velcro hooks, such that the rope surrounds the block and the macrophages and granulation tissue.
- Engage the rope Velcro loops to the matching ball Velcro hooks, such that the rope surrounds the ball.
- Measure the distance between the surface of the wood object and the top surface of the rope at three locations on both implants and, for each object, calculate the average capsule thickness.
- Based on capsule thickness, which implant is more "biocompatible" and why?

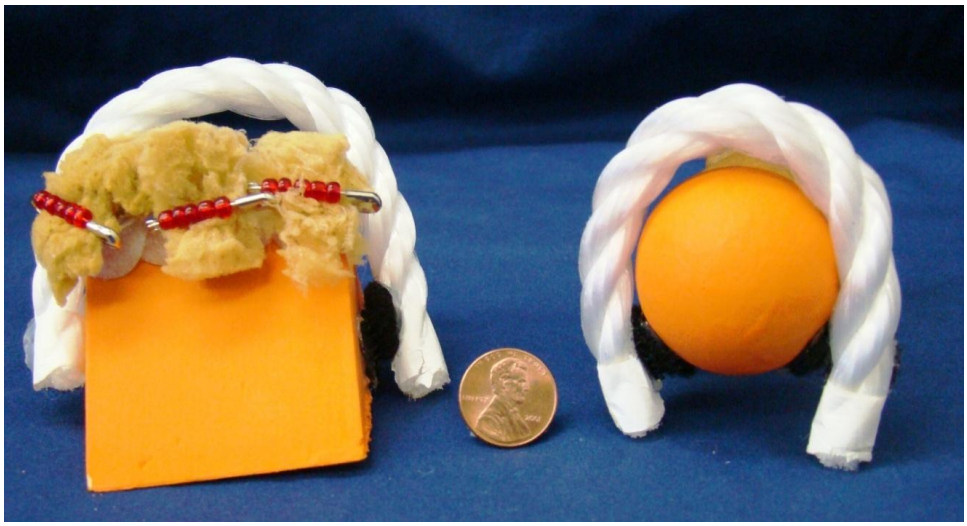

Figure 8.10: Orange implants are surrounded by collagen fibers following implantation. The sharp edges of the pyramid shaped implant cause formation of scar tissue and therefore a much thicker fibrous capsule.

RELEVANCE OF SURFACE TEXTURE OF BIOMATERIALS

Classroom Exercise

In this exercise students will create bead surfaces with different textures. Cells will be combined with beads in a roller bottle, just as they would in the creation of a tissue engineered implant, to observe differences in cell attachment.

Relevance of Surface Texture of Biomaterials

Concepts that will be emphasized include:

1) Many cell types, including fat cells, are termed anchorage dependent. That is, in order to grow, divide, or maintain function, they require a surface of sufficient mechanical stability on which they can attach.

2) Surface topography is a crucial factor in determining cell attachment, division, and function. Anchorage dependent cells often attach better to surfaces of specific roughness than to smooth surfaces.
3) In the body, the protein based extracellular matrix provides the surface of sufficient mechanical stability; in the lab, engineers need to find ways to best mimic the extracellular matrix.

The most relevant National Science Education Standards are:

Science as Inquiry (NS.9-12.1; Abilities Necessary to Do Scientific Inquiry; Understanding About Scientific Inquiry)

Science and Technology (NS.9-12.5; Abilities of Technological Design; Understanding about Science and Technology)

Materials

- Roller bottle for cell culture (as seen in **Figure 8.11)** from lab supply vendor (or substitute 2 liter soda bottles)
- Six small, smooth wooden balls
- Bag of red gift wrapping paper shreds
- Several packages of adhesive white and black Velcro® dots

Figure 8.11: Materials prepared for classroom demonstration. The roller bottle is a culture vessel in which cells will grow. The red paper represents cell culture medium (nutrients for the cells), wooden balls represent cell scaffolds, and black velcro dots represent cells.

Student Activity

- Add a few shreds of red paper to the roller bottle vessel to simulate the cell culture medium, which supplies many nutrients and growth factors to the cells.
- Cover three of the wooden balls with 4 white Velcro® dots. Use only the plastic "hook" ends. The smooth and rough balls will serve as two different tissue engineering scaffolds. The balls are made of the same material, but three of them have been "chemically" modified.
- Cut several black Velcro® dots in half (the fuzzy "loop" end) and fold sticky ends together. These dots will serve as your anchorage-dependent cells.
- Add the six scaffolds and several cells to the cell culture medium in the roller bottle.
- Roll the bottle slowly and observe how the cells attach to the scaffolds.

BIODEGRADABLE MATERIALS FOR DRUG DELIVERY APPLICATIONS

Introduction

The development of new drug delivery systems is important because bulk administration of a drug often leads to excess side effects, systemic toxicity, and drug dilution. By using biodegradable materials, bioengineers can not only better target a region of the body, but can also create slow-releasing delivery vehicles that essentially eliminate high and low peaks of drug dosage.

The degradation of materials is dependent on many factors including pH and temperature. In this exercise, students can observe how coating a drug capsule with an extruded biodegradable polymer can allow the drug capsule to resist degradation in the warm, acidic environment of, for example, the stomach and target the colon at the end of the digestive system. What is normal pH in the stomach? What is physiological temperature?

Materials

- Hot plate (**Figure 8.12)**
- Two glass beakers
- Vinegar
- Empty drug capsules
- Alka Seltzer tablets
- Silly putty
- Play-dough extruder
- Stop watch

Figure 8.12: Materials prepared for classroom demonstration. The vinegar and hot plate will provide the warm, acidic environment of the stomach through which a drug needs to travel. Alka Seltzer tablets will be crushed and loaded into gel capsules and either left bare or covered with silly putty.

Student Activity

- Pour equal amounts of vinegar into two glass beakers and allow vinegar to pre-heat on hot plate to re-create the warm, acidic environment of the stomach
- Crush Alka Seltzer tablets into a fine powder and fill empty capsules
- Extrude a polymer through the play-dough extruder (silly putty works better than play-dough)
- Coat one drug capsule with the polymer and leave the other uncoated
- Put one coated and one uncoated capsule in each of the beakers containing vinegar and observe
- The uncoated capsule should degrade in about 1-2 minutes. The coated capsule should degrade within 45 minutes

CHAPTER 9

CONCLUSIONS

The first step was to modify printing parameters to identify optimal model conditions. Specifically, the effect of stage height on cell viability was evaluated, the relationship between the rate of nozzle firing and the viscosity of a bio-ink identified, and the statistics of cell placement in a printed co-culture pattern determined. It was concluded that the height of the stage had no effect on cell viability when testing distances up to 11.2mm. Since 11.2mm is far beyond the distance at which a discernible pattern would likely print, the stage height does not appear to be of concern when considering cell viability in future experiments. When making observations about the viscosity of a bio-ink and the rate of nozzle firing, the data indicate that the nozzle firing frequency (1/period) must be matched to viscosity. If the firing frequency is too high relative to the viscosity, drop production will cease. Finally, increased bioprinting sample output and better cell adhesion will continue to improve the ability to precisely pattern two or more cell types in 2D and improve studies investigating cell migration, differentiation, and communication. The cell placement experiments demonstrate that the system has sufficient capability to enable development of biological models that better mimic heterogeneity of natural tissue.

The next challenge was to address one of the major limitations of bioprinting, that of cartridge nozzle clogging, by evaluating the effectiveness of ethylenediaminetetraacetic acid as an anti-scalant and anti-aggregant in 2D high-

throughput bioprinting. The results showed that EDTA may be added to cell culture media in order to prevent nozzle failure and to facilitate the high throughput production of 3D complex tissues. The 0.53mM solution of EDTA was the best solution tested because it prevented nozzle failure for the duration of the study, had the greatest proportion of successful drops printed in the cell ejection study, and had no statistically significant toxic effects when cells were suspended in bio-ink solutions for zero minutes and maintained in culture for 24 hours. An approximate concentration of 0.53mM EDTA in HBSS should be incorporated into all bioprinting cell suspension solutions that could trigger salt crystal formation leading to printhead failure.

The next step was to demonstrate the high resolution capability of the custom bioprinting system by printing mono- and co-culture patterns and applying thermal inkjet technology to stain histological samples and cell monolayers, which will be important in the future analysis of test systems. It was found that one key factor in enabling both the speed of attachment and viability of cells during the initial incubation period (immediately following bioprinting) was the collagen substrate on which cells were printed. The addition of a wet collagen substrate gave the cells a readily available attachment point and allowed enough moisture retention to prevent cell stress. also It has been shown that a bioprinting system based on drop-on-demand thermal inkjet technology is a viable technology for depositing a variety of reagents on histological samples. The ability to tailor the amount of reagent based on tissue and protocol is a key benefit of this system.

Following the demonstration of high-resolution bioprinting, high-resolution patterns of murine cells were printed in 2D to evaluate paracrine signaling among adipocytes and cancer cells. Accordingly, D1 and 4T1 cells were printed in co-culture patterns and the effect of 4T1 cells on the proliferation of D1 cells treated with an adipogenic cocktail was evaluated. A variety of post-bioprinting processing methods to increase cell viability and pattern retention were evaluated. Based on the experimental results, it was concluded that, for the purpose of generating heterogeneous tissue test systems, cells should be treated immediately after bioprinting with HBSS, followed by an overlay of collagen, and finally D1 maintenance medium. The combination of HBSS and collagen promote cell attachment and limit migration. The collagen substrate absorbs comparatively large amounts of liquid while keeping the pattern intact, allowing cells to be printed at higher densities. Additionally, staining methods can provide initial insight into cellular relationships and effects of microenvironmental factors, however, quantitative methods of protein and gene analysis will be necessary to glean optimal information from tissue test systems.

The last step was to show that different microenvironmental requirements will be necessary to sustain the stromal and parenchymal portions of breast tissue. It was concluded that the four *in vitro* culture models presented are well-suited for the study of normal and malignant mammary gland development because they can be modulated to mimic a particular *in vivo* environment. Furthermore, the results do support the hypothesis that a stiffer substrate (i.e. beads) will result in altered activity of D1 cells, e.g. inducing them to differentiate.

With respect to education and outreach in bioengineering, the high school classroom demonstration on stem cells appeared to be very useful in helping students understand the major differences between embryonic and adult stem cells and the applications of these cells in bioengineering research. Likely, some of the students in the classes would have fared well with only the slide presentation from which to learn about and better understand stem cell biology; however, because of the wide range of learning styles in any particular classroom, this tactile activity may help reach some of the students who require a more active learning environment. Additionally, the Museum of Science Design Challenges Center did appear to be an appropriate setting for the implementation of teaching modules. In this informal setting, the attention span of the participants appeared to be limited to approximately 5-10 minutes, depending on the age group, so timing of the activity should be limited.

CHAPTER 10

RECOMMENDATIONS FOR FUTURE WORK

1. Continue to match nozzle firing frequencies with the viscosities of bio-inks that will be prevalent in tissue test systems. It will be important to test various concentrations of solutions of collagen, chitosan, alginate, and agarose, for example.
2. Consider methods to keep cells homogeneously suspended in bio-ink solutions so that a more consistent number of cells will be deposited in each drop.
3. Repeat studies to determine the statistics of cell placement using Method 4 post-processing techniques (HBSS, followed by an overlay of collagen, then D1 maintenance medium) to improve cell viability and pattern retention.
4. Combine bioprinting techniques with traditional 3D gel-based macrofabrication techniques to influence ductal branching of mammary epithelial cells. This might be achieved by first creating a 3D gel scaffold consisting of Type I collagen and embedding a pattern of luminal epithelial and myoepithelial cells via bioprinting technology.
5. Refine methods, e.g. laser capture, for harvesting specific clusters of cells from a bioprinted sample so that quantitative gene and protein analysis techniques can be applied.
6. Study the effect of outreach activities on the communication skills of graduate students.